



Cape Peninsula
University of Technology

**HIGH VOLTAGE DIRECT CURRENT (HVDC) IN APPLICATIONS FOR
DISTRIBUTED INDEPENDENT POWER PROVIDERS (IPP)**

by

MARTIAL GIRANEZA

Thesis submitted in fulfillment of the requirements for the degree

Master of Technology: Electrical Engineering

in the Faculty of Engineering

at the Cape Peninsula University of Technology

Supervisor: Professor MTE KAHN

Bellville

December 2013

CPUT copyright information

The dissertation/thesis may not be published either in part (in scholarly, scientific or technical journals), or as a whole (as a monograph), unless permission has been obtained from the
University

DECLARATION

I, Giraneza Martial, declare that the contents of this dissertation/thesis represent my own unaided work, and that the dissertation/thesis has not previously been submitted for academic examination towards any qualification. Furthermore, it represents my own opinions and not necessarily those of the Cape Peninsula University of Technology.

Signed

Date

ABSTRACT

The development of power electronics did remove most of technical limitations that high voltage direct current (HVDC) used to have. HVDC, now, is mostly used for the transmission of bulk power over long distances and for the interconnection of asynchronous grid. Along with the development of the HVDC, the growth of power demand also increased beyond the utilities capacities. Besides the on-going increasing of power demand, the reforms in electricity market have led to the liberalization and the incorporation of Independent power providers in power system operation. Regulations and rules have been established by regulating authority for grid integration of Independent power providers. With the expected increase of penetration level of those new independent power providers, result of economic reason and actual green energy trend, best method of integration of those new power plants are required.

In this research HVDC technology, namely VSC-HVDC is used as interface for connecting independent power providers units to the grid. VSC-HVDC has various advantages such as short-circuit contribution and independent control of active and reactive power. VSC-HVDC advantages are used for a safe integration of IPPs and make them participate to grid stabilization. MATLAB/Simulink simulations of different grid connected, through VSC-HVDC system, IPPs technologies models are performed.

For each IPP technology model, system model performances are studied and dynamics responses during the disturbance are analyzed in MATLAB/ Simulink program. The simulation results show that the model satisfy the standard imposed by the regulating authority in terms of power quality and grid support. Also the results show the effect of the VSC-HVDC in preventing faults propagation from grid to integrated IPPs units.

ACKNOWLEDGEMENTS

My sincere acknowledgement of thanks goes to the Almighty God who has given me the opportunity to successfully complete my study.

To my supervisor, Professor MTE Kahn for his constant supervision, guidance, encouragement and support. I consider myself fortunate to come across such a noble professor, not only for my study but also for my personal development. Without your supervision this thesis would not have been possible.

I express my sincere gratitude to Dr. Raji Atanda for his patience, continuous assistance and encouragement throughout this study.

I am grateful to Mr. Onwuta Onwuta for his wise advices, help and encouragements throughout this journey. I extend my sincere gratitude to Mr. Almaktoof Ali, Mr. Senthil Krishnamurthy and all my colleagues' students at Centre for Distributed Power and Electronic Systems (CDPES) for their academic exchange, support and encouragement.

My thanks go to Mr. Hitimana Christian and Mr. Tuishime Innocent for their support and encouragement.

Lastly I would like to thank my family for their support and encouragement.

The financial assistance of the Centre for Distributed Power and Electronic Systems (CDPES) towards this research is acknowledged. Opinions expressed in this thesis and the conclusions arrived at, are those of the author, and are not necessarily to be attributed to the respective mentioned establishments.

DEDICATION

To my family, may they see in this work the fruit of their love and support

TABLE OF CONTENTS

DECLARATION	II
ABSTRACT	III
ACKNOWLEDGEMENTS	IV
DEDICATION	V
TABLE OF CONTENTS	VI
LIST OF FIGURES	IX
LIST OF TABLES	XII
GLOSSARY	XIII
CHAPTER ONE : INTRODUCTION	1
1.1 OVERVIEW	1
1.2 PROBLEM STATEMENT.....	3
1.3 SCOPE OF THE RESEARCH	3
1.4 BACKGROUND OF STUDY.....	4
1.5 METHODOLOGY	5
1.6 .ORGANIZATION OF THESIS.....	5
CHAPTER TWO: HIGH VOLTAGE DIRECT CURRENT TRANSMISSION	6
2.1. INTRODUCTION.....	6
2.2 CLASSIC HVDC TECHNOLOGY SYSTEM.....	7
2.2.1 Classic HVDC system configuration.....	9
2.2.2 Advantages of HVDC classic.	10
2.2.3 Applications of HVDC classic.....	10
2.2.4 Commercial development	11
2.3 HVDC-VSC BASED SYSTEM	12
2.3.1. Introduction.....	12
2.3.2. System description.....	12
2.3.3. Converters	14
2.3.4 PWM technology.....	18
2.3.5 VSC-HVDC systems control.....	20
2.3.6 HVDC cables	21
2.3.7. HVDC protection	23
2.4. HVDC TRANSMISSION TECHNOLOGIES COMPARISON	24
2.5 SUMMARY	25

CHAPTER THREE : INDEPENDENT POWER PROVIDERS.....	26
3.1. INTRODUCTION.....	26
3.2. WIND ENERGY.....	26
3.2.1 Wind generation.....	26
3.2.2 Wind Turbine Generators.....	31
3.2.3. Wind turbine control.....	36
3.2.4. Wind power plant.....	37
3.2.5 Wind farm grid connection.....	40
3.2.6 Grid requirements for the Interconnection of Wind Farms.....	41
3.3. SOLAR POWER SYSTEMS.....	43
3.3.1 Introduction.....	43
3.3.2 Photovoltaic system.....	43
3.3.3 Maximum-Power-Point-Tracker (MPPT).....	48
3.3.4 PV grid connection.....	49
3.3.5. Concentrated Solar Power (CSP).....	54
3.3.6 Solar power plants impact on the grid.....	56
3.3.7 Superconducting magnet energy storage.....	56
3.4. POWER SYSTEM.....	59
3.4.1 Introduction.....	59
3.4.2 Power system stability.....	60
3.5 SOUTH AFRICA GRID CODE.....	62
3.5.1 Introduction.....	62
3.5.2 Abnormal operating conditions.....	63
3.6 SUMMARY.....	64
CHAPTER FOUR :SYSTEM DESIGN.....	65
4.1. INTRODUCTION.....	65
4.2 MAIN CIRCUIT COMPONENTS AND PARAMETERS.....	66
4.3 WIND FARM.....	66
4.3.1 Introduction.....	66
4.3.2 Frequency regulator.....	67
4.3.3 Synchronous condenser.....	69
4.3.4 Wind turbine.....	70
4.3.5 Asynchronous generator.....	71
4.3.6 Power factor correction capacitor.....	73
4.4. THE GRID.....	73
4.5. CONVERTER TRANSFORMER.....	74
4.6. VOLTAGE SOURCE CONVERTERS.....	74

4.7. FILTERS.....	75
4.8 DC CAPACITORS	77
4.9 HVDC CABLES	78
4.10 CONVERTER CONTROL.....	78
4.11 SOLAR POWER PLANT	81
4.11.2 Solar panels.....	82
4.11.12 controller	83
4.11.13 Storage unit	84
4.11.14 Boost converter.....	84
4.12. SUMMARY	98
CHAPTER FIVE : VSC-HVDC IN APPLICATIONS FOR INDEPENDENT POWER PROVIDER, SIMULATIONS RESULTS	99
5.1 INTRODUCTION.....	99
5.2 INTEGRATION OF THE CONVENTIONAL POWER PLANT (IPP1) THROUGH VSC-HVDC	99
5.2.1 Normal conditions	99
5.2.2. Abnormal conditions	102
5.3 INTEGRATION OF THE WIND POWER PLANT (IPP2) THROUGH VSC-HVDC	104
5.3.1 Introduction	104
5.3.2. Normal condition	104
5.3.3 Abnormal conditions	109
5.4 INTEGRATION OF SOLAR POWER PLANT (IPP3) THROUGH VSC-HVDC.....	115
5.4.1. Introduction	115
5.4.2. Normal working conditions	115
5.3.3 Abnormal conditions	118
5.5 SUMMARY.....	122
CHAPTER SIX : CONCLUSION AND RECOMMENDATION.....	123
6.1 CONCLUSION	123
6.3 FUTURE WORK	124
REFERENCES	125
APPENDICES	138

LIST OF FIGURES

FIGURE 1. 1 ELECTRICITY MARKET MODELS	2
FIGURE 2. 1: HVDC SYSTEM COMPONENTS	7
FIGURE 2. 2: HVDC CONFIGURATION AND OPERATING MODES	9
FIGURE 2. 3: BASIC HVDC-VSC TRANSMISSION SYSTEM	13
FIGURE 2. 4: VSC PHASOR DIAGRAM AND POWER FLOW DIRECTION	14
FIGURE 2. 5: TWO LEVEL THREE PHASE VSC	15
FIGURE 2. 6 : MULTIMODULE VSC DIAGRAM WITH N TWO-LEVEL MODULES	16
FIGURE 2. 7: H-BRIDGE BASED MULTILEVEL DIAGRAM	17
FIGURE 2. 8: DIODE CLAMPED MULTILEVEL CONVERTER SCHEMATIC DIAGRAM	18
FIGURE 2. 9: MASS IMPREGNATED HVDC CABLE	22
FIGURE 2. 10: SELF-CONTAINED FLUID FILLED CABLE	22
FIGURE 2. 11: EXTRUDED CABLE FOR HVDC APPLICATIONS	23
FIGURE 3. 1: WIND POWER GENERATION.....	27
FIGURE 3. 2: VERTICAL WIND TURBINES	28
FIGURE 3. 3: HORIZONTAL WIND TURBINE	29
FIGURE 3. 4: AIR STREAM MOVING TOWARDS A TURBINE.....	30
FIGURE 3. 5: FIXED SPEED SQUIRREL CAGE INDUCTION GENERATOR.....	31
FIGURE 3. 6: DOUBLE FED INDUCTION GENERATOR	32
FIGURE 3. 7: PERMANENT MAGNET SYNCHRONOUS GENERATOR ER.....	33
FIGURE 3. 8: WIND ENERGY CONVERSION SYSTEM.....	36
FIGURE 3. 9 : WIND FARM.....	38
FIGURE 3. 10: RADIAL CONFIGURATION SYSTEM.....	39
FIGURE 3. 11: RING CONFIGURATION SYSTEM.....	40
FIGURE 3. 12: STAR SYSTEM CONFIGURATION	40
FIGURE 3. 13: INDIVIDUAL AND GROUP CONNECTION OF WIND FARM	41
FIGURE 3. 14: PHOTOVOLTAIC CELL	44
FIGURE 3. 15: PHOTOVOLTAIC CELL ELECTRICAL MODEL	44
FIGURE 3. 16: I-V CHARACTERISTIC OF PV CELL.....	45
FIGURE 3. 17: SOLAR ARRAYS.....	47
FIGURE 3. 18: PV CONFIGURATION FOR GRID CONNECTED SYSTEMS.....	48
FIGURE 3. 19: TYPICAL VOLTAGE OR CURRENT MPPT SYSTEM	48
FIGURE 3. 20: PRINCIPLE OF A SINGLE-PHASE GRID CONNECTED PV SYSTEM.....	49
FIGURE 3. 21: CENTRAL PLANT INVERTER CONFIGURATION	50
FIGURE 3. 22: MODULE INTEGRATED INVERTER	51
FIGURE 3. 23: MULTIPLE-STRING DC/DC CONVERTER	51
FIGURE 3. 24: MULTIPLE-STRING INVERTER	51
FIGURE 3. 25: SYNCHRONIZATION METHOD USING FILTERING ON A -B ALPHA AND BETA FRAME	52
FIGURE 3. 26: SYNCHRONISATION METHOD USING FILTERING ON D-Q FRAME	52
FIGURE 3. 27: BASIC TOPOLOGY OF PLL	53
FIGURE 3. 28: GENERAL STRUCTURE OF D-Q PLL METHOD	53
FIGURE 3. 29: PARABOLIC THROUGH CSP PLANT SCHEMATIC	54

FIGURE 3. 30: FRESNEL REFLECTORS	55
FIGURE 3. 31: SOLAR TOWER POWER PLANT	55
FIGURE 3. 32: COMPONENTS OF A SMES SYSTEM.....	57
FIGURE 3. 33: ELECTROMAGNETIC FORCE ON TORROIDAL AND SOLENOID COILS	58
FIGURE 3. 34: GENERATOR-BUS BAR SYSTEM	61
FIGURE 3. 35: MINIMUM FREQUENCY OPERATING RANGE FOR RENEWABLE POWER PLANT	63
FIGURE 3. 36: VOLTAGE RIDE THROUGH CAPABILITY FOR RENEWABLE POWER PLANT	64
FIGURE 4. 1: SYSTEM DESIGN	65
FIGURE 4. 2: ASYNCHRONOUS GENERATOR BASED WIND FARM IN ISOLATED NETWORK.....	67
FIGURE 4. 3 : DISCRETE FREQUENCY REGULATOR PROCESS	68
FIGURE 4. 4: SECONDARY LOADS SWITCHING PROCESS.....	68
FIGURE 4. 5: SYNCHRONOUS CONDENSER EXCITATION SYSTEM	69
FIGURE 4. 6: WIND TURBINE CHARACTERISTIC.....	70
FIGURE 4. 7: WIND TURBINE CONTROL DIAGRAM	71
FIGURE 4. 8 : ASYNCHRONOUS SQUIRREL CAGE MACHINE IN D-Q MODEL	72
FIGURE 4. 9: GRID MODEL.....	74
FIGURE 4. 10: AC HIGH PASS FILTER.....	75
FIGURE 4. 11: HIGH PASS FILTER RESPONSE FREQUENCY CHARACTERISTICS AT 27TH HARMONIC	76
FIGURE 4. 12: HIGH PASS FILTER FREQUENCY RESPONSE CHARACTERISTIC AT 54TH HARMONICS	77
FIGURE 4. 13: VSC-HVDC CONVERTER CONTROL SYSTEM	78
FIGURE 4. 14: DC VOLTAGES AND CURRENTS OF THREE LEVEL BRIDGE.....	81
FIGURE 4. 15: SOLAR PARK CONNECTED TO GRID	82
FIGURE 4. 16: DC-DC BOOST CONVERTER TOPOLOGY	85
FIGURE 4. 17: DC-DC BOOST CONVERTER ON MODE TOPOLOGY	85
FIGURE 4. 18: DC-DC BOOST CONVERTER OFF MODE TOPOLOGY	85
FIGURE 4. 19: ON AND OFF MODES TIME DURATION	86
FIGURE 4. 20: DC-DC BOOST CONVERTER CHARACTERISTIC.....	89
FIGURE 4. 21: INDUCTOR STEADY STATE VOLTAGE AND CURRENT WAVEFORM.....	89
FIGURE 4. 22: DC-DC BOOST CONVERTER CAPACITOR CURRENT AND VOLTAGE WAVEFORMS.....	91
FIGURE 4. 23: INDUCTOR CURRENTS FOR CONTINUOUS CONDUCTION MODE	93
FIGURE 4. 24: INDUCTOR VOLTAGE AND CURRENT WAVEFORMS DURING THE DISCONTINUOUS MODE ..	95
FIGURE 5. 1: IPP 1 CONNECTION TO THE GRID.....	99
FIGURE 5. 2: MEASUREMENT TAKEN AT IPP1 STATION DURING NORMAL CONDITIONS	100
FIGURE 5. 3: MEASUREMENT TAKEN AT GRID SIDE STATION 2 DURING THE NORMAL CONDITION	101
FIGURE 5. 4: IPP1 CONNECTION TO GRID, FAULT TESTING MODEL	102
FIGURE 5. 5: MEASUREMENT AT IPP1 STATION DURING THE FAULTS	103
FIGURE 5. 6: MEASUREMENT TAKEN AT GRID SIDE STATION 2, DURING FAULT CONDITION	104
FIGURE 5. 7: IPP2 CONNECTION TO GRID.....	105
FIGURE 5. 8: MEASUREMENTS TAKEN AT GRID SIDE, STATION 2 DURING THE NORMAL CONDITION	106
FIGURE 5. 9: MEASUREMENT TAKEN AT IPP2 STATION 1 DURING THE NORMAL	107
FIGURE 5. 10: MEASUREMENT TAKEN AT STATION 2 DURING GRID SIDE FREQUENCY VARIATION.....	108
FIGURE 5. 11: MEASUREMENT TAKEN AT IPP2 STATION 1 DURING THE GRID SIDE FREQUENCY VARIATIONS	109
FIGURE 5. 12: IPP2 CONNECTION TO GRID, FAULT TESTING MODEL	110
FIGURE 5. 13: MEASUREMENT TAKEN AT STATION 2 DURING THREE PHASE FAULT ON GRID SIDE.....	111
FIGURE 5. 14: MEASUREMENT TAKEN AT IPP2 STATION DURING THREE PHASE FAULT ON GRID SIDE....	112

FIGURE 5. 15: MEASUREMENT TAKEN AT STATION 2 DURING THE GRID SIDE PHASE ANGLE JUMP 113
FIGURE 5. 16: MEASUREMENT TAKEN AT IPP2 STATION 1 DURING GRID SIDE PHASE ANGLE JUMP 114
FIGURE 5. 17: IPP3 CONNECTION TO THE GRID..... 115
FIGURE 5. 18: MEASUREMENTS TAKEN AT STATION 2 ON GRID SIDE..... 116
FIGURE 5. 19: MEASUREMENT TAKEN AT IPP3 ON STATION..... 117
FIGURE 5. 20: IPP3 CONNECTION TO GRID, FAULT TESTING MODEL 118
FIGURE 5. 21: MEASUREMENT TAKEN AT IPP3 STATION 2 DURING FAULT ON GRID SIDE 119
FIGURE 5. 22: MEASUREMENT TAKEN AT STATION 1 ON IPP3 SIDE DURING THE FAULT ON GRID 120
FIGURE 5. 23: MEASUREMENT TAKEN AT IPP3 STATION 2 DURING GRID SIDE PHASE ANGLE JUMP 121
FIGURE 5. 24: MEASUREMENT TAKEN AT IPP3 STATION DURING GRID SIDE PHASE ANGLE JUMP 122

LIST OF TABLES

TABLE 2. 1: ACTUAL IMPORTANT HVDC PROJECTS	11
TABLE 2. 2 HVDC CLASSIC AND HVDC-VSC COMPARISON	25
TABLE 3. 1: WIND TURBINES TECHNOLOGIES COMPARISON.....	35
TABLE 3. 2: RESULTS OF MEDIUM SIZE SMES COIL.....	58
TABLE 4. 1: ASYNCHRONOUS GENERATOR PARAMETERS USED	71
TABLE 4. 2: SOLAR CELLS PARAMETERS	83

GLOSSARY

CSC:	Current Source Converter
DFIG:	Doubly Fed Induction Generator
DOE:	Department of energy
ESKOM:	Electricity Supply Commission (South African electricity public utility)
FRT:	Fault Ride Through
FSC:	Full Scale Converter
FSGT:	Fixed Speed wind Turbine Generator
HVAC:	High Voltage Alternating Current
HVDC:	High Voltage Direct Current
IGBT:	Insulated Gate Bipolar Junction Transistor
IGCT:	Insulated gate Commutated Thyristor
IPP:	Independent Power Providers
IRP:	Integrated Resource Plan
LVRT:	Low Voltage Fault Ride Through
MATLAB:	Matrix Laboratory
MMC:	Modular Multilevel Converter
MPPT:	Maximum Power Point Tracker
MOSFET:	Metal–Oxide–Semiconductor Field-Effect Transistor
NERSA:	National Energy Regulator of South Africa
NPC:	Neutral-point clamped converter
PCC:	Point of Common Connection
PD:	Proportional Differentiator
PI:	Proportional Integrator
PLL:	Phase Locked Loop
PPL:	Paper Polypropylene laminate cables
PMSG:	Permanent Magnet Synchronous Generator
P.U:	Per Unit system
PV:	Photo-Voltaic
PWM:	Pulse Width Modulation
SCFFC:	Self-Contained Fluid Filled Cables
SHE PWM:	Selective Harmonic Elimination PWM
SPWM:	Sinusoidal PWM
SVPWM:	Space Vector PWM
SMES:	Superconducting Magnetic Energy Storage System
VSC:	Voltage Source Converter
XLPE:	Cross Linked Polyethylene cables

CHAPTER ONE

INTRODUCTION

1.1 Overview

With the liberalization of national utilities services in many countries, the technological development which resulted in high demand of electrical energy that normal grid or the national utilities can't afford and the actual tendency to turn on green energy in conjunction with market driven spirit of investing in renewable energy, the distributed independent power production had seen the day. According to (Bacon & Besant, 2001), the liberalization of electricity market consists of four models:

Model 1 (monopoly) has no competition at all, it is a monopolistic system at all levels of the supply chain. A single company, generally the government utility produces and delivers electricity to the users.

Model 2 (purchasing agency) allows a single buyer or purchasing agency to encourage competition between generators by choosing its sources of electricity from a number of different electricity producers. The agency on-sells electricity to distribution companies and large power users without competition from other suppliers.

Model 3 (wholesale competition) allows distribution companies to purchase electricity directly from generators they choose, transmit this electricity under open access arrangements over the transmission system to their service area, and deliver it over their local grids to their customers, which brings competition into the wholesale supply market but not the retail power market.

Model 4 (retail competition) allows all customers to choose their electricity supplier, which implies full retail competition, under open access for suppliers to the transmission and distribution systems (Bacon & Besant,2001). These four models are shown in Figure.1.1 (Anton, 2001).

Bacon and Besant (2001) have observed that many reform programs in developing countries focus on moving from model 1 to model 3. The key decision is whether to go for model 2 or model 3. Adoption of model 2 in some developing countries has been justified largely as a transition stage to model 3 that is needed to allow time for the generation and distribution sectors to develop sufficiently for the operation of a competitive wholesale electricity market.

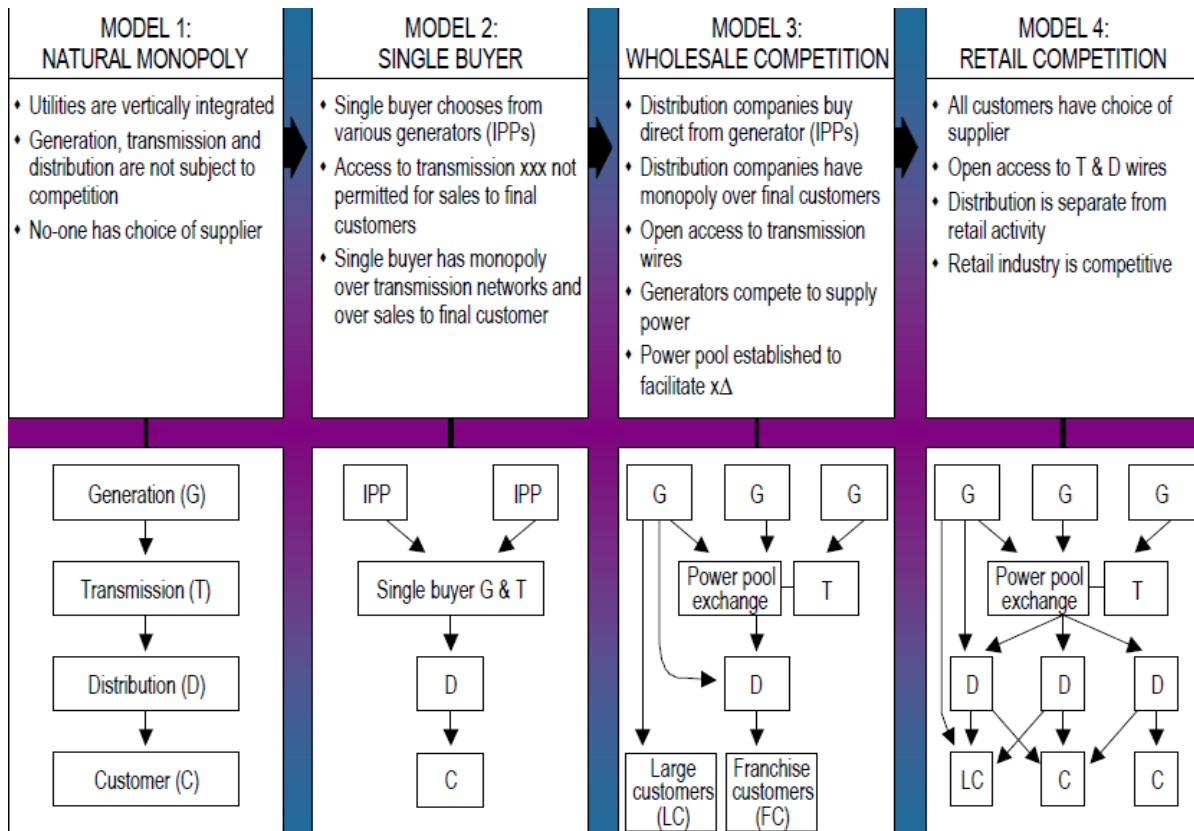


Figure 1. 1 Electricity market models (Anton2001)

South African Republic, like other developing countries, did make the reforms in electricity sector through Electricity Regulation Act (ERA) of 2006 (N°4 of 2006) and many other measures were taken in order to prevent the shortage of power in near future. Like many developing countries South Africa opted for the model 2 where the utilities have authority on transmission and distribution while the Independent Power Providers (IPPs) are occupied with the generation of electrical power to be sold to the utilities; in case of South Africa, it is Electricity Supply Commission (ESKOM). The end users will still get the electrical power from the network of Eskom. All this will be implemented through the power purchase agreements between the government and Independent Power Providers (IPPs).

Alongside with the advantages of having different producers of electrical power, there are also concerns on how to efficiently integrate those distributed generation into conventional power system for reliability and the security of the network. The synchronism between the IPPs, interconnected through the utilities transmission lines, is not easy due to different sources of generation, which may be different in frequency and phase angle for the alternatives current and in magnitude for the direct current sources. Usual requirements needed in order to be interconnected onto utilities electrical transmission system are to maintain certain

constant frequency, a constant magnitude of voltage and certain phase sequences. Those IPPs may also differ in the way they are protected, controlled and their fault protection, etc.

Therefore, their technical and operational differences can make synchronous operation too difficult or expensive to pursue. Thus, the need of an interface between all those IPPs and the utilities grid.

Technological development has made significance advances in power electronics such that, it has been able for now to work with heavy currents either in alternative current form or direct current form. Especially for the High voltage in direct, the advancement in power electronics research made the HVDC to be integrated in electrical power transmission for long distances as well as for special transmission.

This thesis examines ways of applying high voltage direct current (HVDC) technologies as an interface between the normal grid and IPPs in order to overcome or to prevent the difficult operation of synchronization.

1.2 Problem statement

With the increasing growth of IPPs, their integration into the national grids is more becoming a challenge. The synchronization of those nonutility's operated generators as well as their reliability, is requiring high level of technical compatibility and operational coordination which grows in complexity and cost with the scale and inherent differences within the IPPs to be integrated in the grid.

How to overcome this technical challenge of synchronization and the complexity of it, for a safe, reliable and better integration of IPPs within utilities grid, by the use of HVDC technologies.

1.3 Scope of the research

The current study, *high voltage direct current(HVDC) in applications for Independent Power Provider(IPP)*, is limited to technical aspect of the interconnecting the IPPs, through HVDC technologies, into utilities transmission grid. The economic, social and political aspects of this problem are not treated in this thesis. Even though all those aspect are somehow on different scale embedded in the problem but still the technical aspect is the leading one for the safe and reliable operation of integration of IPPs.

The study is concentrated on the grid interconnection of IPPs renewable projects, in western cape, and the behavior of the grid at the interconnection point after the introduction of HVDC technologies; as well as the behavior of those Independent power providers (IPP), in different working conditions of the grid, steady state, dynamic state and fault conditions.

1.4 Background of study

The power blackout that faced South Africa in 2008, caused by the power demand which exceeded the resources available at the moment, was a warning to the government on the future similar problem if nothing is done. South Africa government reacted, beside immediate measures that have been taken, by introducing a long-term electricity capacity plan; the Integrated Resource Plan (IRP2010). The IRP2010 had the objectives, among others, of developing a sustainable electrical power investments strategy for generation capacity and supporting infrastructure for South Africa over the 20 years ahead. According to the IRP 2010, beside the capacity required to replace decommissioned plant, more than 41346 MW of new capacity are required in order to meet the demand in 2030. In this plan specific emphasis is put on diversifying the electrical power supply technologies to include nuclear, gas, biomass, and renewable (wind, solar, hydro). The renewable energies of 3725 MW are included in those needed new capacity for the CO₂ emissions decrease.

In respect of the IRP2010, the department of energy lunches a renewable energy IPP procurement program in August 2011 that has contributed to South Africa's energy diversity. Divided into 2 windows, the window 1 had 28 bidders approved by National Energy Regulator of South Africa (NERSA) with 1416 MW. The preferred bids for the window 2 of the renewable energy were announced this May 2012, with a capacity of 1043, 9MW, and nineteen bidders were selected. At the end of the two windows a total of 47 new power plants, owned by independent power providers (IPPs) will be integrated into South African grid.

Actually, 27 power plants operated by Eskom producing more than 98 % of South African electricity are connected to South African grid (Eskom, 2011). With the implementation of the integration resource plan (2010), especially the renewable energy IPP procurement, an increase of more than 100% of grid connected power plants is expected. With only both window of this renewable IPP procurement 47 power stations are expected to be introduced in the grid and there are still about 1165 MW not yet allocated (DoE, 2012).

The sources of power generation for those IPPs are mainly hydro, biomass, biogas, solar, gas and wind. Those resources are different in nature, their power generation models are also different and thus, their outputs are different in magnitude, phase, frequency and the power factor. The grid interconnection of these asynchronous generation point requires a huge and complex synchronization operation.

By using High Voltage Direct Current (HVDC) technology, which normally is preferred for long bulk power transmission, as an interface between the grid and power station it is possible to overcome the synchronization operation complexity; plus the obtaining of a buffer or firewall against eventual cascading failures from one part of the grid, that may harm the power stations (Bahrman, 2007).

1.5 Methodology

For this research to adequately reach completion the following methods were used:

- Literature survey: In depth review of related theories were collected from books, relevant journals, internet search engines, submitted works related to this research.and interaction with experienced people in the subject.
- Modeling and simulation: IPPs and VSC-HVDC Models were developed and simulated using MATLAB /Simulink in order to well understand the behavior of integrated IPP through HVDC technologies in the grid.
- South African grid code for renewable energies was considered as the reference for evaluation of IPPs performance.

Grid faults simulations were carried out to investigate the integrated IPPs response and to draw the best method of integration.

1.6 .Organization of thesis

The thesis is organized into six chapters:

Chapter 1 gives a brief introduction on the electricity market reforms, concept of IPPs and South Africa electrical energy policy. Research methodologies and objectives are also discussed.

Chapter 2 reviews literature on HVDC transmission concepts, technologies and applications. VSC-HVDC transmission concept is also in depth explained. VSC-HVDC operating principle, structure of VSC-HVDC, advantages and disadvantages are fully discussed.

Chapter 3 presents the independent power providers technologies. Solar energy and wind energy technologies are reviewed as well as the power system and grid code.

Chapter 4 presents the system design and modeling. Mathematical derivation and overall structure of the system to be tested are discussed. The Selection of appropriate parameter values of system components is given in detail.

Chapter 5 discusses the simulation scenarios and results obtained. Analysis of VSC-HVDC grid integrated IPPs performance under different working conditions is discussed as well.

Chapter 6 presents conclusions of the study and recommendations for future work.

CHAPTER TWO

HIGH VOLTAGE DIRECT CURRENT TRANSMISSION

2.1. Introduction

In the beginning of industrialized era, the electrical energy took the advantage on the steam energy that was serving for long period. The electricity available or generated at the moment was direct current. The first electric central station in the world was built in 1882 by Thomas A. Edison in New York. The generator used was a direct current, so was the first electrical power transmission line constructed at that moment. The direct current was finally supplanted by the alternating current (AC) due to two things: the introduction of induction motors, the workhorse in industries and work with AC; and the availability of transformer with its easier ability of changing voltage level from transmission or distribution level to users' level. Hence, the AC became useful commercially and domestically (Kala & Sadrul, 2007).

As world economy and development increased, the demand of electricity increased as well, putting the power systems on the challenges of looking for more bulk power even far from the load centers. The transmission of such quantities of electrical power over long distances from remote area to the load centers using the HVAC transmission systems was economically inefficient due to the losses in the lines and consequently the required high amount of the lines to overcome that issue. As it was recognized early in the 1920's that there was advantages in the use of DC transmission in more challenging applications, the idea of transmitting electrical power in DC emerged again, but stacked due to the lack of necessary technologies in AC/DC vice versa conversion. The problem was resolved by the invention of high voltage mercury rectifier valves and especially by the introduction of thyristors valve into HVDC applications, around 1970 (Owen, 2009).

Till recently the traditional HVDC thyristor based, known also as HVDC classic, stood only for the conversion of AC/DC and DC back to AC. Different from the HVDC classic, the new type of HVDC on the market now, is based mostly on IGBTs and has more advantages over classic HVDC. The converters are VSCs (Voltage Sources Converters) operating at high switching frequencies. The new type of HVDC is commercialized as either HVDC Light (Kjell, 2001) or HVDC Plus (Schettler, et al., 2000) .

2.2 Classic HVDC technology system

HVDC as a technology system it has many components that interact together to make the whole running, as it can be seen on Figure.2.1

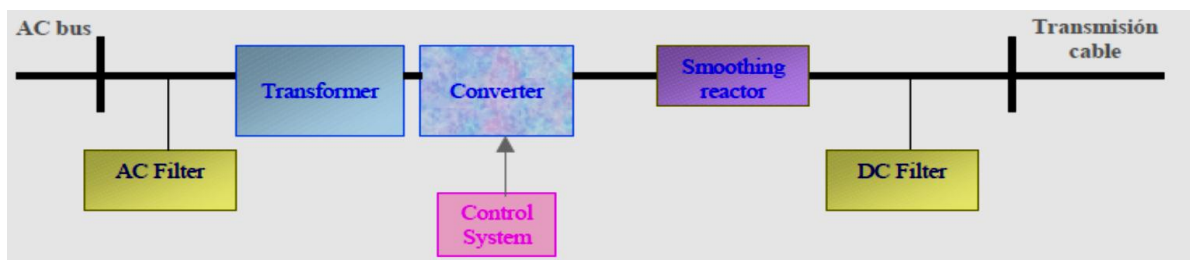


Figure 2. 1: HVDC system components (Larruskain et al, 2005)

The AC power from the bus bar is transformed after filtration and is converted into dc and passed through smoothing reactors then into DC filter before being sent into transmission lines. The reverse process is done at the receiving end where the DC is brought back into AC.

A. Harmonic Filters: harmonics are generated by the no-linear loads, that draw a non-linear sinusoidal current from AC sources (Robert, 2001). HVDC converters being a nonlinear load, generate harmonics that are absorbed by AC filters which in turn supply reactive power. DC filter circuit must be used as well as active filters in order to reduce dc ripple voltage generated by the converters. Such voltages ripple within a certain range of frequency can create interference into telephone circuits in the vicinity of the DC lines. On the other hand the DC filter is not necessary for cable transmission or for Back to Back substation. The active DC filters are most preferred in the modern installations (Zhang, 1994).

B. Transformers: the AC bus voltage has to be transformed to the required entry voltage of the converters. The Converter transforms the voltage level of the AC bus bar to the required entry voltage level of the converter.

C. Smoothing reactors designed as linear reactors their functions are the prevention of the intermittent current, limitation of the DC fault currents and the prevention of resonance in the DC circuits (Padiyar, 2005)

D. Control and Protection, like AC systems for the DC systems faults are generally caused by the malfunctioning of the equipment and controllers or by the failure of insulation caused by external sources such as lightning and pollutions.

For the disruption of the power transmission, control and protection are set by means of switching and control equipment, such as surge arrester, high speed DC switches, earth electrodes (Padiyar, 2005) .

A HVDC station requires considerable land because the transformers, filters and phase correction capacitors are placed outdoors. However, the valves and control equipment are placed in a closed air-conditioned/heated building; this distribution is due to the fact that the completely enclosed system requires a large building and is too expensive (Larruskain, et al., 2005)

E. Converters

Generally the power electronic converters are used where electrical power parameters have to be changed; these parameters may be frequency, voltage or current. Concerning the HVDC system the conversion is the fundamental process that takes place at ends, sending and receiving end. With conversion from AC to DC and DC to AC, respectively. Modern HVDC converters are thyristor based.

According to the commutation method used within them, there are two categories of converters (Amirnaser & Iravani, 2010; Roberto & Sharma, 2000):

1. *Line Commutated Converters (LCC)*. Also called natural commutated converters, they are the most used in the HVDC systems as of today. The commutation is done by the AC system voltage itself. The thyristor is the key component in the conversion process, with the ability of blocking high voltages (up to 10 kV), high current carrying capability and being a controllable semiconductor; it is feasible to build up a thyristor valve, that can operate at high voltages. They are operated at net frequency (50 or 60 Hz) and controlled by means of controlling angle, thus the transmitted power is quickly and efficiently controlled. Besides the merit of line commutated converters, it is still vulnerable to the commutation failure when connected to weak networks. From where the idea of the Capacitor Commutated Converters, which use the commutation capacitors. By this method the weakness of line commutated converter are reduced even in presence of weak networks.
2. *Forced Commutated Converters*. They are also known as *Voltage Source Converters (VSC)*. Their difference from line commutated converter (LCC) is that they are built up with semiconductors with the ability not only to turn-on but also to turn-off. Gate turn-off thyristor (GTO) or Insulated gate bipolar transistor are semiconductors generally used in this kind of converters. The conversion is done by Pulse Width Modulation (PWM) which gives to the VSC converter the ability of variation of phase angle and amplitude within a certain range. They have as well high commutation frequency, possibilities to control active and reactive power independently; therefore they can be a support for very weak AC system (Roberto & Sharma, 2000; Qahraman, et al., 2006).

2.2.1 Classic HVDC system configuration

There are various configurations' ways for HVDC operations. Figure.2.2 shows different common system configurations and operating modes in use for HVDC transmission. The mostly used configuration for modern overhead HVDC transmission lines is bipolar with a single pole at each terminal. A bipolar is a combination of 2 poles which shares a common return or ground. This configuration is also preferred in case of failure of one pole, half of the power may still available through monopole operations.

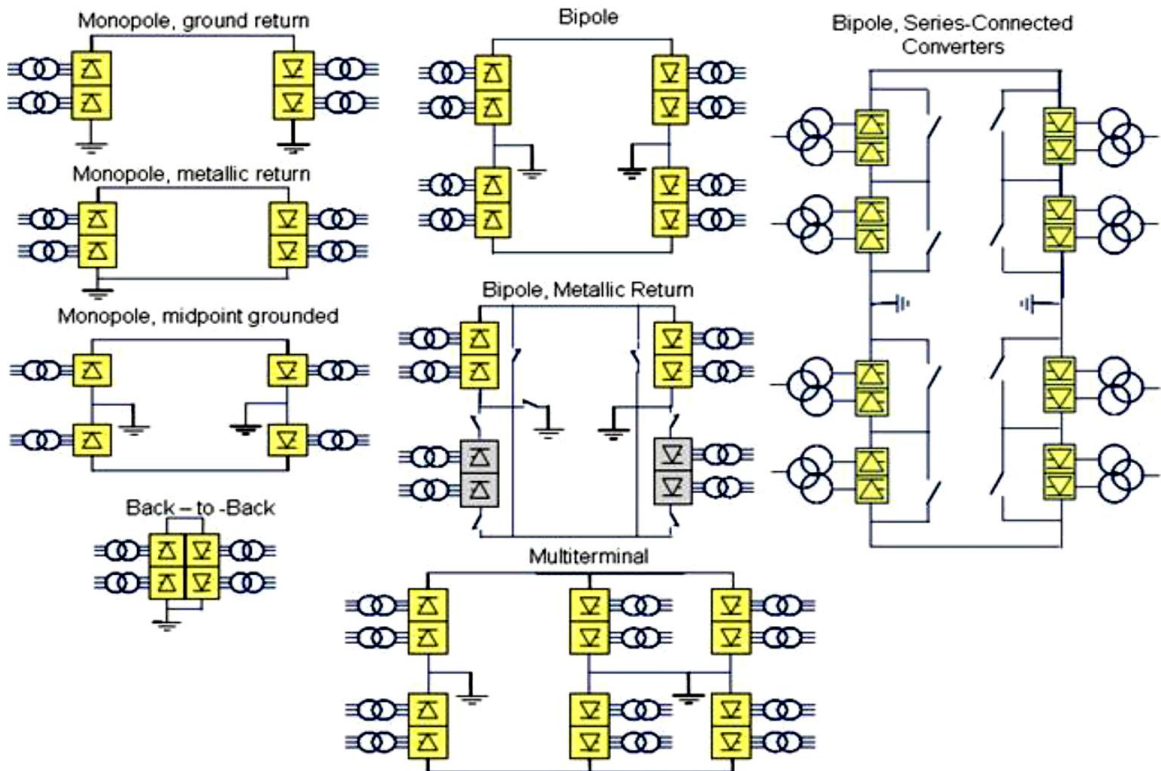


Figure 2. 2: HVDC configuration and operating modes (Bahrman & Brian, 2007)

For normal balanced operation there is no earth current. Emergency ground or earth return operation can be minimized during monopole outages by using the opposite pole line for metallic return via pole and converter bypass switches at each end. This is valid during converter outages as well as during line insulation failures where the remaining insulation has strength to withstand the low resistive voltage drop in the metallic return path. In a power pool with bulk power HVDC transmission, above $\pm 500\text{kV}$, variations of bipolar operation, like series connected converters, are performed in order to avoid the energy unavailability for individual converter outages or partial line insulation failure (Bahrman & Brian, 2007; Siemens, 2005).

2.2.2 Advantages of HVDC classic.

The HVDC classic system beside the long transmission of bulk electrical at economical cost, it has also other merits that are not easier to get in conventional AC transmission system, such as (Abhijit & Halder, 2011):

- There is no skin effect as much there is in AC system, thus the current density in HVDC transmission might be higher.
- HVDC links do not suffer stability problem in interconnected power system as they can run independently, plus they do not increase the short circuit current in the link point .thus no need of new calibration of circuit breaker in the existing network.
- HVDC transmission system does not need shunt compensators, as it is the case for AC long distance transmission lines.
- HVDC system use less conductors, thus the construction of transmission is simple. The line losses are less compared to AC transmission systems.
- In HVDC systems there are fewer coronas therefore less radio interference and there is not charging current, which put the HVDC system cables away from high dielectric losses.
- HVDC has got the ability to change the magnitude and the direction of power flow easily.
- The HVDC converters can act, through the gate control, as fault current dumper during fault in the DC lines.

2.2.3 Applications of HVDC classic

The main application of HVDC system was the delivery of bulk electrical power from remote power plant, to the load centers. Most of power plants are located several hundred kilometers from the costumers and far enough for the HVAC transmission to be efficient in terms of losses. Besides that, there are other applications in which can HVDC classic system be found, like in:

- Interconnections of asynchronous electrical power networks by using back to back configurations. HVDC does not contribute to short-circuit current of the interconnected system.
- Increasing of AC transmitting capacity by either upgrading the latter or by over building new HVDC overhead lines onto the normal AC lines.
- Stabilization of network, with the diversified power electronics equipment that HVDC classic systems have, they can be used to control the power flow.
- To deliver the power into congested load areas. Where new transmission right of way are impossible to obtain.

2.2.4 Commercial development

Gotland had in 1954 the first commercial HVDC project in the World. Built in the Baltic sea between the Swedish mainland and Gotland island, the project consisted in the transfer of power generated from Gotland island wind park to the main land (Asplund, et al., 2003). From this project, research were going on in order to optimize the concept of DC transmission and of power electronics components technology. The results were the introduction of thyristors in 1960's.

As it can be seen from Tab.2.1, there are several HVDC thyristor based transmission systems all around the world. They were constructed for the long transmission from the generation power point, mostly hydropower plant, to load centers.

Table 2. 1: Actual important HVDC projects (Asplund, 2004)

Project	Power MW	Distance KM	Voltage +/- KV
Cabora Bassa, South Africa, Mozambique	1930	1920	550
Inga- Shaba, Republic of Congo	560	1700	500
Nelson River Canada	4000	940	500
Itaipu Brazil	6300	790	600
Quebec- New England	2000	1480	450
Pacific Intertie USA	3000	1360	500
Geszuba- Shanghai	1200	1000	500
New Zealand	560	600	350
Skagerrak Denmark	440	240	250/350
TSQ China	2000	800	500
Three Gorges- Changzhou	3000	890	500
Three Gorges- Guandong	3000	940	500

In continental Europe, the first project of connection between England and France started in 1961, with the linkage of Lydd nuclear power station in Great Britain to the French station at Echingen inverter station. Operated at voltage of 100 kV and 800 A, it was a bipolar cables

64km long. It was later in 1981, replaced by two new 72 Km bipolar submarine cables operating at 270 KV with power transfer capability of 2000 Megawatts (Goodrich & Andersen, 1987).

The Italian HVDC transmission, linking Sardinia, Corsica to Italy went in operation in 1965. Consisted of submarine cables of 103 km linking Italy to Corsica and 15 km linking Sardinia to Corsica, the system is a multipoint system that facilitates energy exchange among the multiple several static invertors distributed between Italy, Corsica and Sardinia. It has also three overhead lines, one on each region: Italy mainland, Corsica and Sardinia. With a length of 50 km, 167 km and 87 km respectively. This installation operating at 200kV has power transfer capability of 200 MW (Mazzoldi, et al., 1989) .

In Japan, since 1960 many HVDC transmission systems were built to interconnect different archipelagos. In 1965 Japan eastern and western networks were interconnected through Sakuma HVDC convertor station .The station has power capacity of 300 MW. Five years later in 1970, two new convertors were put in service, with 37.5 MW, 125 kV, at Sakuma testing station. The installed convertors were thyristor based (Horiuchi & Kato, 1974).

2.3 HVDC-VSC based system

2.3.1. Introduction

The HVDC system, in its previous introduction, was using current source convertors mostly they were thyristor based. With this technology the commutation of the valves were done by the line or network. The commutation is initiated by the polarity change of the AC voltage. As technology goes on developing the introduction of new higher rated power semiconductor like Insulated-Gate Bipolar Transistor (IGBT), Gate Turn Off thyristors (GTO) and integrated gate-commutated thyristors (IGCT) had made possible the appearance of voltage source convertors (VSC).

The HVDC-VSC is new technology based on high rated VSC convertors, themselves based on IGBT. The AC waveform is achieved by the use of power width modulation (PWM) techniques. The PWM technique gives the possibility to change the magnitude, phase angle and the waveform of the fundamental component. Those changes can be made nearly instantaneously by the variation of PWM pattern (Padiyar, 2007).

2.3.2. System description

The HVDC-VSC concept consists in transmitting a high voltage direct current from the rectifier to inverter, as it can be noticed on Figure.2.3; the transmission can be implemented either by a back to back configuration or through DC cables. From one AC side network to the other.

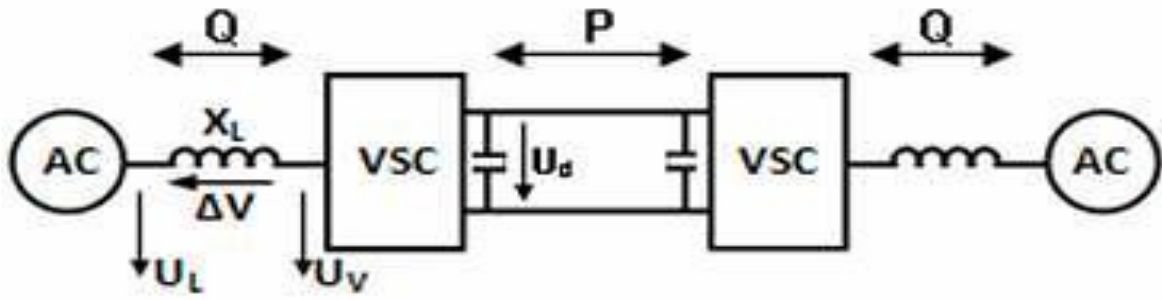


Figure 2. 3: Basic HVDC-VSC transmission system

The converters are connected to an AC grid through three phase reactors and transformer. The power flowing from right side to left side, the voltage U_V the fundamental voltage at the converter transformer with leakage reactance X_L is proportional to the DC voltage U_d coming from the other VSC on sending end. Thus,

$$U_V = K_u U_d \quad (1)$$

The proportionality coefficient K_u in Equation (1), is subject of variations depending on the commutation number per cycle, the pulse width modulation is a control technique used by the converter for varying the output voltage in VSC. Thus the power transmitted would be controlled by the control of valve side voltage U_V . By assuming the transformer resistance low to be taken into account, so the active power P and reactive power Q are given by the

$$P = U_d \cdot I_d = \frac{U_L \cdot U_V}{X_L} \sin \delta \quad (2)$$

$$Q = \frac{U_L \cdot (U_L - U_V \cos \delta)}{X_L} \quad (3)$$

Where I_d is the DC side current, U_L the AC side voltage and δ the phase shift between U_L and U_V from Equation (2), the active power is related both to the DC current and voltage and in turn to phase angle δ the flow direction of active power is determined by the value of phase angle δ . With positive angle the power will flow towards the converter from the AC side, at that moment the VSC will be acting as a rectifier. For the reactive power the flow direction is primary given, as it can be noticed in Equation (3), by the difference between the AC side voltage and the converter output voltage. The phase angle δ has its share in the variation of the converter output. The reactive power will flow from the side with higher voltage magnitude to the lower magnitude voltage side. As it can be seen from Equation (4) and Figure.2.4, the ability of controlling the angle, using the PWM techniques most of time, allows to the VSC the

independent control of both reactive and active power which is its advantage (Khatir, et al., 2009).

$$P^2 + \left[Q - \frac{U_L^2}{X_L}\right]^2 = \left[\frac{U_L * U_V}{X_L}\right]^2 \quad (4)$$

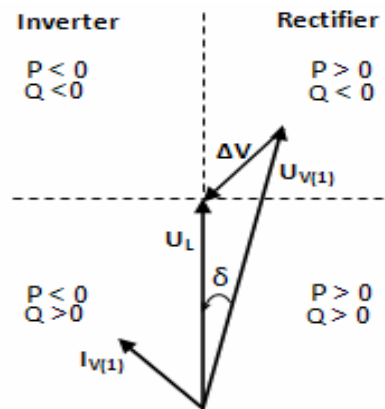


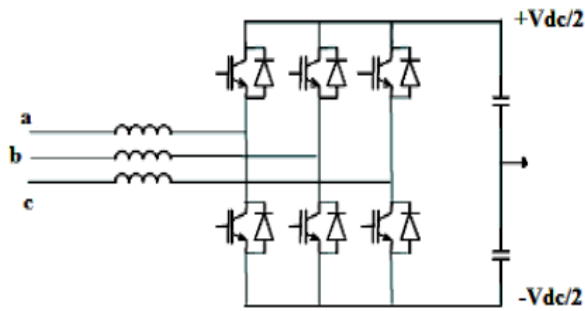
Figure 2. 4: VSC phasor diagram and power flow direction (Khatil, e t al.2009)

2.3.3. Converters

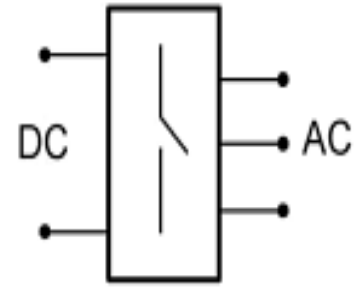
The HVDC VSC transmission system is based on VSC converters. Three phase converters of different configuration are used. Most of the VSC configurations are the two levels, multilevel and multimodal.

1. Two levels converters

The two levels VSC converters are based on two levels half-bridge circuits, as it can be seen on Figure.2.5, of a three phase half bridge with six valves, each valve consisting of an IGBT and an anti-parallel diode. The converter is called two levels since it can supply two voltage levels of $\pm V_{dc}/2$ to the AC side depending on which group of valves is on. Two half bridge VSC may be connected in parallel on their DC side to make a two level full bridge, called also H-bridge converter. The advantage in doing that is the AC voltage is now twice of the half bridge AC voltage. For two levels converters switching, various Pulse Width Modulation (PWM) are used (Shri, et al., 2012).



a) Three phase two level VSC



b) three phase two level VSC symbolic

Figure 2.5: Two level three phase VSC

2. Multimode converters

For high voltage applications, the usual switch cells that compose a VSC can't withstand voltages and currents requirements. In order to remedy that challenge, series or parallel associations of switches cells are made. The set of such association of switches is called valve. The insulated gate bipolar transistor (IGBT) valves are the mostly used. The number of IGBTs in association is determined by the power required and the power handling capability of the semiconductor, the actual IGBTs can handle 2.5 kV at switching frequency of 2 kHz. With the continuous research, higher power devices are expected. A VSC converter with that IGBT of that standard can handle 800 A ac line currents, voltages of 150kV and power ratings up to 140 MVA. Although the association of switches, a limitation of the number of switches to be grouped is set by form factor, off-state voltage distribution, and simultaneous-gating requirements. Those factors make two levels VSC inadequate for high power. The alternative ways was the association of several modules of two levels VSC. Like it can be seen from Figure.2.6 numerous two levels VSC are associated to form a multimodule converter. Besides the high power handling capability of that kind of converters, the modularity is the key for the low cost production (Padiyar, 2008; Amirnaser & Iravani, 2010 Shri, *et al.*, 2012).

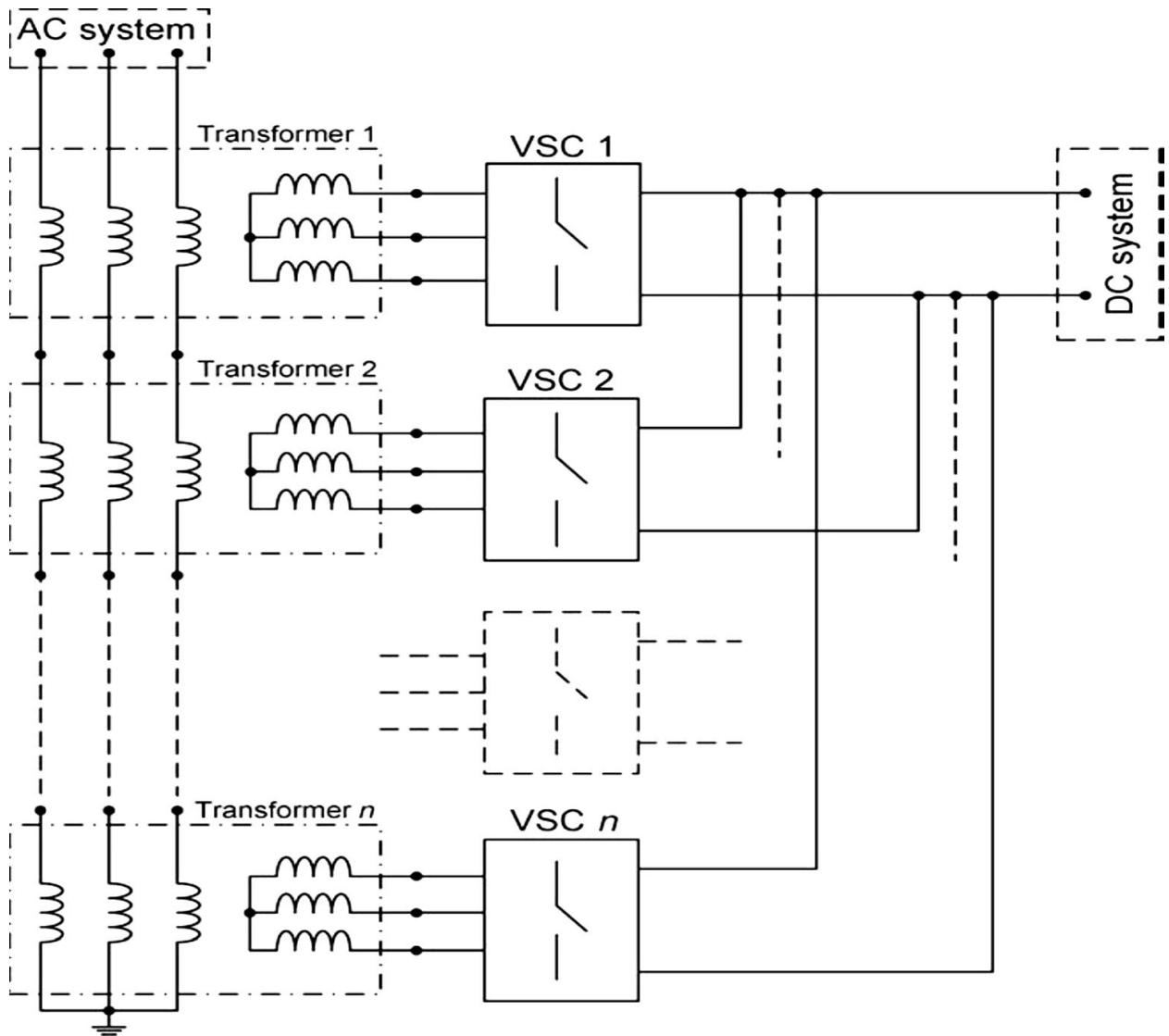


Figure 2. 6 : Multimodal VSC diagram with N two-level modules (Amirnasir and Iravani 2010)

3. Multilevel converters

The other configuration used by VSC systems to fulfil the voltage and current requirements in order to be used in high power applications is the multilevel conversion. It consists of associate series of power semiconductor switches with various voltage dc sources to perform the power conversion by synthesizing a staircase voltage waveform. Thus more different voltage levels at the AC side are possible to get .Multilevel converters have got improved performance than two level converters and they are as well very complex and onerous than the two level converters (Bimal, 2000; Andrzej, 2010).

Figure.2.7 represents the schematic diagram of multilevel VSC and from it we can see the difference between multilevel and multimodule VSC is that the latter use a single source while the multilevel VSC use several DC sources. There are three configurations of multilevel VSC (Rodríguez, et al., 2007):

- The H-bridge-based multilevel VSC
- The diode-clamped multilevel VSC.
- The capacitor-clamped multilevel VSC

- **The H-bridge-based multilevel VSC**

The H-bridge multilevel VSC, Figure 2.7 known as well as cascaded H-bridge multilevel VSC consists of multiple converter modules connected together in series connection; with several DC sources isolated one from the other, the output from the modules is added together to have high power levels. Which might be seen as a disadvantage but on the hand the fact of having multiple sources may be exploited in connecting solar arrays (Guanjun, et al., 2008; Colak, et al., 2010) .

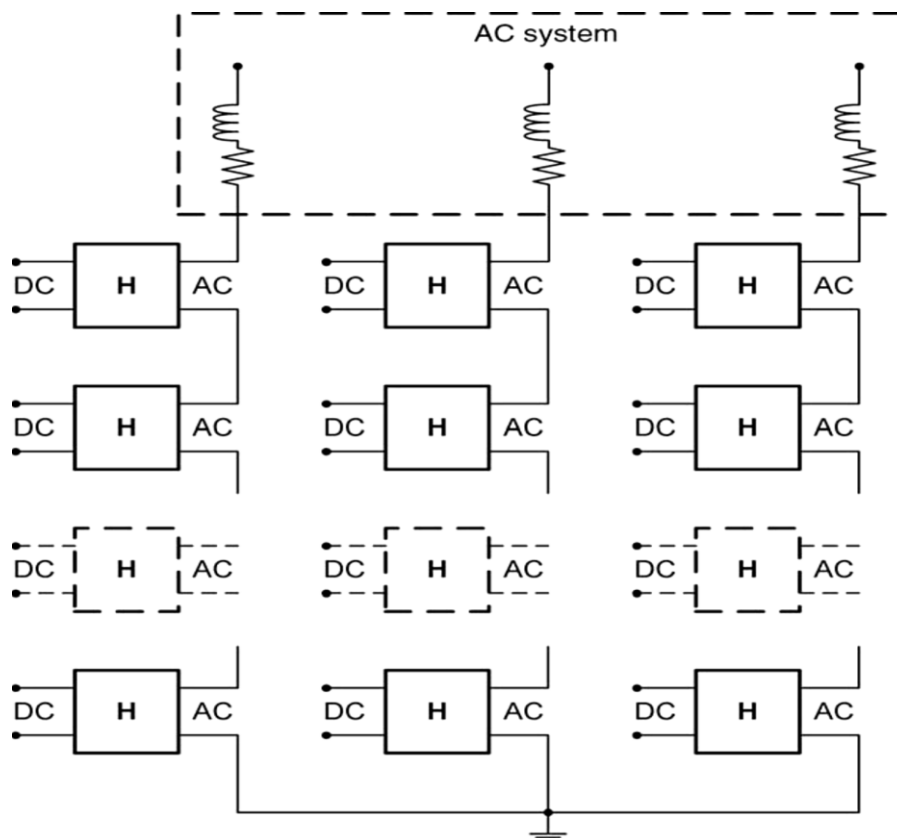


Figure 2. 7: H-Bridge based multilevel diagram (Amirnaser and Irvani 2010)

- **The diode-clamped multilevel VSC.**

Introduced by Nabae, Takashi, and Akagi in 1981 this configuration is derivation of two level converters with an addition of diodes that maintain the DC source voltage in order to achieve different steps in output voltage (Rodríguez, et al., 2002). The key role of the diodes is to limit the voltage stress across the switches. The concept consists of a series association of switches to achieve sinusoidal look output voltage. Figures 2.8 (a) and (b) represent a

schematic diagram of a single phase, three and five level diode-clamped converter respectively, also called the neutral-point clamped (NPC) inverter due to fact that the mid voltage level was taken as neutral point n . According to (Colak, et al., 2010), besides the three level, four to six level converters are as well in service. The higher the number of voltage levels, the higher is the quality of the output voltage and more closer to sinusoidal waveform, paradoxically the control circuit are more complex and more devices are needed: as for n number of level $(n-1)$ voltage sources or capacitors, $2(n-1)$ switching devices S_n and $(n-1)(n-2)$ diodes D_n have to be used (Bindeshwar, et al., 2012; Andersen, et al., 2002).

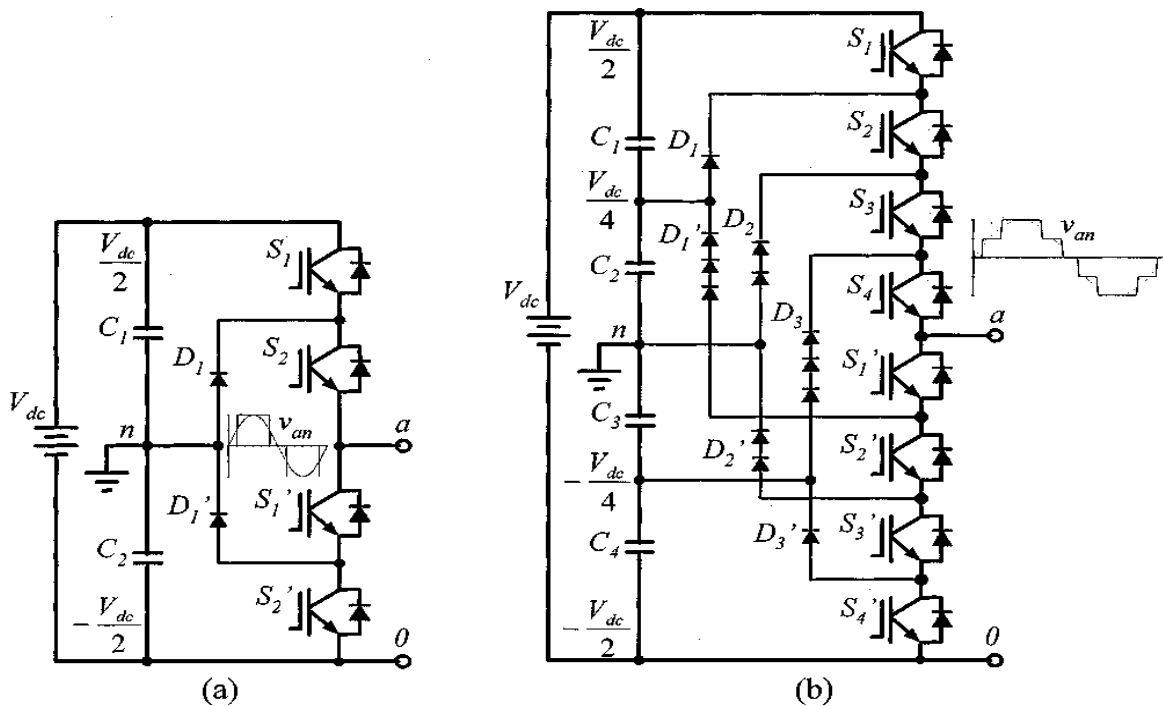


Figure 2.8: Diode clamped multilevel converter schematic diagram (Bindeshwar, et al., 2012)

- **The capacitor-clamped multilevel VSC**

The capacitor-clamped multilevel VSC is another configuration of multilevel converters which involves large size capacitors, with the advantage of reducing the need of filter or their size and the control on power flow real and reactive (Clark, et al., 1994). The number of capacitors used in this configuration is determined by the square of number of level intended. The configuration suits for industry drives applications not for HVDC ones (Arrillaga, et al., 2007).

2.3.4 PWM technology

Pulse width modulation method is one of different power control strategies used in a VSC-HVDC system; it allows the system to control independently the active and reactive power. The

PWM allows the AC output of voltages with fewer harmonics. Various PWM techniques have been developed to achieve an efficient control strategy, most popular are:

- Selective Harmonic Elimination PWM (SHE PWM).
- Space vector PWM (SVPM).
- Sinusoidal PWM (SPWM).

- **Selective Harmonic Elimination PWM (SHE PWM).**

Selective Harmonics elimination PWM technique was introduced in 1964 by Turnbull. Later on in 1970's it was perfected by Patel and Hoft for the thyristor based inverters. It was meant for lower order two and three levels inverter harmonic's elimination (Turnbull, 1964; Patel & Hoft, 1974). The method is now days applied to multilevel inverters.

SHE PWM concept is based on the devices switching time evaluation and the switching sequences such that the harmonics of certain order are suppressed from the synthesized output voltage waveform. This method is efficient in eliminating harmonics of specific order or harmonics in a specific band of frequencies (Sahali & Ferrah, 2003).

- **Space vector PWM (SVPM).**

The space vector PWM method is actually finding its way in power converters switching, during the last decade several works were published and it has been seen as the most efficient but on the hand is complex (Neacsu, 2001). SVPM is a digital technique consisting in developing pulses voltages based on space vector theory using Clarke transform as platform (Serrano, 1993). Compared to the other PWM techniques SVPM is getting more attention due to its efficient use of supply voltage and low harmonic distortion in both output voltage and current. But the merits it has got are shaded by the complexity associated to its circuit (Bose, 2002).

- **Sinusoidal PWM (SPWM).**

The sinusoidal PWM consists in a comparison between a sinusoidal (sine wave) signal with a certain low frequency and a carrier signal, triangular, with a high frequency. From this comparison converters switching pulses are generated (Acha, et al., 2002).

Sinusoidal PWM technique is widely used. Thanks to its less switching loss, simple implementation and other advantages compared to the other methods. The converter output frequency is controlled through the adjustment of the sinusoidal signal frequency while the magnitude of this sinusoidal or modulating signal is used to control the voltage output. Different variations of this technique, harmonic injection, third harmonic injection and multicarrier have been developed to match the converter's applications (Michael & Phoivos, 1988; Zhenyu, et al., 1997; Colak, et al., 2010)

2.3.5 VSC-HVDC systems control.

VSC-HVDC gained consideration over the classic HVDC due to its control abilities, like the independent control of both active and reactive power. Several methods are used to achieve this control. They can be classified into direct method or vector power angle control, vector current control and power synchronization control.

Power angle control is a direct method of power control consisting in controlling the VSC voltage phase angle which in turn will have direct effect on active power flow, while the reactive power is controlled through the variation of VSC voltage magnitude. This method is the easiest for implementation but it has a disadvantage of its limited control bandwidth and the lack of control over the current flowing into converter (Svensson, 1998).

Vector current control overcame the power angle control system's weaknesses of none control over the current flowing to the converter and limited control bandwidth. The current flowing to the converter is a huge concern as the VSC does not possess any over-current capability. To avoid the converter to be tripped during the disturbance, in cases of VSC grid connected, the current flow has to be well controlled.

The vector current control consist in control of the instantaneous active and reactive power independently using the fast inner current control loop, which in turn use the dq decomposition technique with the grid voltage as phase reference to achieve the control. The d component is used by outer loop to control direct voltage, while q component is used to control reactive power. The vector current based VSC are dominant in Adjustable Drives Inverters (ADS), and Doubly Feed Induction Generators (DFIG) wind turbines and all grid connected VSCs (Kazmierkowsk & Malesani, 1998; Svensson, 1998).

The vector control method has got merits over the direct method in that the vector current controlled VSC less suffer from the grid disturbance, inherent protection against over current and possibility of using the control to damp line harmonics and improve other quality issues (Abbey, 2007).

In spite the performances VSC based on vector-current control has got, there are some drawback that raise when connected to a weak A.C .grid ; like the low frequency resonances that may interfere with the fast inner current control loop, which limit the performances of the converter (Harnefors, et al., 2007).

Power synchronization control was developed with the idea to overcome the drawbacks the vector control has shown while connected to the weak ac system. The method consists in the use of the ac network internal synchronization mechanism. This method has got some similarity with the power angle control method in the way of using power angle and voltage magnitude for the active power and reactive control, but it differs from the other methods in the no use of Phase Locked Loop (PLL) (Zhang, et al., 2010).

2.3.6 HVDC cables

The earlier HVDC cables were made for the submarine power transmission connection of two or more power systems separated by a sea. With actual trends of power demand, the most of the load centers being the already densely populated areas and more to that the saturation of the existing infrastructures to carry the supplement of energy needed; the only option remaining is the use of underground HVDC cables to deliver power to those areas. The recent introduction of VSC-HVDC will increase the use of HVDC cables. The advantages that HVDC cables have got, like less eddy current losses, are shaded by the temperature dependence of its insulation.

For HVDC cables, different types of cables have been developed; and they may be classified, according to their insulation technology, into three types namely Mass impregnated (MI), self-contained fluid-filled cables (SCFF) and extruded cables.

A. Mass Impregnated cables

The mass impregnated cables are composed of copper or aluminum conductor, insulated with special paper impregnated with high viscosity compound. They are the mostly used in submarine transmission since 50's. With the ability to carry 500 kV/DC and conductor up to 2500 mm² cross section, these cables are reliable for long bulk power transmission (Benato, et al., 2010).

The mass impregnated HVDC cables, Figure 2.9, are either used in submarine or underground systems. They are furnished most of the time with the polyethylene sheath, as protection in case of underground system. For land installations, only armoring is provided when high pulling tension are involved. Due to transportation constraint related to the size of the cable up to 1000m may be installed without joint in land application. In submarine installations on other it is possible to realise quite long continuous distances with less joints. normally MI cables are rated to operate to up to 55°C of conductor temperatures. Recently a novel insulation technique in HVDC using paper polypropylene laminate (PPL) increased the maximum conducting temperature to 85°C and the transfer capability to 600 kV (Gianluigi, 2013)

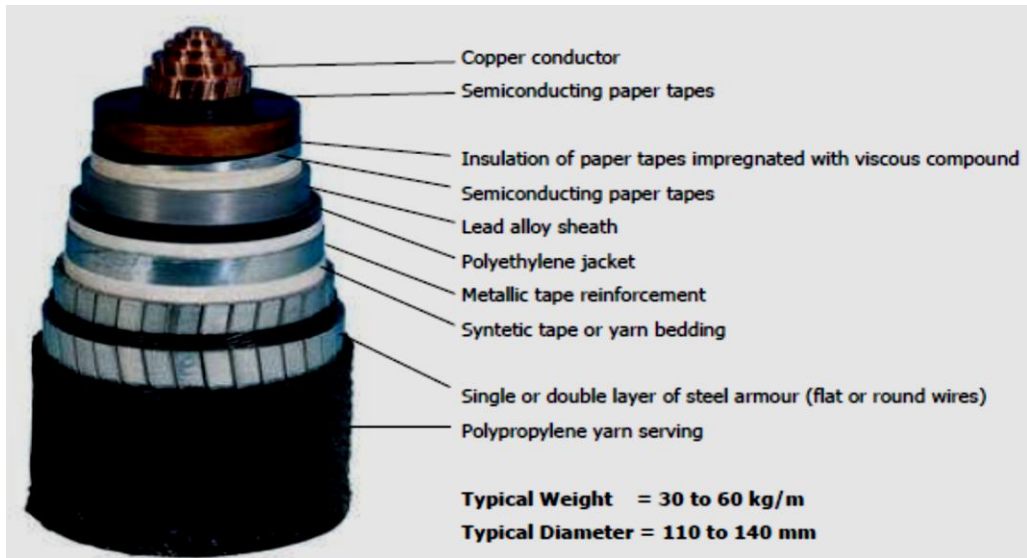


Figure 2. 9: Mass impregnated HVDC cable (Europacable, 2011)

B. Self-contained fluid-filled cables (SCFF)

These types of cables were introduced to improve the mass impregnated cables challenges. Those challenges are mainly the risk of creation cavities into cables insulation due to the rapid changes in temperature. Those cavities in turn will give raise to partial discharges within the insulation, thus untimely aging of the cable. Figure 2.10 shows a self-contained fluid cable, it consists of a single core structure with a fluid channel, oil impregnated paper and the protection all around .The oil in the channel maintains paper insulation pressure. The fluid used is either a gas or oil. Nitrogen is used in case of the gas insulation; it is filled into the conductor through hole inside the conductor. While for the oil, pressurized low-viscosity oil is used (Chan-Ki, et al., 2009).



Figure 2.10: Self-contained fluid filled cable (Europacable, 2011)

Self-contained fluid filled cables can normally be used in high voltages up to 600 kV DC but for short distances in order to maintain fluid pressure constant during thermal transients. The SCFF cables presently transmit up to 500 kV DC with a conductor cross section of 3000 mm² (Ernesto, 2009) . Although this type of cables has got merits, on the other hand there is concern of accidental leak results of environment effects, manual intrusions, manufacturing defects, etc. The leak would be of huge ecological impact for environment. Several researches have been done but so far none of the leak detection methods developed is reliable (Hao, et al., 2010)

C. Extruded cables

The HVDC use of extruded cables was challenged by the space charge build up within the insulation due to the constant DC voltages, resulting in partial discharges. Nowadays with on-going research the extruded cables have found applications with VSC-HVDC based transmission, particularly when bipolar mode is involved (Marzinotto & Mazzanti, 2011).

Extrude cable for HVDC applications, Figure.2.11, has as got some advantages over the mass impregnated like being lighter ,flexible and ability to use prefabricated molded joint make the extrude cables affordable than masse impregnated one for long land cable application (Bahrman & Brian, 2007). According to Ernesto (2009) the extruded cable can withstand, when used in VSC-HVDC transmission based, up to 300kV DC and 800 MW of power transfer.



Figure 2.11: Extruded cable for HVDC applications (Europacable, 2011)

2.3.7. HVDC protection

The protection system is the major part in any power system, the localization and the isolation of the fault source is the key role, especially in the HVDC system where expensive and very sensible devices are involved. The classic HVDC transmission system protection is different from the VSC-HVDC: the latter transmission system is based on voltage source converter where the over current is the main protection concern, while for the current source converter

(CSC) based classic HVDC there is no such concerns due the fact that the currents are regulated by large smooth converter thus making the system robust to short circuit currents (Jin, et al., 2010).

The basic faults likely to rise in an HVDC system are:

- Positive line to ground fault.
- Negative line to ground fault.
- Positive line to negative line fault.
- Overcurrent.
- Overvoltage.

For the VSC-HVDC system the line to ground fault are rare because the underground cable are used. Beside improper installation, cable aging and failure of insulation due to the environment nearby the cables, the human activity may harm the cables. The accidental damage to the buried cable during the construction activities is the most likely to happen. The fault may rise at the instant or later as the damaged insulation will lead to the failure of the insulation and causing the current to short cut to the ground. For the converter connected to an AC source. A damaging Overcurrent demand appear within the converter (Jie, et al., 2010)

2.4. HVDC transmission technologies comparison

As discussed in previous sections High Voltage Direct Current transmission is divided into two technologies namely the HVDC classic, which is based line current commutation and HVDC based on Voltage Source Converter (HVDC-VSC). Each technology has certain advantages over the other the depending onto circumstantial needs and requirements, Table 2.2 below gives a comparison of their features. As it can be seen VSC-HVDC has got a lot of advantages in terms of power flow control, voltage regulation as well the fault ride through capability. Thus, the preference of this Voltage Source Voltage high voltage direct current (VSC-HVDC) for grid connected renewable power plant.

Table 2. 2 HVDC classic and HVDC-VSC comparison (Chaudhary, et al., 2008)

		LCC-based HVDC	VSC-based HVDC
1	Size range single convertor	150 – 1500 MW	50 – 550 MW
2	Convertor/Semiconductor technology	Line commutated, Thyristor	Self commutated, IGBT
3	Relative volume	4 – 6 times	1
4	Type of cable	Mass Impregnated Paper Oil/Paper	XLPE
5	Control of active power	Yes	yes
6	Control of reactive power	No (only switched regulation)	Yes, continuous control
7	Voltage control	Limited	Extensive
8	Fault ride-through	No	Yes
9	Black start capability	No	Yes
10	Minimum short circuit capability in AC grid	>2.0 x rated power	No requirement
11	Power reversal with-out interruption	No	Yes
12	Generator needed on off-shore platform	Yes	No requirement
13	Minimum DC power flow	5-10% of rated power	No minimum DC power
14	Typical losses per convertor	0.8%	1.6%
15	Operating experience	> 20 years	8 years
16	Operating experience off-shore	No	Yes

2.5 Summary

This chapter provides an overview of High Voltage Direct Current transmission. A short history is given; characteristics and applications of different HVDC technology are discussed. An emphasis is made on VSC-HVDC transmission system, a literature review of working principle, challenges, components, and control theory are provided.

CHAPTER THREE

INDEPENDENT POWER PROVIDERS

3.1. Introduction

The Independent Power Providers (IPP) concept was introduced by the reforms in electricity market, as discussed in Chapter 1. Most of those IPPs are in renewable energies such solar, wind and small hydro power.

In this chapter, renewable energy technologies for electrical power generation that are used by IPPs are discussed. Focus is made on wind and solar energy.

3.2. Wind energy

The wind energy has been in use for the human kind, since ancient civilization around 200 B.C, in Persia, for grinding mills. Later in 13th century AD the wind mills sprint all over Europe (Mathew, 2006). Among the green energy available now, the wind has been of huge of importance to human kind all along the civilizations, from milling grain, pumping water to propelling ships. And by now is continuing to serve by producing the electrical power. According to Dr. Gary L. Johnson (2001) the first production of electrical power by the wind was in Denmark in 1890.

3.2.1 Wind generation.

The wind energy is used for a long time in farms to grind grains or pump water in the form of a wind mill. The principle is to convert the kinetic energy from the wind to the mechanical energy. This principle is applied to the wind energy in the power system. A wind turbine captures the kinetic energy from the flowing air and changes it to the mechanical energy. A generator installed in the wind turbine converts the mechanical energy to the electrical energy. As shown in Figure 3.1, the kinetic energy of the wind turns the rotor blades of the wind turbine. This results in revolving of the shaft of the generator, which is mounted on the rotor blades. The generator converts the mechanical energy from the rotating shaft to the electrical energy. The power cable transmits the electrical power to a transformer. The transformer steps up the generated voltages before being transmitted.

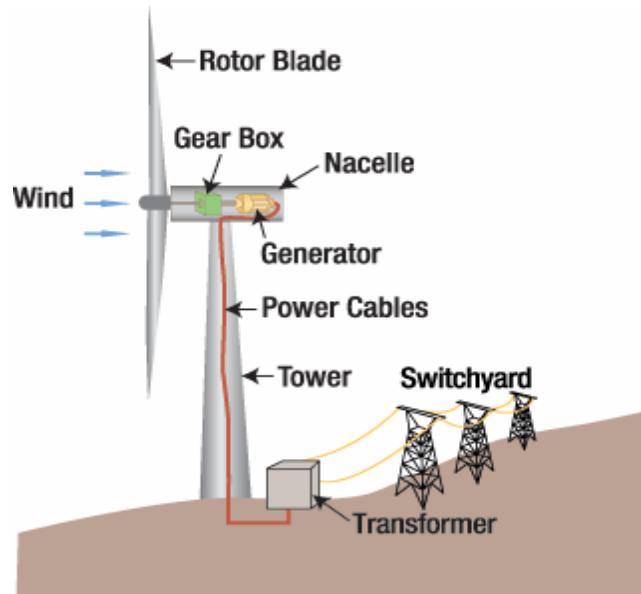


Figure 3. 1 Wind power generation (TVA, 2011)

1. Wind turbine

The wind turbine is an important feature in the wind generation, as it is the one which transfer the kinetic energy of the wind to the generator in the nacelle. The wind turbines are of different types and they are classified according to their rotor rotation axis orientation: vertical and horizontal wind turbines (EERE, 2011). As it can be seen on Figure 3.2, of the different types of vertical wind turbines, the rotor axis is vertical.



Figure 3.2. a) Darrieus winds turbine

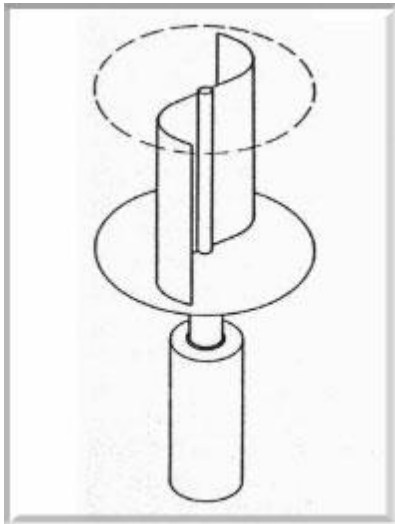


Figure.3.2 b) Savonius wind turbine



Figure 3.2 c) H-rotor wind turbine

Figure 3.2 Vertical wind turbines (squidoo, 2012)

Modern vertical wind turbines started by Darrieus turbine but later, faces problem of power controllability, however their low cost installation and maintenance encourages researches in their amelioration. Through the progress H-rotor and Savonius turbines did see the day. While keeping their low maintaining cost and they still have a low efficiency for them to be used as large electricity generators. Only the Savonius turbines are currently in use for water pumping with 25% power efficiency. The vertical wind turbines are built with two or three blades (Eric, 2006).

The horizontal wind turbines are more popular type of wind turbines, Similar to the vertical wind turbines, the horizontal wind turbines can be built with two or three blades. As it can be seen on Figure 3.3, the horizontal wind turbine has a control system that controls the speed of rotor. The anemometer measures the wind speed and transmits the data to the controller. The pitch angle of the rotor blades is controlled by the controller to attain the maximum wind power and to limit the mechanical power in case of the strong wind. The rotor blades are pitched to decrease the angle of attack from the wind when the rated power is reached. The yaw drive can turn the wind turbine compartment or so called nacelle according to the direction of the wind vane

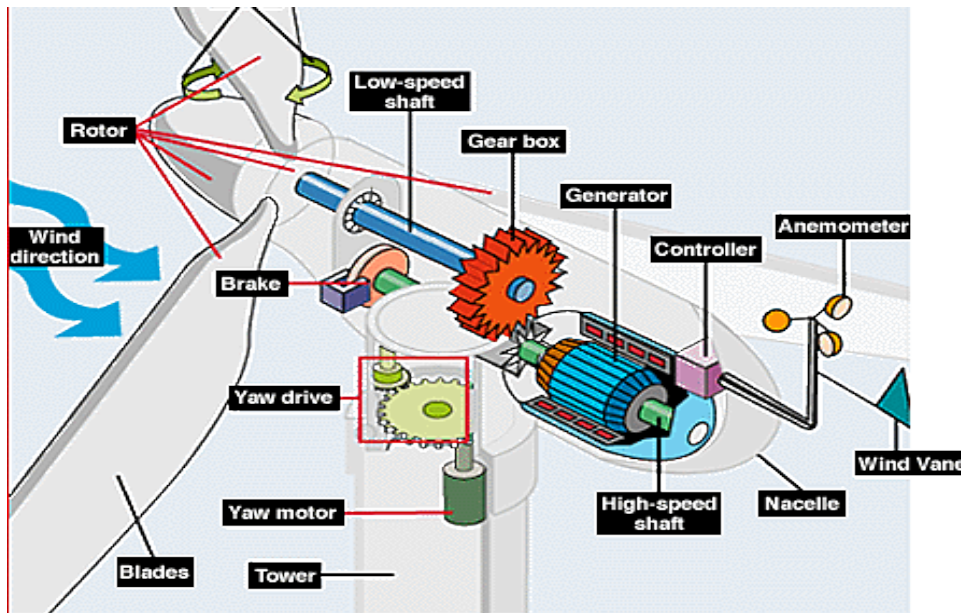


Figure 3.3: Horizontal wind turbine (EERE, 2011)

In addition to the pitch control, the maximum power from the wind can be limited by passive stall control for small and medium-size wind turbines. The stall control avoids the rotation of the blades. Contrarily to the pitch-angle control, passive stall control has fixed pitch-angle rotor blades. The passive stall control relates to the design of the rotor blades that leads to turbulence or so called stall on the back of the blades to reduce the power extracted from the wind. As the capacity of wind turbines is increasing, active stall control is used for large wind turbines. The active stall control is similar to the pitch-angle control. The rotor blades are rotated to obtain the maximum power extract. When the extracted power reaches the rated power, opposite to the pitch-angle control, the active stall control turns the rotor blades to increase the angle of attack from the wind to provoke the turbulence (Ragheb, 2009) .

Wind turbines can be distinguished into 2 categories, fixed speed and variable speed wind turbines. The fixed speed wind turbines are connected directly to the utility grid and operate with the synchronous speed of the grid angular frequency regardless of the wind speed. The fluctuations in the wind generate mechanical stresses to the generator. Furthermore, since the wind generation system is connected to the utility grid directly, the fluctuations of the wind appear on the electrical side. The variable speed wind turbines operate in an opposite way. The speed of the generator is varied according to the wind speed solving the problem of the mechanical stresses. As a result, the output voltages of the generator have variable amplitudes and frequencies. Hence there must be a grid interconnection to convert the variable magnitude and frequency voltages of the wind turbines to the synchronous frequency of the supply grid. The indirect connection with the grid interconnection reduces the problems caused from the mechanical stresses(Manwell *et al*,2009; Tong, 2010).

2. Wind power energy

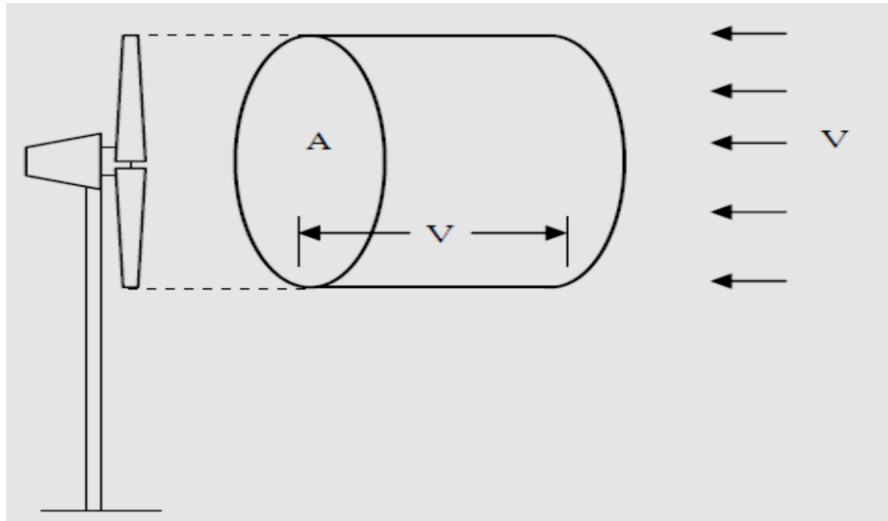


Figure 3. 4: Air stream moving towards a turbine (Sathyajith, 2006)

The wind energy consists of converting, by turbines, the kinetic energy of the mass of wind into mechanical energy then into electrical energy by means of generators. The kinetic energy carried by the mass of wind and flowing at speed V crossing the wind rotor with cross section area A , as shown on Figure 3.4, will be described by energy Equation (3.1) (Sathyajith, 2006):

$$E = \frac{1}{2} \rho_a v V^2 \quad (3.1)$$

where ρ_a is the density of air and v is the volume of air parcel available to the rotor. The air parcel interacting with the rotor per unit time has a cross-sectional area equal to that of the rotor (A_T) and thickness equal to the wind velocity (V). thus the energy per unit time, that is power P , can be expressed as:

$$P = \frac{1}{2} \rho_a A_T V^3 \quad (3.2)$$

As it can be seen from Equation (3.2) of power, there are various factors involved in power stream of wind transmitted to the turbine, but the most prominent factor deciding the power available into the wind stream is the velocity (Bianchi *et al* 2007).

3.2.2 Wind Turbine Generators

The currently on market available utility size wind turbine generators model can be grouped into four categories according to the generation technology used inside (Vijay & Ayyanar, 2012):

1. Fixed speed wind turbine generator, based on squirrel cage generator (FSGT).
2. Limited variable speed wind turbine generator, based on wound rotor induction generator.
3. Variable speed with partial scale frequency converter known also as double fed induction generator (DFIG).
4. Variable speed with full scale frequency converter or permanent magnet synchronous machine (PMSG).

1. Fixed speed wind turbine generator.

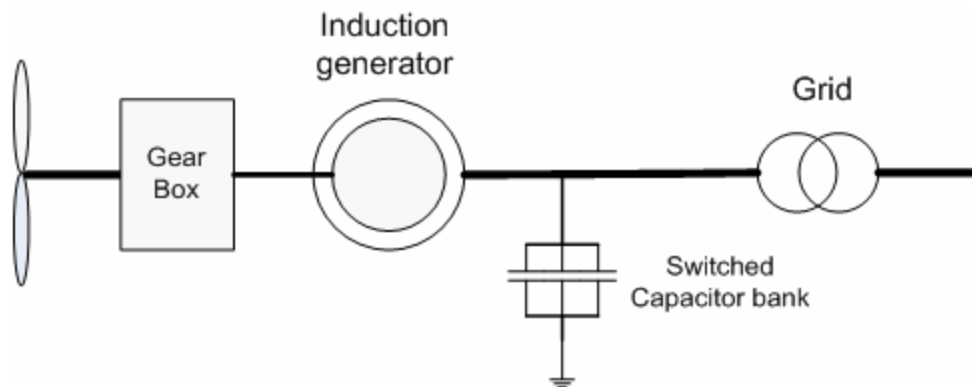


Figure 3. 5: Fixed speed squirrel cage induction generator (Vijay & Ayyanar, 2012)

Fixed speed wind turbines incorporate both squirrel cage induction generator (SCIG) and wound rotor induction generator. As it is shown on Figure 3.5 the turbine is directly connected to the grid through a step-up transformer and in parallel with capacitor bank providing the reactive power compensation. The system is cheaper on one hand, but the on the hand when connected to grid high inrush current develops during start up. Although a soft-starter, thyristor based, is used as mechanism to prevent those current by providing a smooth start-up, any wind fluctuation would result into the fluctuation of the mechanical torque and the electrical power. While the mechanical torque fluctuations cause high mechanical stress, the electrical power fluctuations lead to voltage fluctuation and flicker effects in the case of weak grids. Such wind turbines use stall control, pitch control, or active stall control (Hansen, 2005).

Stall controlled turbines also known as type A0, they are simple, economical and robust on one hand and on other hand they do not have control of the power during the connection sequence. The pitch controlled turbines, known as well as type A1, resolves the power controllability

problem and allowing controlled start up and emergency stopping. However it suffers of loss of control during the high wind speed because the pitching mechanism time response is too high to follow the sudden change in wind speed thus the power generated fluctuations. An active stall controlled turbine, type A2, are trying to overcome the previous drawbacks of stall and pitch control by basically maintaining all the power quality characteristics of the stall-regulated system. Active stall control and pitch mechanism combination and flexible coupling of the blades to the hub result in an improved overall system, allowing emergency stopping and startups; but also in high cost system. (Bianchi, et al., 2008; Hansen, 2005)

2. Limited variable speed generator

The configuration of limited variable speed is like the same as for the fixed speed generator, the only difference reside into the introduction of a variable resistor into the rotor. The resistance is controlled by a power converter. The generator is directly connected to the grid. A capacitor bank performs the reactive power compensation. A smoother grid connection is achieved through a soft-starter.

The variation of rotor resistance allows control the speed, between 2 to 5%, therefore the output power in the system. The method is also known as dynamic slip control. (Frede & Chen, 2006).

3. Variable speed with partial scale frequency converter

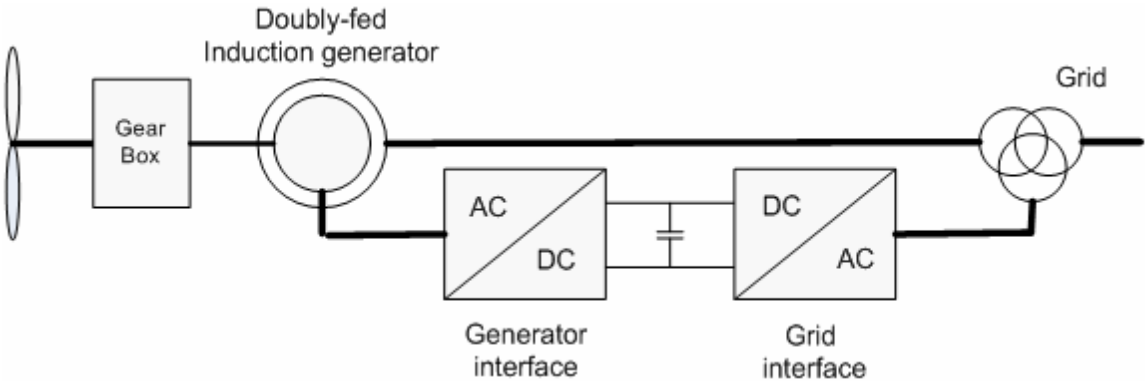


Figure 3.6: Double fed induction generator (Vijay & Ayyanar, 2012)

Known also as double fed induction generator , DFIG system, Figure 3.6, consists of a Wound Rotor Induction Generator (WRIG) with the stator windings directly connected to the constant frequency three-phase grid and with the rotor windings connected via slip rings to grid through a partial scale frequency voltage source converter, 30% of the generator power rating. The generator rotor is able to run at variables speed, typically between -40 to +30% of the synchronous speed, which makes the system able to run either in sub or super-synchronous

mode. During the super-synchronous mode the power is delivered to the grid through both rotor and stator, while the reverse is observed when running in sub synchronous mode. The stator is connected directly to the grid via the step up transformer, The double feed induction generators are the most adopted in MW wind power generation. The reason is the many advantages associated with them such as, the ability to support the grid during the disturbance or for voltage regulation by feeding or taking the reactive power, no need of soft starter and no reactive compensation. More than 60% of the installed worldwide wind turbines are of this type (Qiong-zhong, et al., 2011; Rechsteiner, 2008), this is due to the less cost compared to the permanent magnet one and to the short comings of the previous generator at fixed speed.

4. Variable speed with full scale frequency converter or permanent magnet synchronous generator (PMSG).

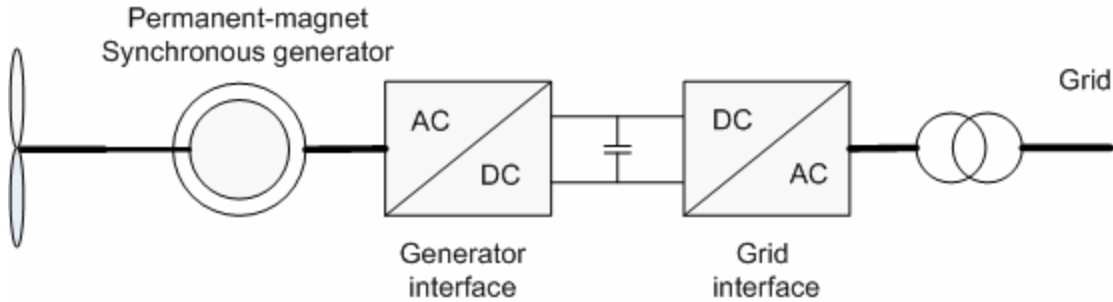


Figure 3.7: Permanent magnet synchronous generator with full scale converter (Vijay & Ayyanar, 2012)

The permanent magnet synchronous wind generator system, Figure 3.7, consist of full power converter acting as the turbine interface to the grid. The AC power from the generator is converted by a back to back converter, before being sent to the grid via a step up transformer. The rotor is a permanent magnet and not gear box are used. Thus the turbine is running at low mechanic speed which requires multi pole in order to remain within synchronous speed. The drawback of the multipole concept of the PMSG generator is the increase in the size of the turbine, in order to accommodate the large number of poles. But on the other hand the omission of gearbox reduces the weight, losses, and costs and maintenance demands of the turbine and increases the efficiency making it more better compared to the other variable speed wind generator types (Polinder, et al., 2005; Grauers, 1996).The full scale back to back voltage source converter connecting the turbine generator to the grid gives a full controllability of the system. Besides the full controllability of the system allowed by the full scale converter , this

latter decouples the generator system from the grid hence allowing the fault ride through and grid support to be simple to perform (Muller, et al., 2002; Pena, et al., 1996).

5. New wind turbine category

With now day's trends for green energy the research and development of new model or the optimization of the existing ones is the priority of the many manufactures of wind turbines technologies. The new wind turbines configuration have started seeing the day like, multibrid ,clipper, voithdrive and windflow configurations (Thomas, 2012)

A Multibrid concept is the combination of the variable speed permanent magnetic synchronous wind generator concept with a gearbox and the fixed speed wind generator without the gearbox. A planetary gear or a single stage gearbox is used instead of three stage standard gearboxes and with the stator of the PMSG they are both incorporated directly into the machine housing while the rotor is connected to the output of the planetary gear box. The stator is connected to the grid via converter. Multibrid wind turbines generator system is developed by Areva and seen as promising in future (Roberto, et al., 2011)

Clipper configuration consists in into the splitting of one big Permanent magnetic synchronous generator into four small size generators. The ideal is the continuous service of the turbines even during the failure of one all more generators within the turbines. This is achieved through the overall control of the turbine. Yet the power deliver during the failure of generator is less but the turbine will not be tripped off the grid (Thomas, 2012; Thresher & Laxson, 2006)

Voith concept is a full variable speed wind turbine with synchronous generator combined with a novel drive train known as WinDrive. These latter acts as a torque balancing device which converse the variable input speeds from the turbine into the constant speeds output connected to the synchronous generator. The variation of the rotor speeds, result of wind speeds variations; do not affect the synchronous generator which runs at constant synchronous speed. Therefore, the elimination of frequency converter (Jamieson, 2011).

Wind flow configuration it is a two blade turbine running at limited variable speed. The limit is imposed by a torque limiting gearbox. It absorbs the variations in the turbine rotor speed and same time driving the generator at constant. The synchronous generator running at a constant speed, it is directly connected or synchronized to the grid without the need to interface power electronics devices.

The double fed induction generator wind turbine is the preferred turbine currently on the market but the main disadvantage of it is the existence of slip ring brush, where the idea of developing a new model of DFIG with no brush, the same idea is being applied to the double fed reluctance

generator. However this technology is still on technical stage and they need a complex control. Table 3.1 (Hyong & Dylan, 2010), is showing the advantages and disadvantages of each type of 4 type plus the new derivatives of double feed generators.

Table3. 1: Wind turbines technologies comparison (Hyong & Dylan, 2010)

Generator Concept (Type)	Advantages	Disadvantages
SCIG (FSWT)	<ul style="list-style-type: none"> • Easier to design, construct and control • Robust operation • Low cost 	<ul style="list-style-type: none"> • Low energy yield • No active/reactive power controllability • High mechanical stress • High losses on gear
PMSG (VSWT-FSPC)	<ul style="list-style-type: none"> • Highest energy yield • Higher active/reactive power controllability • Absence of brush/slip ring • Low mechanical stress • No copper losses on rotor 	<ul style="list-style-type: none"> • High cost of PM material • Demagnetisation of PM • Complex construction process • Higher cost on PEC • Higher losses on PEC • Large size
WRSG (VSWT-FSPC)	<ul style="list-style-type: none"> • High energy yield • Higher active/reactive power controllability • Absence of brush/slip ring • Low mechanical stress 	<ul style="list-style-type: none"> • Higher cost of copper winding • Higher cost on PEC • Higher losses on PEC • Large size
DFIG (VSWT-PSPC)	<ul style="list-style-type: none"> • High energy yield • High active/reactive power controllability • Lower cost on PEC • Lower losses by PEC • Less mechanical stress • Compact size 	<ul style="list-style-type: none"> • Existence of brush/slip ring • High losses on gear
BDFIG (VSWT-PSPC)	<ul style="list-style-type: none"> • Higher energy yield • High active/reactive power controllability • Lower cost on PEC • Lower losses by PEC • Absence of brush/slip ring • Less mechanical stress • Compact size 	<ul style="list-style-type: none"> • Early technical stage • Complex controllability, design and assembly • High losses on gear
BDFRG (VSWT-PSPC)	<ul style="list-style-type: none"> • Higher energy yield • High active/reactive power controllability • Lower cost on PEC • Lower losses by PEC • Absence of brush/slip ring • No copper losses on rotor • Less mechanical stress • Easier construction 	<ul style="list-style-type: none"> • Early technical stage • Complex controllability and rotor design • High losses on gear • Larger size than DFIG

From the table 3.1 we can set the comparison using the criteria common to all the type above, like the energy yield, reliability, cost, grid support and availability on the market. The Permanent Magnet synchronous Generator (PMSG) has high energy yield but with the drawback high cost of power converter, while the squirrel cage induction generator (SCIG) is cheaper but with low yield energy, due to its fixed speed, compared to PMSG between 10 and 15%less (Anders, 1996).

According to Hyong and Dylan (2010) the squirrel cage synchronous generator(SCIG) in terms of cost is the cheapest and the wound rotor synchronous generator(WRSG) has the highest cost.In terms of reliability the Double fed induction generator (DFIG) is suffering from its brushes and slipping which are subject of possible failures but on the other hand eventhough the DFIG can not fully support the grid ,due to the stator that absorbs the fault effects from the grid.The brushless double fed induction generator (BDFIG) and brushless double fed reluctance generator (BDFRG) overcame the handicap during the disturbance or fault operation of the grid (Shao, et al., 2009; Jovanovic, 2009) .The DFIG , SCIG , WRSG and PMSG are the currety on market turbines, with high share of DFIG.

3.2.3. Wind turbine control

The control of wind turbine is required in order to achieve full performance operation. The control system provides a safe operation, optimized power output and long structural life which in turn ensure the low maintenance costs. The wind turbine system is composed of different parts that are interacting to produce electrical power output. As shown in Figure 3.8, the wind turbine can be looked at from three different angles or aspects, which are aeronautical, mechanical and electrical aspect.

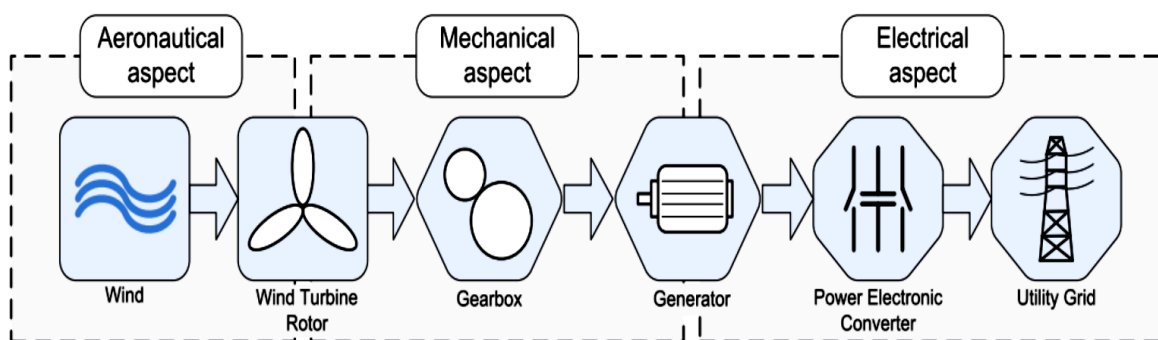


Figure 3.8: Wind energy conversion system (Hyong & Dylan, 2010)

The control of wind turbines involves the combinations of all three aspects and they intercommunicate each for an efficient operation of the turbine. The turbine power output is determined by the rotational speed of turbine, directly proportional to wind speeds. The control is needed to control or to limit the input aerodynamic power to the wind turbine. The methods

mainly used for this control which is known also as aerodynamic power control are stall, pitch and active stall. Stall control concept is that during the high wind speeds, the blades are set to stall and then there is no need of pitch mechanism (Burton, et al., 2001).

The pitch control concept is to affect the turbine rotational speed by turning the turbine blades around their longitudinal axis. During the high speed winds, the output power of the generator start becoming too high in reference to the rated power, the turbine electronics controllers will slightly pitch the blades out of the wind. Thus reducing the power performance coefficient and in turn the rotational speed of the turbine. The reverse is done during the drops of wind the blades are turned back towards the wind, at an angle that maximizes the wind power capture. The pitching action takes place all along the rotation of the turbine, which do make the synchronization of blades angles adjustment complex. Electrical and hydraulic actuators are used in pitching of blades. Almost all variable-speed wind turbines use pitch control (Johnsson, 1985; Marian, et al., 2002).

Active stall turbine control is a stall controlled with variable pitch angle that can be controlled till the stall angle. In order to limit the output power during the high speed winds, the active stall controlled turbine is set in the way that during the low speed, it will act as a conventional pitch controlled turbine. The power output is almost at maximum independently of the prevailing wind speeds and without overloading the drive train of turbine (Marian, et al., 2002; Florin, et al., 2005)

3.2.4. Wind power plant

A wind power plant or wind park consists of a group of tens or up to few hundred wind turbines in the same location aggregated to generate high power. They can be onshore or offshore, but the offshore wind farm generates more stable power than onshore wind farm because the wind speed offshore is higher and steadier. Figure 3.9 shows an onshore and offshore wind farm. The power produced may be feed into grid or not. In the latter case, we say a stand-alone system. The turbines in farm are spaced with a distance equal to three times of their rotor radius, one from each other in order to avoid the turbulance from one turbine blades to affect the other nearby turbines.the same is applied to the row of turbines ,where the interspacing might be 10 times turbine diameter (Sathyajith, 2006).



Figure 3.9 a) offshore wind farm



Figure 3.9 b) onshore wind farm

Figure 3.9 : Wind farm (Sathyajith, 2006)

The total power output of a wind farm is the contribution of every individual turbine in the farm. The turbines are connected together through a network of cables, step up transformers, switching equipment, protection relays and feeders before their output to be sent into the grid. This collection system is configured by selecting and routing the cables with respect to reliability in terms of redundancy, protection system, fault location and service restoration system. There are three types of network configuration or feeder topology that have various redundancy schemes: Radial, ring and star network or configuration (Müfit, et al., 2011).

A radial configuration, Figure 3.10, consists in connecting the feeder to each wind turbine in one continuous string until the last turbine. The main advantage is the configuration is economic as the cost of cables is low due to tapering between the turbines. But on the hand the system present a poor reliability as any fault on cable or switch gear fault on hub end results in an interruption of power delivery of the entire row. Despite the reliability handicap the radial system is popular especially in offshore and land-based wind park (Sheng & Vassilios, 2010).

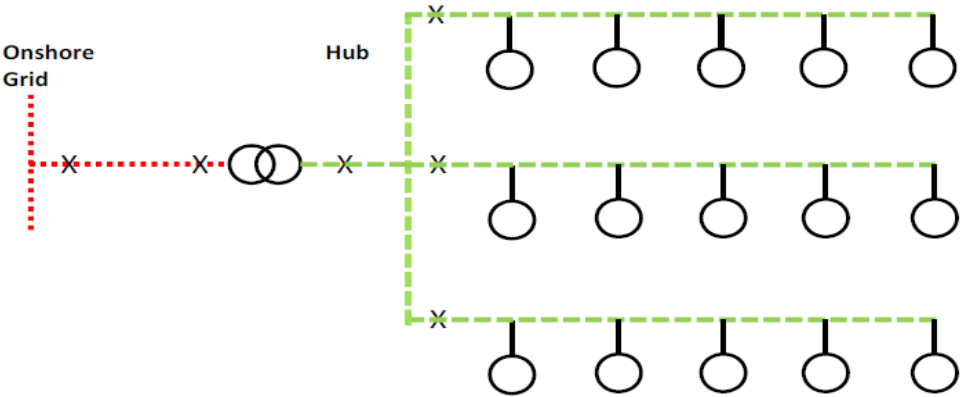


Figure 3.10: Radial configuration system (Himanshu, et al., 2012)

The ring configuration, Figure 3.11, is a realised by providing a redundant way for every turbine on the row, instead of one way to the hub. Thus more reliability is gained, but at an extra cost of high rated and long cables. More variations of ring configurations are like double sided, multiple hub ring configuration (Twidell & Gaudioisi, 2009)

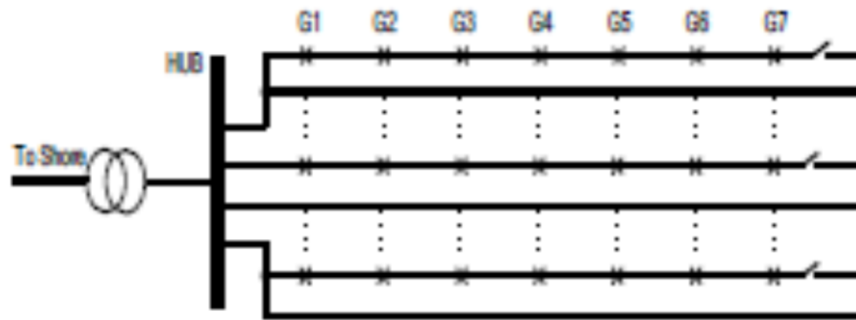


Figure 3. 11: Ring configuration system (Sheng & Vassilios, 2010)

The star topology Figure 3.12 provides high reliability at low cost, in terms of reducing the cable ratings. All the turbines are feeding in a central point which in turns connects to the hub .the long radial cables connecting the turbines to the central collecting point are rated to the turbines output, while short, high rated cables are used to connect to the hub. This configuration use complex switchgear at the wind turbine, which increases the cost the configuration (Wang & Li, 2009; Himanshu, et al., 2012)

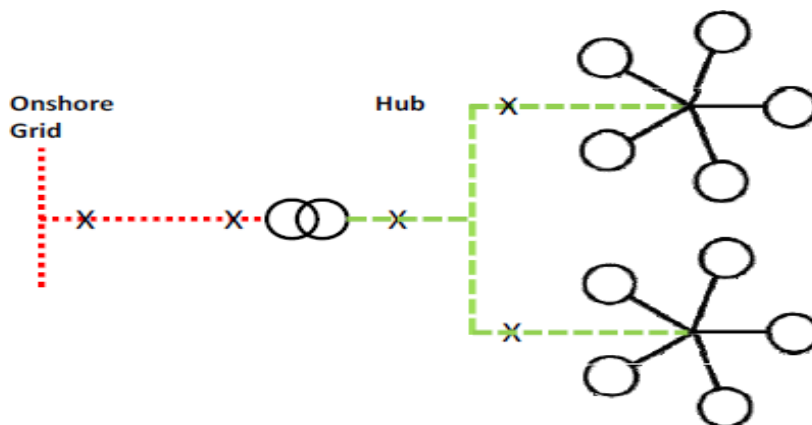


Figure 3. 12: Star system configuration (Himanshu, et al., 2012)

3.2.5 Wind farm grid connection

The wind speed is different in each location of a wind farm, meaning that the wind turbine rotor blades rotate following the wind speed in their vicinity. Power produced depending on the wind speed, in the wind farm variable magnitude and frequency outputs are observed. Thus a direct connection to the grid is not feasible, rather power electronics interfaces are used to connect turbine. The power from different turbines in the farm has to be summed together before being fed into the grid. Figure 3.13 shows a group and individual connection of wind farm, with the group connection the variable speed concept is no longer since all wind turbines are connected to one converter. Hence they must operate with same speed. Differently, the individual connection supports the concept of the variable speed. Moreover, this type of the connection

provides reliability to the power system since only one converter is crucial, which is the grid-side converter. When one of the rotor-side converters is out of operation, other wind turbines can supply the power. For the group connection, both converters are critical. An eventually fault in either converter results in failure of the wind power plant (Blaabjerg & Chen, 2006).

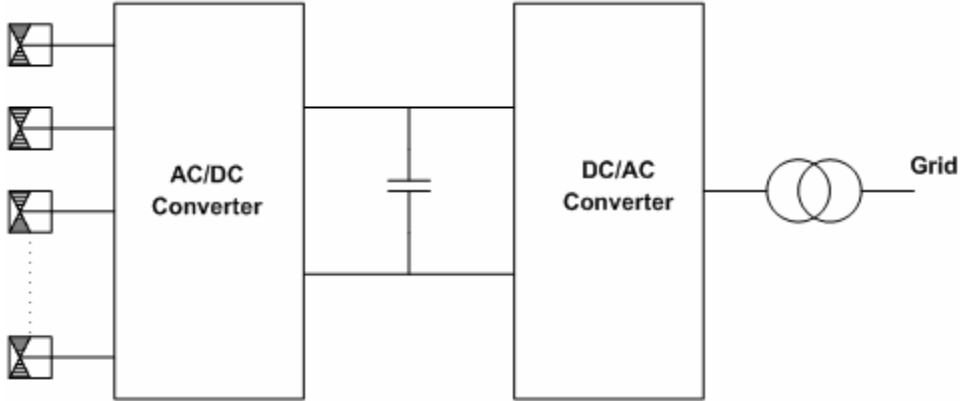


Figure 3.13 a) Group connection

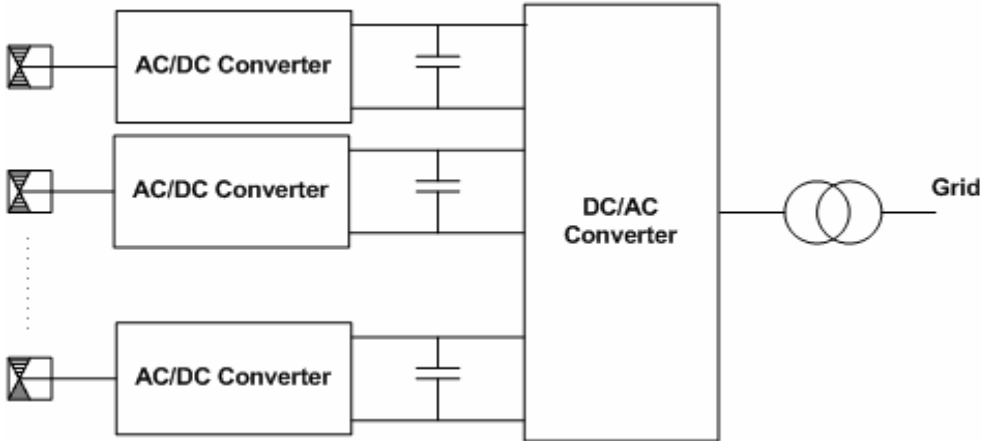


Figure 3.13 b) Individual connections

Figure 3. 13: Individual and group connection of wind farm (Blaabjerg & Chen, 2006)

3.2.6 Grid requirements for the Interconnection of Wind Farms

The integration of large scale wind farms into the grid has severe impacts on the power system operation (EL-Shimy, et al., 2008). Normally, wind turbines were not required to participate in frequency and voltage control; but with their increasing integration in the grid in recent years, wind farm performance in the power system has gained attention. Consequently, some grid codes have been set to specify the steady state and dynamic requirements that wind turbines and wind farms must meet in order to be connected to the grid (Chen, 2005).

Many countries have set different criteria through the grid codes for the wind energy integration into the grid (Willi & Johnsen, 2006). Among the common criteria for the grid interconnection: voltage control, reactive power control, frequency control and fault ride through capabilities.

Voltage control is important as the utility and customer equipment are designed to operate at a certain voltage rating. However the wind power has a characteristic of voltage variations, which made the grid to allow the wind a certain range of voltage variation in respect to the grid or to the point of connection voltage (Ackerman, 2005). The range depends on the duration of variations either for a long or limited period of time. For nominal continuous operation the variations is generally set to $\pm 10\%$ of the nominal voltage (Willi & Johnsen, 2006; NERSA, 2012).

Reactive power control has an effect on voltage magnitude as the total power is the sum of active and reactive power. There must be a balance between the supply and the demand of reactive power. According to the output power produced, the conventional generator's Automatic Voltage Regulator (AVR) decides the amount of reactive power to supply or absorb from the grid. A mismatch between the demand and the supply of reactive power would cause the system voltage to change. Thus the variation of reactive power is constrained to the variation of system voltage (Inigo, et al., 2007)

Frequency control is essential in order for wind plant to integrate the grid. The active power output from the generators is proportional to the input power to the generator (steam turbines, hydro, wind, etc.). The active power available in interconnected system is set by the available rotational energy of all generator interconnected. Thus the generators have to match the load demand, otherwise a decrease in frequency occur through the network. The reverse will happen in case of excess of generation, with the increase of frequency beyond the rated value. The frequency can be taken as an indicator of balance or imbalance between the generation and the load demand, thus a strict regulation is done during the imbalance through primary frequency control, secondary frequency control or tertiary frequency control (Ackerman, 2005; Inigo, et al., 2007). The generator are rated to operate within a frequency range closer to the grid frequency nominal value, mostly between 49.5 and 50.5 Hz in Europe, while in south Africa for continuous operation range during the disturbance is between 49-52 Hz (NERSA, 2012) .

Fault ride through capability is required to all wind technology by the code grid in order to integrate the grid. The wind farm are required to remain connected during the short circuit fault on the lines, which is followed by a voltage decrease to zero all along the transmission system. The disturbance is felt on the grid and the wind turbines normally very sensitive to the voltage sags, even transient drops over 70%, will disconnect from the grid. Thus creating imbalance between the power generation and the load demand and in turn the grid system

instability enhancement, which may results in cascaded trip off of other plants and finally a black out. That's why the wind farms are required to ride through the fault and remain connected to the grid by reducing their lines voltages in order to minimize the losses and to restore their previous normal conditions after fault clearance (Inigo, et al., 2007)

3.3. Solar power systems

3.3.1 Introduction

The solar energy has been used for many years in ancient civilization as source of energy for heating (Mervyn *et al*, 2011).the solar electrical power production is a conversion of sunlight energy into electricity. The conversion might be a direct conversion or an indirect conversion. The direct conversion use the photovoltaic effect of materials while the indirect conversion will use Concentrated Solar Power to convert the sunlight energy into heat energy for producing steam that will drive a synchronous generator, which will in turn produce electrical energy (Paul, 2005).

3.3.2 Photovoltaic system

A photovoltaic system (PV) is a combination of several different components such as battery system, DC/AC converters, and other power conditioning devices in addition to the solar panels themselves.

1. Solar cell

They are photovoltaic semiconductor cells compounded in a solar panel, which converts sunlight energy into Direct Current. Photovoltaic cell is a p-n semiconductors which when the sunlight falls on it, the photons energy making up the light are absorbed by it and cause a brake of semiconductors electrons bonds. Thus generating a flow of charge carriers, an electric current in the semiconductor (Eduardo, 1994), as it can be seen on Figure 3.14

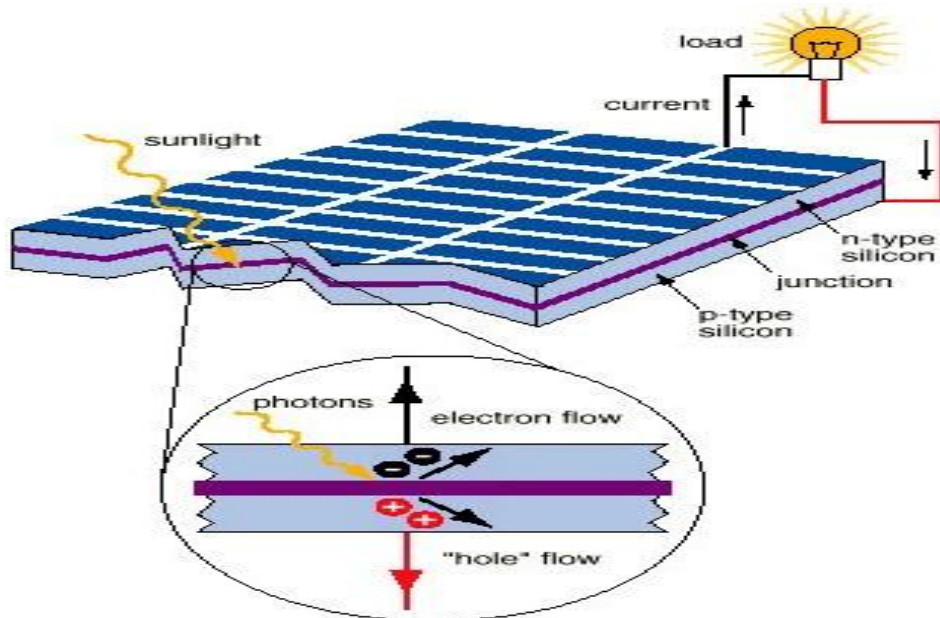


Figure 3.14: Photovoltaic cell (Castellano, 2010)

The photon energy carried by the sunlight falling on the p-n semiconductor cell is absorbed by electrons, this excess of energy initiates a broken up of electrons bindings. The electrons freed are moving towards n-region, while the holes are moving towards the p-region, this flow of charges carries up to the contacts of the cell, results in voltage across it, as the electric load is connected on the circuit the electricity can flow and bulb lights up. If the circuit is open the voltage will still be available on the electric contacts of the cell. Some of electrons freed fail to reach the electrical contacts of the cell, therefore don't participate to electricity generation and they are recombined to an atom through recombination processes. The voltage generated will be function of multiple factors such as solar radiation of the cell, as well as the material properties of the cell semiconductor (Kichartz, 2009; Markvart, 1994; Castellano, 2010).

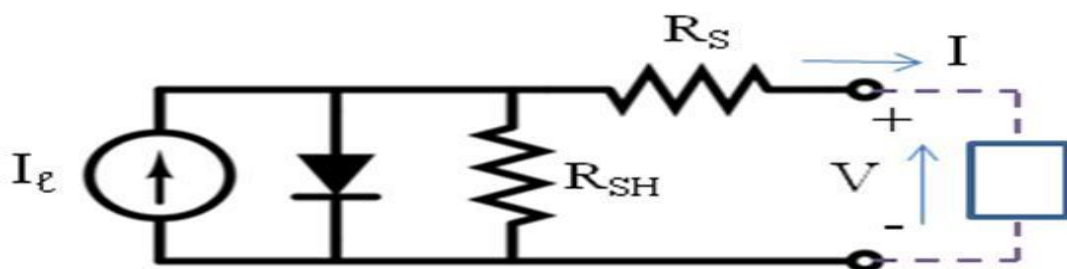


Figure 3. 15: Photovoltaic cell electrical model (Hough, 2006)

In Figure 3.15, the equivalent circuit of the solar cell is shown where the solar cell current output I_{ℓ} flows in parallel through either the junction represented by the diode, the resistances R_S , R_{SH} representing the power dissipation and the load. The shunt R_{SH} and series R_S resistances would be, in case of ideal cell, infinite and zero respectively. The load current I will equal

$$I = I_l - I_0 \left(\exp \frac{q(V+I \cdot R_S)}{n \cdot k \cdot T} - 1 \right) - \frac{V + I \cdot R_S}{R_{SH}} \quad (3.3)$$

Where I_0 is the reverse saturation current of the diode, q is the elementary charge 1.6×10^{-19} Coulombs, k , Boltzmann's constant with value 1.38×10^{-23} J/K, T is the cell temperature in Kelvin, n the diode ideality factor $1 < n < 2$ and V is the measured cell voltage (Hough, 2006; NI, 2012). From that equation of load current, by assuming the cell ideal and setting V as zero like in short circuit condition I_{sc} and setting the current to zero as in open circuit condition V_{oc} we get a characteristic shown below.

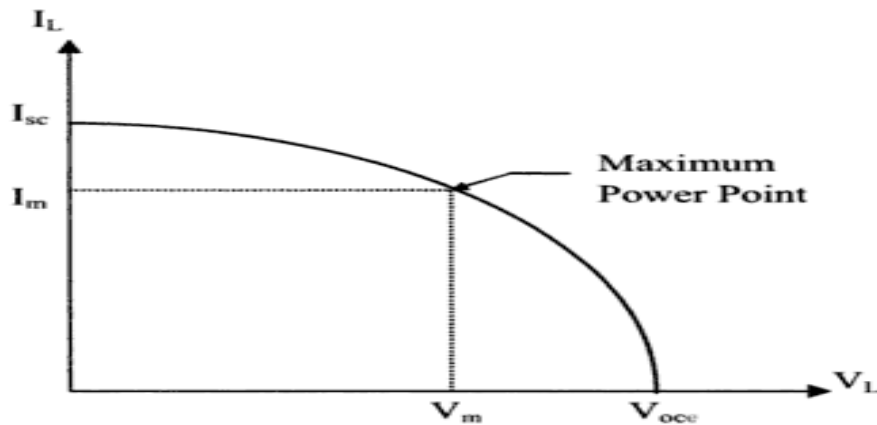


Figure 3. 16: I-V characteristic of PV cell (Hough, 2006)

From the characteristic of the solar cell above, Figure 3.16, the maximum power provided by the cell is at the point of high value of the product of the voltage and current, represented by I_m and V_m . Therefore the maximum power is the product of I_{sc} , V_{oc} and the fill-factor FF (Markvart, 1994) ,

$$P_{max} = V_m I_m = FF V_{oc} I_{sc} \quad (3.4)$$

2. PV cell technology

Different cell technologies are currently on the market. The main factors according to, a good a cell is evaluated are the energy PV energy conversion efficiency and the initial cost per watt capacity produced .The factor determines the economic viability of the technology. The goals when creating a new technology is to raise the conversion efficiency and same time minimizing the losses within the cell by improving the quality of the cell. Various types of cells are available on market and others in laboratories where researches are still continuing for high efficient cells.

Among the cell available: single crystalline silicon, polycrystalline /semi crystalline silicon, thin-film cell, amorphous silicon, Spherical cell, concentrator cell, multijunction cell (Krauter, 2006).

Silicon based cells are popular on market, the low cost of the technology is due to the fact of their abundance in nature, the long lifetime more than 25 years and high crystalline structure stability. The efficiency is key point of the success of the silicon based photovoltaic cells, the current available modules have an efficiency ranging between 11 and 14% .However the process of manufacturing of it, is slow and costly compared to polycrystalline and semi crystalline which have a fast and cheaper manufacturing process but also with a reduced efficiency. While amorphous and thin cell require less raw material, they are still under research in order to improve the efficiency for amorphous which half of the crystalline cell technology. Same as amorphous cell technology, the concentrator cell require fewer raw materials but on other hand it requires optic material to concentrate solar sun on the cell. An efficiency of 37% has been claimed under laboratory conditions. Similar high efficiency has been achieved for multijunction cell under laboratories conditions and researches still on for better efficiency (Mukund, 2006; Tomas, 1994).

3. Solar panel

The individual solar cell can generate a half of volt, in order to have more power 36 solar cells are connected in series and encapsulated together to form a module. The module framework protects cells from weather and other physical hazards. The module they are themselves interconnected to form a panel (Solar Energy International, 2004).

According to the required power to be generated, solar panels are electrically associated together to form an array. The series connection and the number of panel involved is governed by the needed output current ,while the parallel connected panels number is determined by the required output voltage. Figure 3.17 shows a set of panels forming an array (Prasad & Snow, 2005).



Figure 3. 17: Solar arrays (SolarCatskills, 2011)

4. Power conditioning devices

There are various devices for the power control within a PV system, depending to the design of the latter; we may found the battery charge regulators that must prevent excessive discharge and overcharge of batteries. In case of a small generation around 100W, shunt regulators are indicated to prevent the undesired power to flow to batteries. For large PV generators relay and solid state devices might be used to isolate the batteries from the panels. Like the overcharge, the excessive discharge of batteries is harmful to them in term of life cycle. Converters for the DC/AC conversion, monitoring equipment and other control elements are of significance role in the optimization of the transfer of energy from the arrays to the load and batteries (Tomas, 1994).

5. Solar Power Plant

There are two different exploitation methods for using the sun energy, a direct and indirect method. The direct methods the sun energy is converted into electricity by photovoltaic panels, while the indirect method the sun energy is converted into heat before being converted into electricity by concentrated solar techniques (Fereidoon, 2010).

6. Photovoltaic power station

The power station consists of multiple PV arrays connected together and converting the sunlight energy directly into a DC power. The PV arrays may be with a sun tracking system for better solar capture or a fixed system that stay in one position. The power produced will be feed into the grid in the case of grid-connected system. The converters are used to convert the DC output current into alternating current which will be transformed at high voltage as needed by the grid. The large PV converters are controlled by pulse width modulation control techniques hence the harmonics issues (David & Camm, 2012).

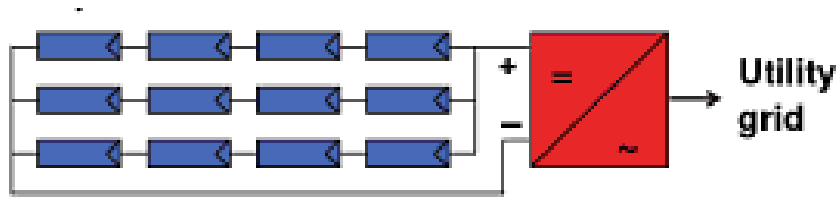


Figure 3.18: PV configuration for grid connected systems (Heinrich, 2012)

For grid connected system as it can be seen on Figure 3.18, series and parallel connections are made to achieve the desired output current and voltage, the DC output is the sent to the grid via the converter. The converter is the interface element between the grid and the system, thus the most critical elements in the whole system (Boxwell, 2010; Heinrich, 2012).

3.3.3 Maximum-Power-Point-Tracker (MPPT)

During the operation of solar cell the maximum power output is obtained at a certain point of voltage and current. The solar cell characteristic on Figure 3.16 is showing the point on the knee of the graph, which is the maximum power point. As this point is changing depending on moment and environment conditions in which the cell is undergoing, there is need to keep on tracking the maximum power point in order to achieve the maximum output power. Figure 3.19 shows the arrangement for the MPP tracking.

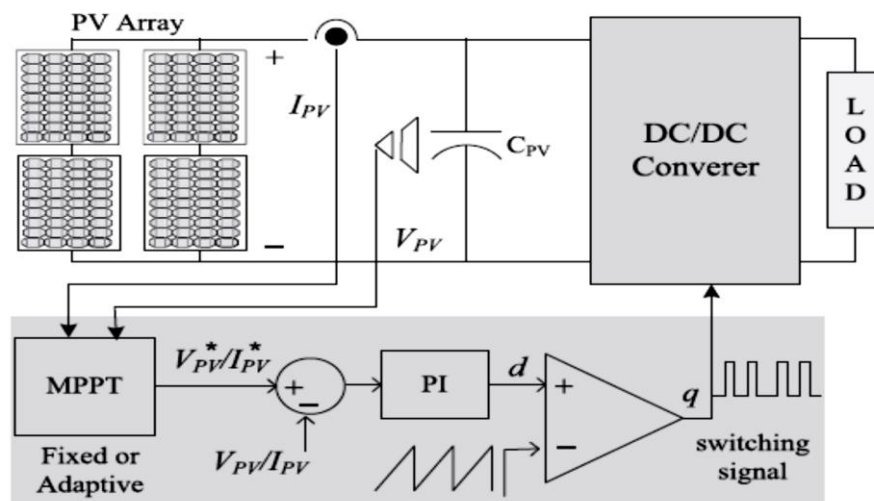


Figure 3.19: Typical voltage or current MPPT system (Kashif & Zainal, 2013).

Different methods are used to track the maximum point; they are divided into 2 categories namely conventional maximum power point tracking and the soft computing maximum power point tracking method. The conventional techniques enclose namely the Perturb and Observe (P&O), Incremental Conductance (IC) and the Hill Climbing (HC), while for the computational

technique the Fuzzy Logic Controller (FLC), Artificial Neural Network (ANN) and Evolutionary Algorithms (EA) are the main methods used (Kashif & Zainal, 2013). Perturb and Observe method techniques consist in introduction of a perturbation in the operating voltage and current then observe the reaction of the operating at the converter in case of an increment in operating point it means that the converter is not yet at MPP. A new perturbation will be introduced until the MPP is reached from that point any more increase will not have any effect of increasing the operating point rather it will evolve around the MPP. The same method is used for Hill climbing technique, but instead of perturbation of voltage and current, it is the duty cycle which is disturbed and still the working point will be observed to see the change in towards the MPP. Quite different with the previous methods, the Incremental conductance consist in comparison of the ratio of derivative of conductance with the instantaneous conductance. the idea is that the MPP point corresponds to point where the 1st derivative of power is equal to zero. (Bidyadhar & Raseswari, 2013). The computational techniques currently available and different variations are discussed in Kashif & Zainal (2013).

3.3.4 PV grid connection

1. Introduction

PV power plant integration or connection to the grid consists in injecting the power generated into the transmission, as it is shown on Figure 3.20 where a single phase PV generator connection to the grid is shown as an example, the integration system consists a PV generator ,inverter, monitoring or control equipment and grid transformer. The DC voltage produced by the PV generator or arrays is converted into AC before being sent into the grid through the grid transformer. The key elements in the whole system is the inverter which is controlling not only the output power from arrays but also is in charge of the synchronization with the grid.

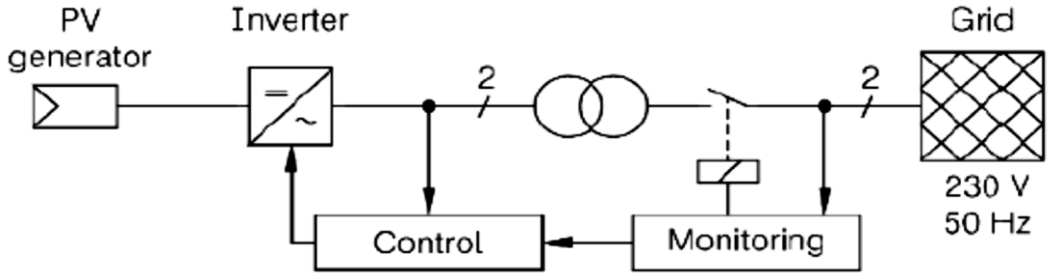


Figure 3. 20: Principle of a single-phase grid connected PV system (Schutz, et al., 2008)

2. Inverter for grid connected PV

Actual grid connected PV systems are self-commutated PWM inverters based, with pulse frequencies ranging from 10 kHz to 25 kHz. While the old inverter inverters were line commutated and thyristor based, the currently are most of them MOSFET or IGBT based. Older line-commutated inverter types often used to have power quality problems and therefore

they are disappearing from the market. PV inverter with high-frequency transformer are used as well. The latter is often used to reduce transformer's core volume, thus the weight even though it's costly. (Schutz, et al., 2008)

There are 4 types of inverter configurations or arrangements in order to achieve his task of PV output power conditioning and synchronization with the grid. Namely: the central-plant inverter, multiple-string dc–dc converter with single-output inverter, multiple-string inverter and module-integrated inverter configuration.

The central plant inverter consist of a large rated inverter to summer up the all PV arrays DC output power and convert it to AC power, as it is shown on Figure 3.21, several panels are connected together to a single DC bus. This configuration, Central inverters, offer the best monitoring possibility as only one data interface and one processing unit is needed. On other hand no individual MPP tracking is possible. The failure of the inverter will affect the entire system. This is avoided by the use of module integrated inverter configuration, Figure 3.22, where each module has its own small inverter and the outputs of those inverters are sent to the grid. Same as central inverter configuration, the multiple-string dc/dc converter with single output inverter on Figure 3.23, the DC/AC converter is the heart of the system. The failure of the converter affects the entire system. To prevent that situation the multiple-string inverter may be the best configuration. As it is shown on Figure 3.24, it consists of several modules connected in series on the dc side to form a string. The output from each string is converted and transmitted to grid through a smaller individual inverter. Many such inverters are connected in parallel on the ac side. This arrangement is not badly affected by shading of the panels. It is also not seriously affected by inverter failure (Nayar, et al., 2001; Schutz, et al., 2008).

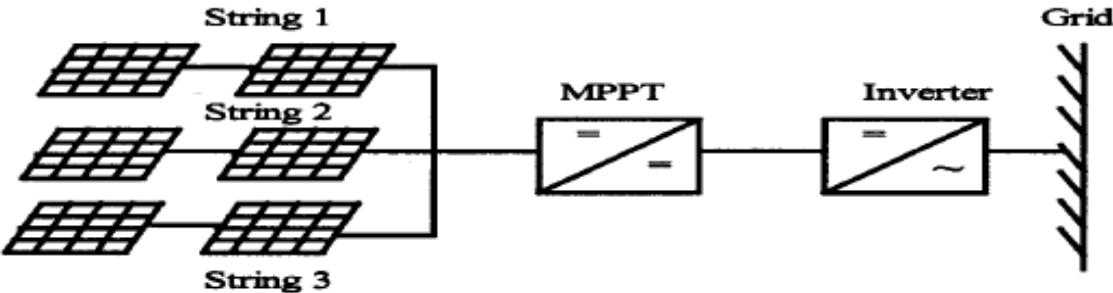


Figure 3.21: Central plant inverter configuration

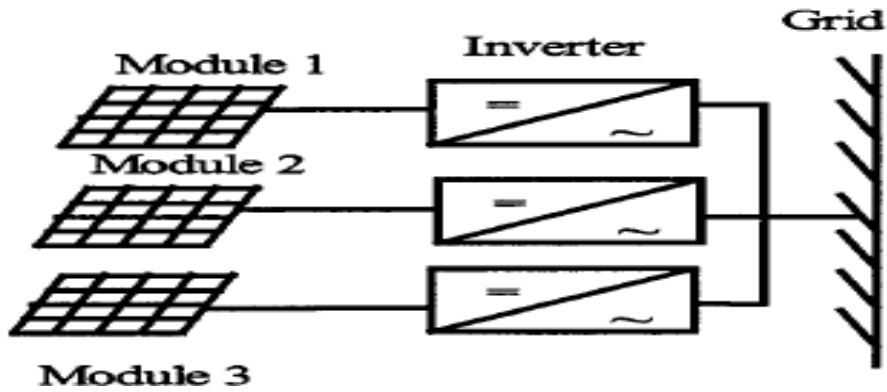


Figure 3. 22: Module integrated inverter

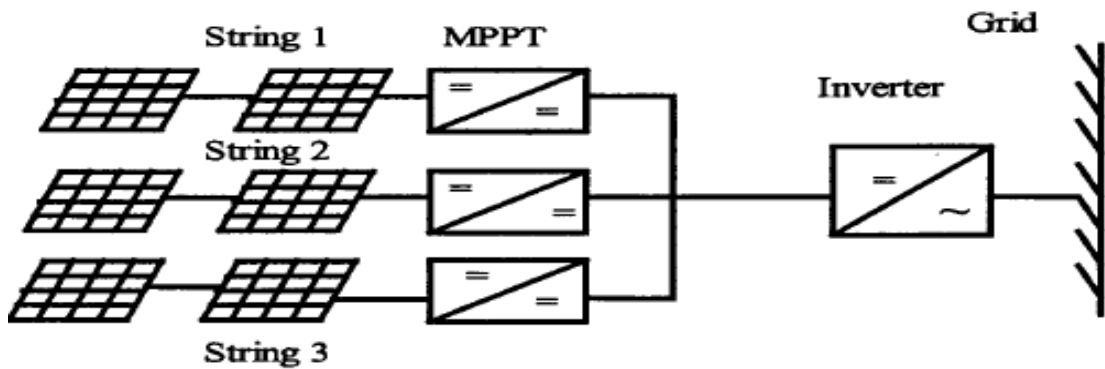


Figure 3. 23: Multiple-string DC/DC converter

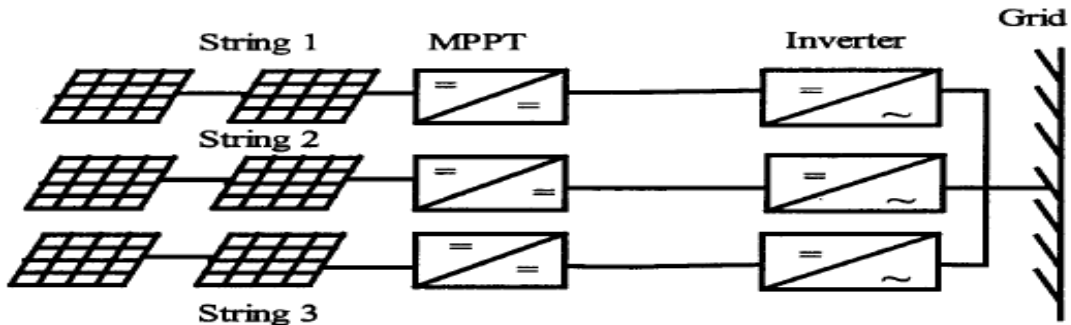


Figure 3. 24: Multiple-string inverter

3. PV power grid integration

The integration or tie to the grid of PV power plant is achieved through the converter. Like any other power source generation, in order to be integrated into grid, the PV power plant has to synchronize with the grid and comply with the grid codes. The converter acting as interface between the PV power plant and grid is hosting the grid synchronization unit. Through the latter the synchronization with the grid is carried out.

Synchronization consists in duplicating the grid signal characteristics: frequency, phase angle and voltage magnitude; to the converter output signal before being injected into grid. Different three phase synchronization methods or techniques are used by grid connected converters: filtering techniques, phase locked loop and adaptive notch filter (ANF) based techniques. The

choice of the one or another synchronization technique depends to his proficiency in tracking the phase and frequency variations of the grid signal, the ability to rejects harmonics and disturbances that exist in grid signal, and finally the implementation simplicity and cost of the technique (Yazdani, et al., 2009).

Filtering techniques concept consists in filtering the grid signal or voltages in an α - β stationary reference or in d-q synchronous rotating reference frame. As it is shown on Figure 3.25, the three phase grid voltages (U_a, U_b, U_c) are transformed into α - β reference frame. The resulting α - β stationary frame components (U_α, U_β) are filtered using low pass filter, notch filters, space vector, etc. The filtered two components are used to calculate the phase angle θ , and it is that angle that the converter will follow while injecting the power into the grid. The same concept is applied when using the d-q synchronous rotating reference frame filtering, as it is shown on Figure 3.26. The d-q filtering is easier to design, but like the α - β techniques the filtering methods used shows weakness to extract the phase during grid disturbances. Moreover delays are introduced by the filters thus the need of proper design or use of compensation for delays (Adrian, et al., 2005; Blaabjerg, et al., 2006).

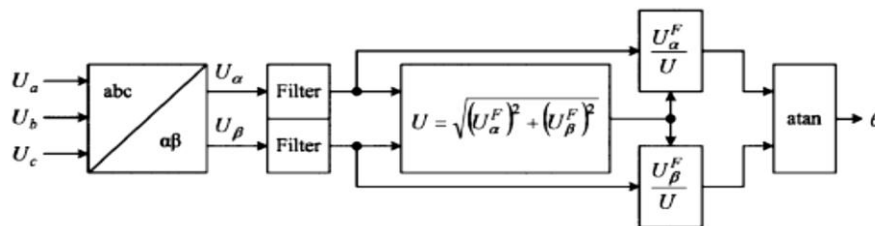


Figure 3. 25: Synchronization method using filtering on α - β alpha and beta frame (Yazdani, et al., 2009)

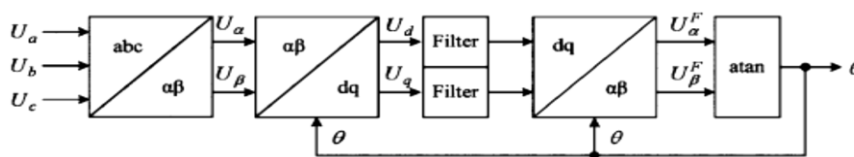


Figure 3. 26: Synchronisation method using filtering on d-q frame (Yazdani, et al., 2009)

The phase locked loop (PLL) method for synchronization concept is based on phase locked loop technique. The PLL consist in recovering and synthesizing the grid signal parameters, namely the frequency and the phase angle θ . The concept, as it is shown Figure 3.27, is that PLL makes the output signal X_o to track the reference signal X_i in frequency and in phase. For the grid synchronization in three phase systems the phase locked loop implemented in d-q synchronous reference frame shown on Figure 3.28, is the common structure used. It

composed of two main parts the transformation part and the PLL part. The latter is the one that determine the whole system dynamics as the transformation part has not dynamics. The PLL implemented in d-q synchronous reference frame suffer during the utility disturbances of voltage. Various scheme of the PLL called also synchronous reference frame methods have seen the day to improve the performance during the unbalance occurrence (Guan & James, 1996; Yazdani, et al., 2009).

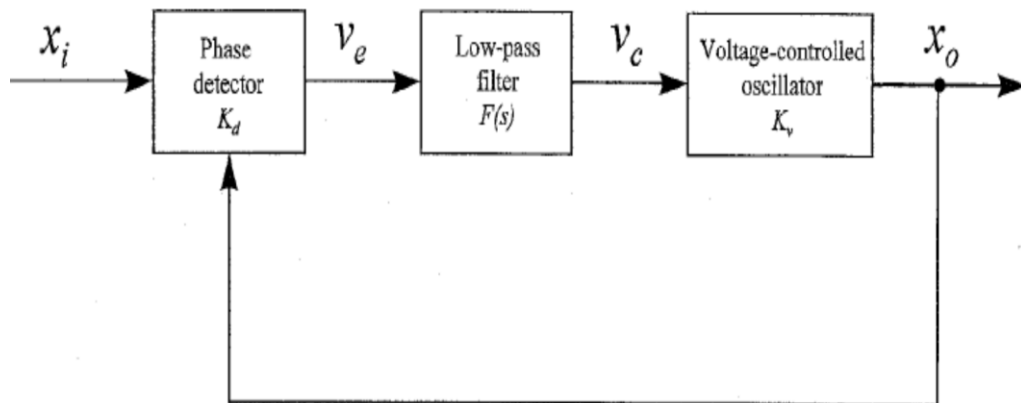


Figure 3. 27: Basic topology of PLL (Guan & James, 1996)

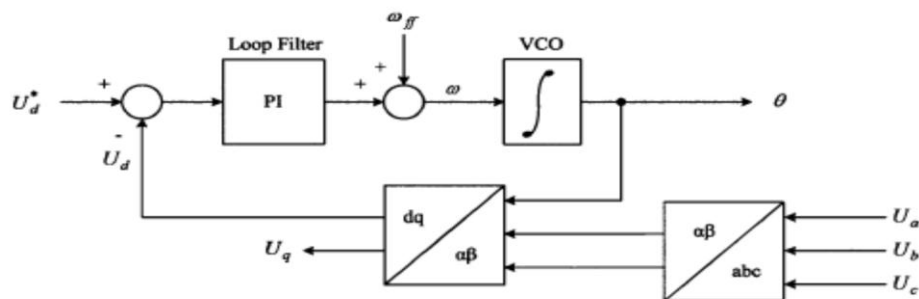


Figure 3. 28: General structure of d-q PLL method (Yazdani, et al., 2009)

The adaptive phase locked loop (PLL) methods consist of using three PLL systems instead of one, as usual for the PLL method. As it is presented in (Jovcic, 2003), the implementation of a PLL on each phase will have a good performance than using a single common system for all three phases. With this system large and heavy algorithm for the control is required, however with this system every phase is monitored individually which makes this method suitable for grid phases monitoring.

3.3.5. Concentrated Solar Power (CSP)

The concentrated solar power plant working principle consists of capturing the sunlight energy and converting it into thermal energy and using the heat gained to produce steam that will run a steam turbine of an alternator. The sunlight is concentrated on working fluid and through heat exchange process the steam is produced. Various techniques are used for concentrating or focus the sun light onto the working fluid: parabolic through collectors, solar power tower, linear Fresnel system (Fereidoon, 2010).

- **Parabolic through collectors**

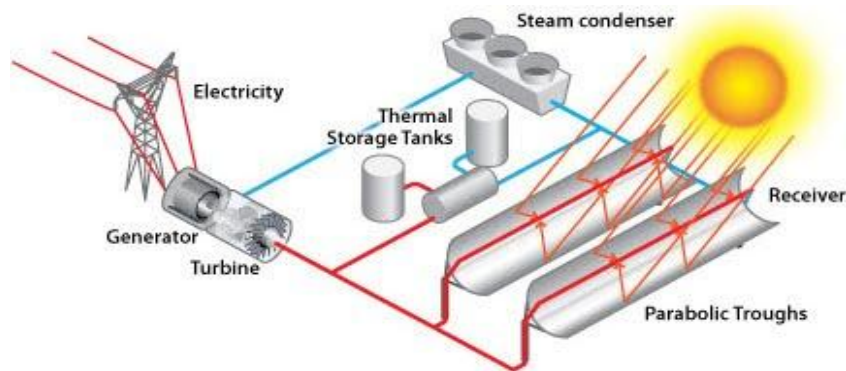


Figure 3. 29: Parabolic through CSP plant schematic (NREL, 2010)

As it can be seen on the Figure 3.29, parabolic reflectors concentrate sunlight rays onto the pipe transversally passing through the reflectors. The fluid heated, generally oil, will generate the steam through the heat exchange process to run the steam turbine generator. The size and the number of parabolic are dependent on the amount of electrical power to be generated. The excess of heat generated during the day may be stored for several hours of night electricity generation and during the cloudy days (Tushar & Mark, 2011).

- **Linear Fresnel system**

Linear Fresnel system, Figure 3.30 works on the same principle as the parabolic through, the difference is in that rather than using a parabolic reflectors, multiple single linear reflector are used to focus the sun light to one or more pipe positioned over them, through which a fluid flows. (Nayar, et al., 2001; Schutz, et al., 2008)

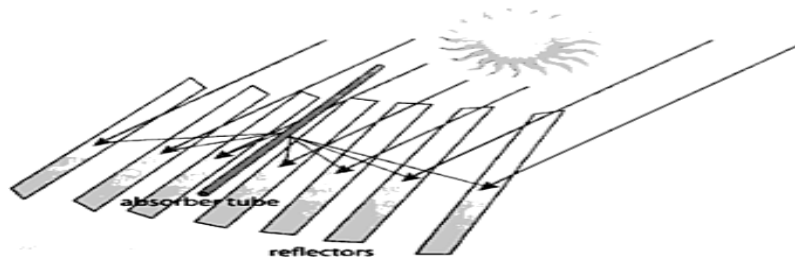


Figure 3. 30: Fresnel reflectors (Volker, 2009)

- **Solar power tower**

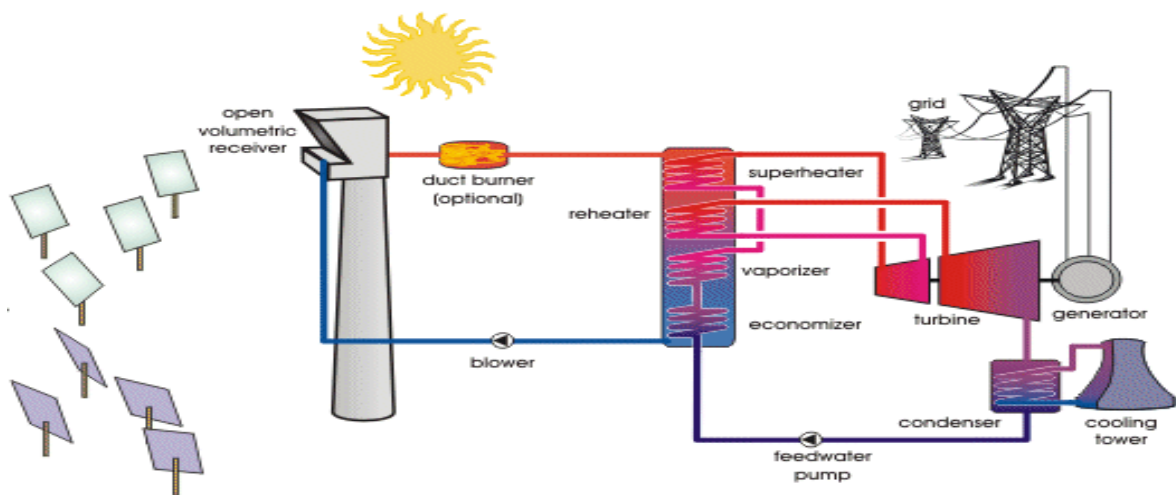


Figure 3.31: Solar tower power plant (Volker, 2009)

As it can be seen from Figure 3.31, a solar tower power plant consists of sun tracking reflective mirrors (heliostats) that concentrate the sun light onto the receiver in the tower. The heliostat surrounding the tower sun tracking is done by computer for good efficiency. The fluid is heated up to 1000°C then through the heat exchange the steam is generated to run the steam turbine that drives the generator. The alternating current power generated will be transformed before being transmitted in the grid (DGS, 2005).

- **Heat storage system in CSP**

CSP generates electrical power in the same way as conventional power plants, but using solar energy as input energy. The heat energy is efficiently generated during the clear sky day. The use of heat storage system greatly improves the CSP system’s ability to provide power at a constant rate despite significant disturbances in the amount of solar radiation available. With heat storage system CSP can be used as dispatchable source of power and thus allowing flexibility to the grid during the peak demand of energy. Different heat energy technologies are

used in CSP plant, according to their concept they can be classified into: active storage and passive. With the active storage, forced convection heat takes place onto the storage material which is the transfer fluid. While for passive storage systems the heat transfer fluid get the convection done within the storage material where it has to pass for charging or discharging on a solid material. Molten salts mineral and synthetic oils are the mainly fluid used (Luisa, et al., 2012; Antoni, et al., 2010).

3.3.6 Solar power plants impact on the grid

Solar power plant integration and their increasing penetration especially, PV rises concerns on the possible negative effect to the grid stability. The power system inertia is based on rotating generators and is a vital characteristic that stability of the system is based on. The reaction of the system to the disturbances or imbalances depends on its inertia. A power system with lower with a low inertia tends to respond fast to the load variations and in turn to the frequency changes.

The continuous integration of renewable energies, leads to the use of them during the low load situations while the conventional are on standby for the peak load period. in that moment the system is more exposed to disturbances.

Besides stability challenges due to the high penetration of large scale PV Park into the grid, large scale PV have more technical impacts on the grid as presented in (Yuan, et al., 2013). Studies have been conducted by (Wang, et al., 2008; Rakibuzzaman, et al., 2012) onto the impact of large scale solar PV on grid voltage profile.

3.3.7 Superconducting magnet energy storage

1. Introduction

The first superconducting magnetic energy storage (SMES) system was implemented in Los Alamos National Laboratory in 1974. The idea of application of SMES into power system resulted from the ability of the system quick response with high efficiency. Those characteristics are used in load leveling, dynamic stability, transient stability, frequency regulation, transmission enhancement and power quality optimization.

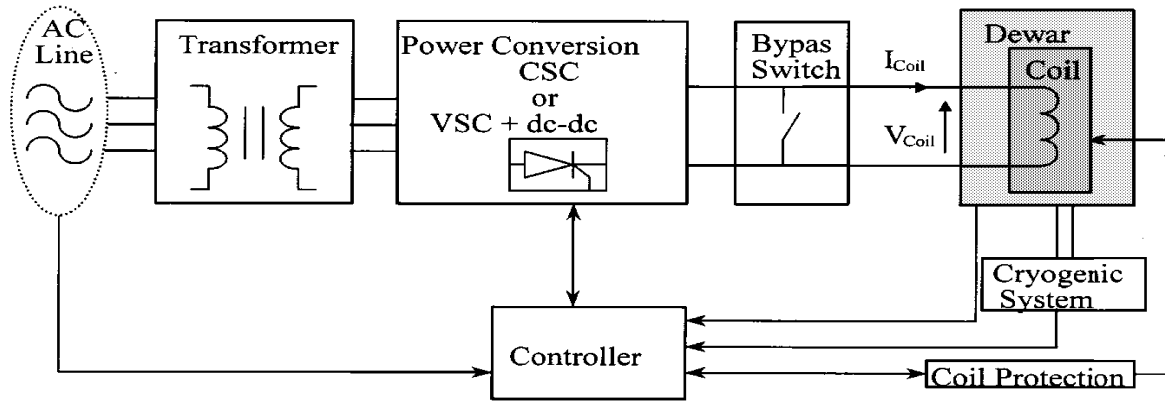


Figure 3.32: Components of a SMES system (Paulo, et al., 2001)

The superconducting magnetic energy storage system consists in storing energy in magnetic field generated by a direct current (DC) current flowing through the superconducting coil. The superconducting state for the coil is achieved at low temperature, thus the large coil is maintained at cryogenic temperature through a cryostat that contains liquid helium or nitrogen. The inductively stored energy into the coil with inductance L , flowing DC current I and voltage V across the coil can be retrieved from the SMES instantaneously and will be flowing out during a period ranging from fractions to several hours. The stored energy into SMES is given by the Equation (3.5) (Paulo, et al., 2001) :

$$E = \frac{1}{2} LI^2 \quad E = \frac{dE}{dt} = LI \frac{dI}{dt} = VI \quad (3.5)$$

2. System components

As it is shown on Figure 3.32, the SMES consists of transformer interfaced between the AC network and the converter, large superconducting coil, control system, protection system and the cryogenic system. The transformer acts as interface between the converter and the network by stepping up the current flowing from the AC network to the converter during the charging of SMES. The reverse process is performed while the SMES is discharging into the network (Piotr, 2008).

Voltage source converter (VSC) and current source converter (CSC) are generally the types power conditioning systems used in the SMES for the interconnection of the system to the grid. A DC/DC chopper may be added to the system to reduce the stress on transformer and converter by adjusting the current flow between the SMES coil and the converter. VSC are used in large SMES while the CSC is used in medium and mini-sized SMES. However in case of high power parallel connection of CSCs can be used. The CSC power conditioning type is simple and of easy control than the VSC power conditioning type. Moreover the CSC type is much

faster than VSC type in terms of power exchange due to the fact that the SMES keep energy in dc current form. The control of SMES coil charge and discharge is performed the converter and chopper if present. (Ju, et al., 2007; Paulo, et al., 2001; Piotr, 2008).

SMES coil is the heat of an SMES system, thus they are specially designed, following the Virial law in order to optimize the mass according to the intended energy storage capability of the SMES (Boom, 1991). The superconducting coils are either of torroidal or solenoid types, the torroidal types is suitable for medium and small sized SMES. Solenoid type is suitable for large SMES with the benefits of having a simple structure and on the hand it has leaking magnetic fields. Therefore, the idea of using torroidal types in multistage structure. This reduces the magnetic field leakage and the floor space. The leakage in solenoid coil as shown on Figure 3.33.b is due to the fact that the electromagnetic force is outward. Hence, the increase of the stress on the shedding results in magnetic field leakage. The SMES solenoid coil construction design insist on achieving high amount of energy storage with less superconducting material ,less weight and less space used by the SMES. The usual cross sectional shape used for solenoid coil is rectangular, but the research of new types variants of it are undergoing with purpose of reducing effectively the losses (Kanamaru & Amemiya, 1991). In (Ju, et al., 2007) medium sized coils for SMES are designed follow the Virial and the results are shown in Table 3.2, where it can be seen that the dimension of the coil varies according to the capacity of the SMES.

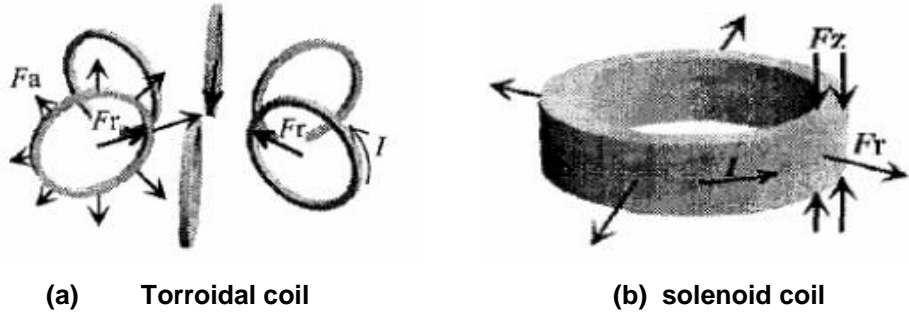


Figure 3.33: Electromagnetic force on torroidal and solenoid coils (Ju, et al., 2007)

Table 3. 2: Results of medium size SMES coil (Ju, et al., 2007)

SMES coil capacity /MWh	Interior hole /m	Height /m	Operating current /kA
1	5	8	50
5	8	12	50
10	10.5	15	75
20	13.5	17.5	100

Rapid absorb and release of great power in short time like milliseconds, that is the stress the SMES are subject to, thus the SMES coil should be more stable than conventional coils. The operation in rated range, prevent the damages to the system. The SMES coil may lose superconductivity, due to the overheating and high voltage arcing. This may result in the loss of the stored energy in the form of heat with critical damages to the SMES coil. Whereby the need for the protection system that should reduce the energy exhaustion, prevent the wire overheating and continuously monitor the superconductivity of the coils (Ju, et al., 2007). The superconductivity in SMES coil is measured through temperature, pressure, and ultrasonic flow velocity and voltage detection methods (Lord & Bule, 1991; Ninomiya & Sakaniwa, 1989; Makoto & Takaai, 1999). The protection of SMES should rapidly detect the superconductivity and quench the heat without damaging the coils.

The superconductivity of the SMES depends on the cooling system or cryogenic system. It consists of refrigeration device made out of stainless steel and liquefied helium as refrigerant. Two methods are used actually, the immersion of SMES coils into the liquid helium or the forced circulation of the liquid helium through the coil conductors. The immersion method is good in terms of stability while on the hand it is not the case for AC losses and voltage proof; The forced circulation method provide high performances in machine intensity, ac losses and over voltage on one hand and on the hand it has a low stability performance. With those two methods, complex cryogenic liquid systems and liquid compensation are involved for the SMES to run for long time. To avoid that complexity, the cryocooler has been proposed in place of liquid helium for magnet cooling.

3. Advantages:

1. Long term lossless repetition of energy storage, conversion efficiency 95% while the battery storage repeat number in general is 1000 to 2000 times
2. SMES through the converter connected to the grid, have fast response speed (ms).
3. Can build large power and large energy system; in addition to vacuum and refrigeration system without rotating part, so the device has a long service life.
4. Build will not be limited by the place and the maintenance is simple, no pollution (Xuesong, et al., 2012)

3.4. Power system

3.4.1 Introduction

The modern power system consist in general, the production of electrical energy and its transport to the consumers. As the consumers or loads are distributed and located far from the production units, networks of interconnected lines and cables is used to transmit power to various locations. The electrical power network system is composed of generators, transformers, transmission lines, protective devices, customers, etc. The electrical power

network can be divided into three categories: the transmission network, Sub transmission network and distributions system. (Momoh & El-Hawary, 1999):

- a) Transmission system: they interconnect the generating units to the main loads centers .they are pillars of the network, their operating voltage level is the highest, 230 KV and above. The output voltages from the generating units, which are in the range of 11-35 KV, have to be stepped up by transformers in order to be connected to the transmission level. The capacity of those generating units or power plants connected to it, is large. The generating units are mostly steam or gas turbines and hydro. With the increasing of wind power capacity, they are also connected as well as the concentrated solar power plant.
- b) Sub-transmission system: The sub-transmission network also known as the medium voltage transmission network is the interconnection between the transmission network and the distribution networks, they transfer electrical power generated by large power plants in the transmission network to the distribution network and to the large industrial customers. They operate at voltage level between the transmission level and distribution level, typically 34.5 KV to 138 KV.
- c) Distribution system: The operating voltage in this level is between 4KV and 34.5 KV. In this level, the power supplied to the customers can be either from the sub-transmission level or directly from distribution power plants. Small renewable energy power plants as wind turbines, solar cells, fuel cells, micro turbines, etc. can be connected to those distribution networks.

3.4.2 Power system stability

The electrical energy consummation, or load demand , is keep changing .from the simple fact of switching on or to the start of a heavy electrical machines , all have a big impact on the generation and transmission of electrical power. There is an equilibrium the between the generation the transmission and the consumption, the loss of equilibrium points leads to failure of critical elements of the system such as generation units or transmission lines (Kahn, et al., 2008) .A single element failure may end up in a cascading failure of other elements, to finally resulting in power outages. Hence, the importance of power system stability understanding.

Power system stability deals with the ability of the power system, after disturbances to recover its equilibrium points or conditions. The system recovering its original equilibrium points after minor or small disturbances is called oscillation stability or dynamic stability. The small disturbances are caused by the load changes, variations of excitation field circuits, and changes in mechanical torques. A system that regains from large or major disturbances and attains new equilibrium points is called to be in transient stability. The large disturbances are caused mainly

by the loss of a large generator or a short circuit of a transmission line (Grigsby, 2007). The dynamic stability is determined by the rotor angle stability and voltage stability (Kundur, 1994).

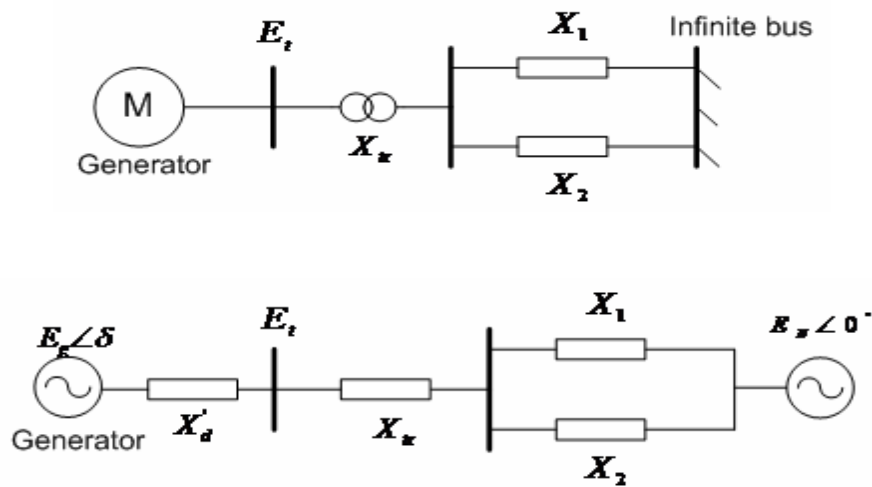


Figure 3. 34: Generator-bus bar system

Rotor angles stability is related to the synchronization between the generating units. As depicted in Figure 3.34, a synchronous generator is connected to an infinite bus representing a robust system. The later can be substituted by a constant voltage source, while the generator is represented by a voltage source after the transient reactance X_d' . The active power produced by the generator to the infinite bus is given by Equation (3.6) below:

$$P_e = \frac{E_g E_N}{X_T} \sin \delta \quad (3.6)$$

Where

δ : is the rotor angle

X_T : The total reactance of the system given by $X_{tx} + X_d' + (X_1 X_2)$

X_1 and X_2 : infinite bus reactance.

X_{tx} : transmission reactance

E_g : generator output voltage

E_N : voltage at infinite bus

As it can be seen from Equation (3.6) the power transferred to the infinite bus bar is proportional to the rotor angle δ . The electrical power produced by the generator is proportional to the mechanical power supplied to the shaft. Thus any unbalance between the two powers will result in change of rotor speed, with the increase in the rotor speed in case mechanical power is greater than the electrical power and decrease in the rotor speed in other case. In both case the rotor angle of the generator will no longer be in phase with the infinite bus angle or other

generating unit's rotor angle. Therefore, a loss of synchronism with the system occurs (Kundur, 1994).

The loss of synchronism by a generator has an effect on output voltage and frequency. The loss of synchronism means that the rotor is not running at the same speed as the expected for the generation of voltages at the system or infinite bus frequency. The mismatch between the rotating stator field and the rotor field, results in isolation of the generator by the protection system. This is due to the instability in output power, current and voltage.

Voltage stability is defined as the capability of a power system to keep voltages at all buses in the system in admissible range during the normal operation conditions and after recovering from the disturbances. The increase in load demand as well as change in the system condition generates a progressive and uncontrollable drop in voltage. However, the major factor behind the instability is the inability of the system to meet the reactive power demand (Farmer, 2001).

3.5 South Africa grid code

3.5.1 Introduction

The actual South Africa grid codes find its roots in the electricity act 4 of 2006. It is there to specify the minimum technical and design requirements for renewable power plant to be connected on the transmission or distribution system. The code classifies the renewable power plant according to the power produced, hence there are category A; grouping all renewable power plant with power produced up to 1 MVA, category B with power produced ranging from 1MVA to 20 MVA and category C for those power plant with power produced greater than 20 MVA.

According to (NERSA, 2012) the characteristics of electrical power to be evaluated against the technical parameters set the by the code are:

- Voltage and current quality, i.e. magnitude, harmonics distortions, flicker, unbalance
- Voltage events i.e. voltage sag or dips, voltage swells , voltage transients
- Supply interruptions
- Frequency of supply

For the normal operating conditions the grid code requires, the renewable power of category B and C to be able of operating within a voltage range of $\pm 10\%$ around the nominal voltage at the point of common connection. While for the frequency, the nominal value is 50 Hz, a deviation till 52 Hz is permitted for a period less than 4 seconds beyond which a disconnection from the grid is recommended. Same recommendation is applied, when frequency on the grid goes down to 47 Hz for a period longer than 200 ms, as shown on Figure 3.35. For the synchronization with the grid the renewable power plant of category B and C should be permitted to the grid once the voltage at point of connection is within $\pm 5\%$ around the nominal voltage.

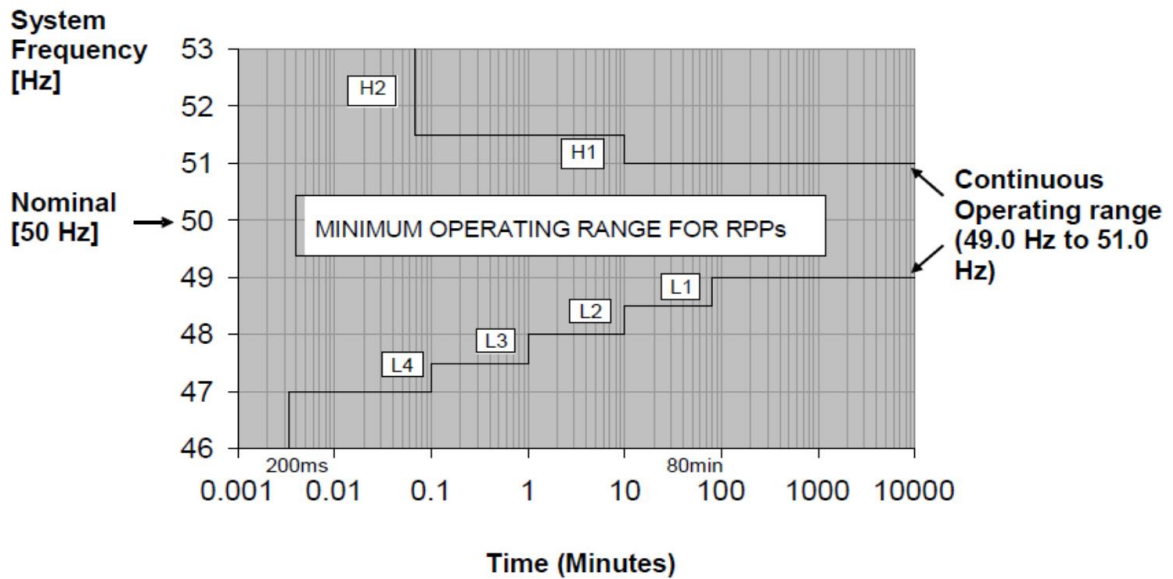


Figure 3. 35: Minimum frequency operating range for renewable power plant (NERSA, 2012)

3.5.2 Abnormal operating conditions

The code requires from the renewable power plant to be able to stay connected onto the grid for a certain time during the fault on the grid at point of connection. Known as the fault ride through capability, the category B and C power plants are required to withstand sudden rise or drop of voltage for a precise period of time. As it can be seen from Figure 3.36, they shall be able to handle and stay connected when during a sudden rise up to 10% of nominal voltage at the point of connection for a period of 2 seconds.

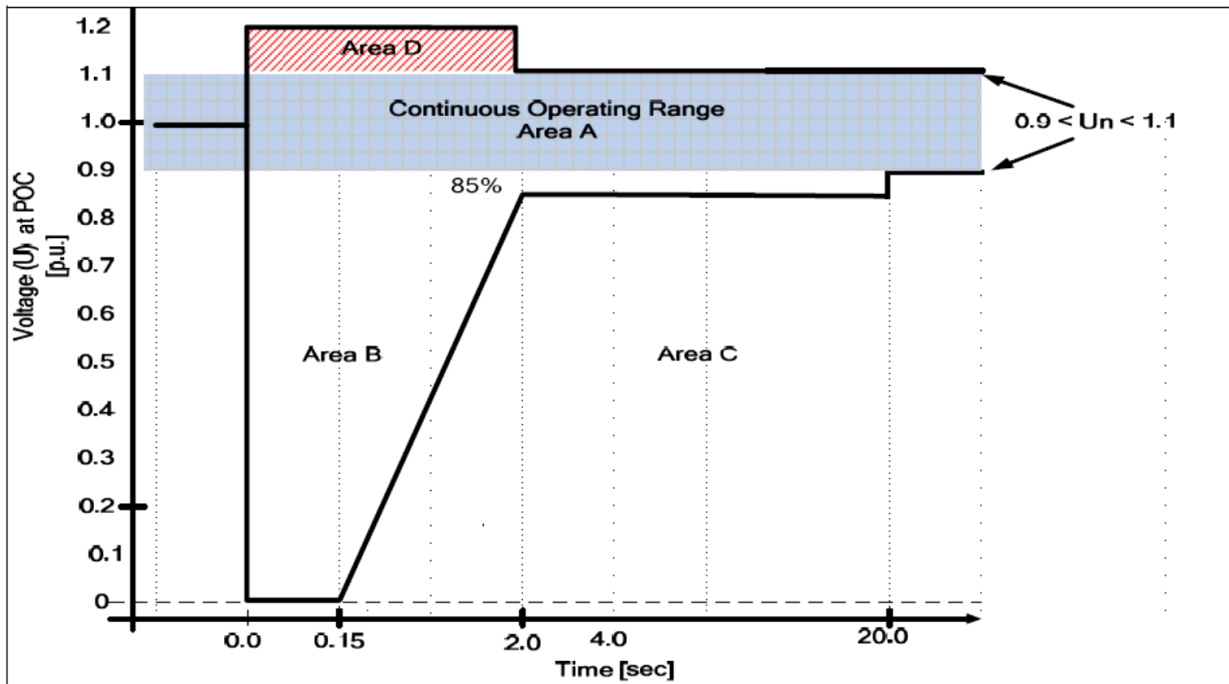


Figure 3. 36: Voltage ride through capability for renewable power plant, B and C category (Nersa, 2012)

3.6 summary

This chapter discussed some of technologies that are used by Independent Power Providers (IPPs). Photovoltaic solar power plant, wind energies grid interconnection systems are reviewed, Superconducting magnetic energy storage system (SMES) is looked at also. Power system overview is given as well as power system stability literature review. South African Grid code requirements for renewables energy plant are provided.

CHAPTER FOUR

SYSTEM DESIGN

4.1. Introduction

The system for application of High Voltage Direct Current (HVDC) technologies for distributed Independent Power Providers (IPPs) is achieved by integration of those IPPs to the grid through Voltage Source Converter based HVDC system (VSC-HVDC). The latter acts as an interface between grid and IPPs. The VSC-HVDC is preferred over the HVDC classic. As described in Chapter 2 in comparison of both technologies, VSC-HVDC has interesting features than classic HVDC. Therefore those advantages of VSC-HVDC are capitalized on for a successful IPP's integration, compliant to the grid code. Figure 4.1 shows the system configuration where the IPPs: solar park, wind farm and conventional generator; are all connected to the grid through the HDVC-VSC link. The grid is driven by the synchronous generator G1.

A 200 MW conventional power plant, 150 MW wind farm and 60 MW solar power plants with VSC-HVDC connection to the grid are considered for system testing. Energy storage system is connected in parallel with solar IPP plant in order to replace the later during the night or in case of shut down or insufficient output.

In this chapter, different components of the system are described. Some of the main circuit parameters were assumed on the basis of system ratings, while others were determined.

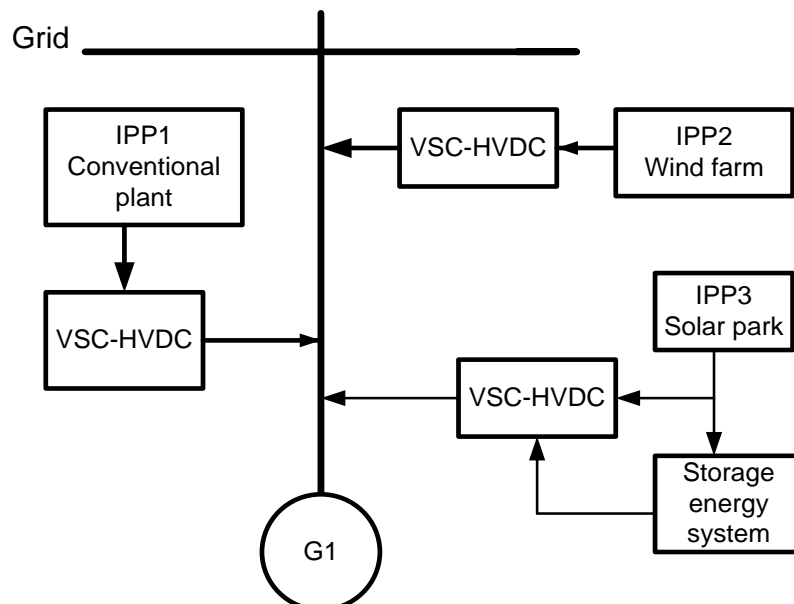


Figure 4. 1: System design

4.2 Main circuit components and parameters

The system to study consists of the following main components:

1. A wind farm
2. A solar power plant
3. Three-winding transformers
4. HVDC-Voltage source converters
5. Converter transformers
6. HVDC cables

4.3 Wind farm

4.3.1 Introduction

A no storage wind-diesel model system is considered to make a wind farm. The idea is to have an independent wind power plant that supply an isolated network, but at the same time is called to supply the grid when necessary. As it can be seen from Figure 4.2, the wind farm model is composed of an asynchronous wind generator, capacitor banks, a synchronous condenser, power control equipment and loads connected to it.

An asynchronous generator and a diesel driven synchronous condenser are required to supply customer load and secondary load. During high wind speeds, when wind power exceeds the load demand, the synchronous machine is used as a condenser. The excitation system of the condenser will control the grid voltage at its nominal value.

Secondary load bank is used for the regulation of system frequency by absorbing the excess of power produced. This is achieved by setting, a sets of three phase resistors in series with GTO thyristors switches which are switched accordingly to the deviation of the frequency from the nominal value. Each set of load resistor is made in the way that it is possible to vary it by steps of 1.75 MW for the current experiment.

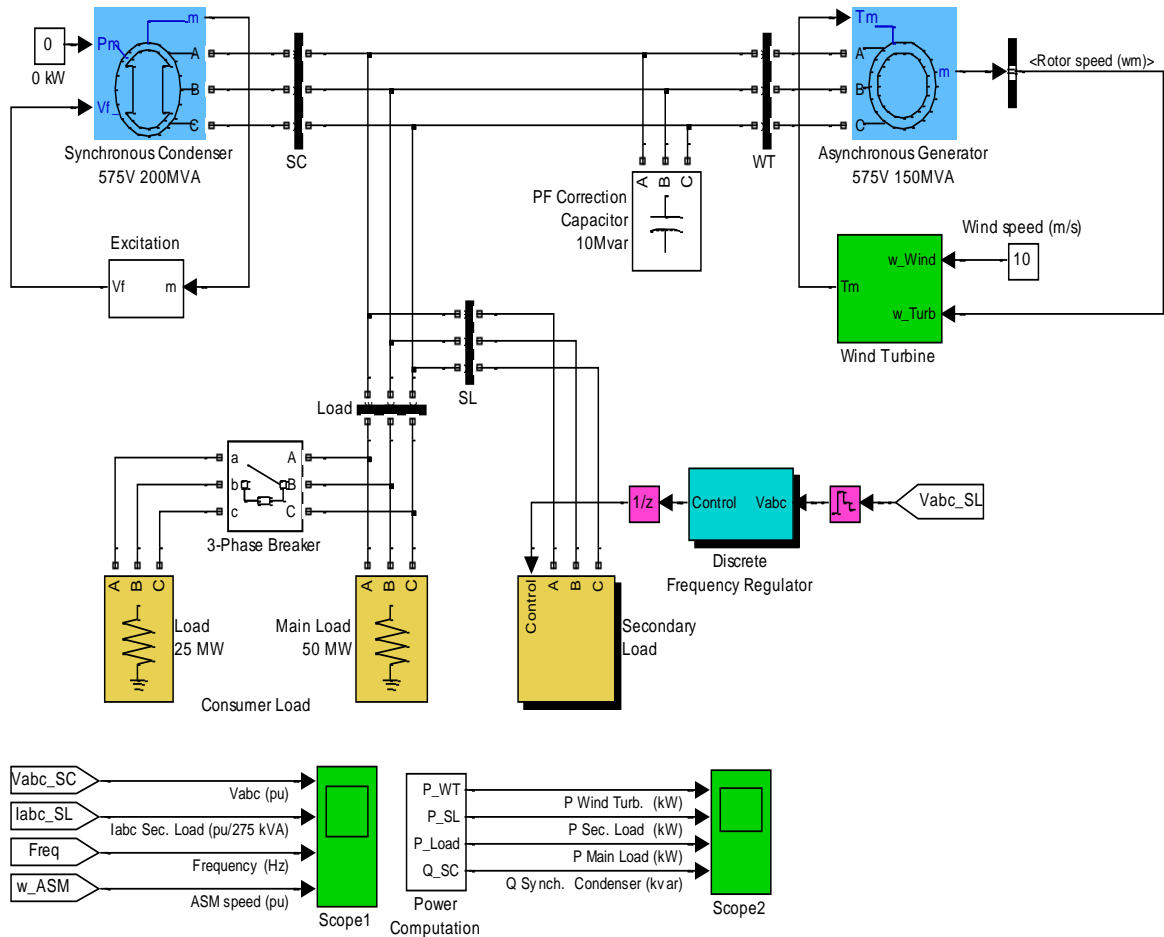


Figure 4.2: Asynchronous generator based wind farm in isolated network

4.3.2 Frequency regulator

The frequency control is performed by the discrete frequency regulator unit or block, As shown in Figure 4.3. It is based on standard three phase locked loop (PLL) system for frequency system measurement. A comparison between the measured frequency and the reference frequency (60 Hz in the current experiment) is made to get frequency error. The latter is processed through the integrator in order to get the phase error. The phase error is applied to a proportional differential (PD) controller to generate a signal that represents the required secondary load power. The signal from the PD is then converted into 8-bit digital signal that controls the switches of the eight three-phase secondary loads shown in Figure 4.4. However, the switching is performed at zero crossing of voltage in order to prevent disturbances.

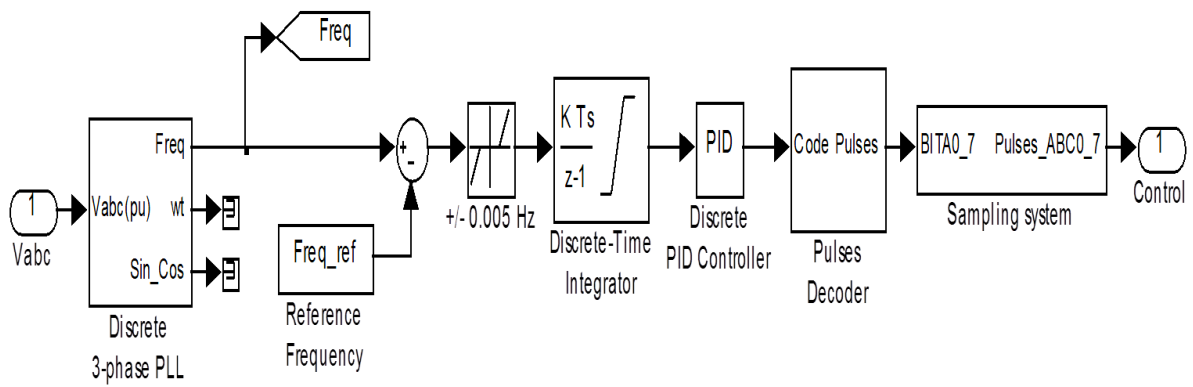


Figure 4.3 : Discrete frequency regulator process

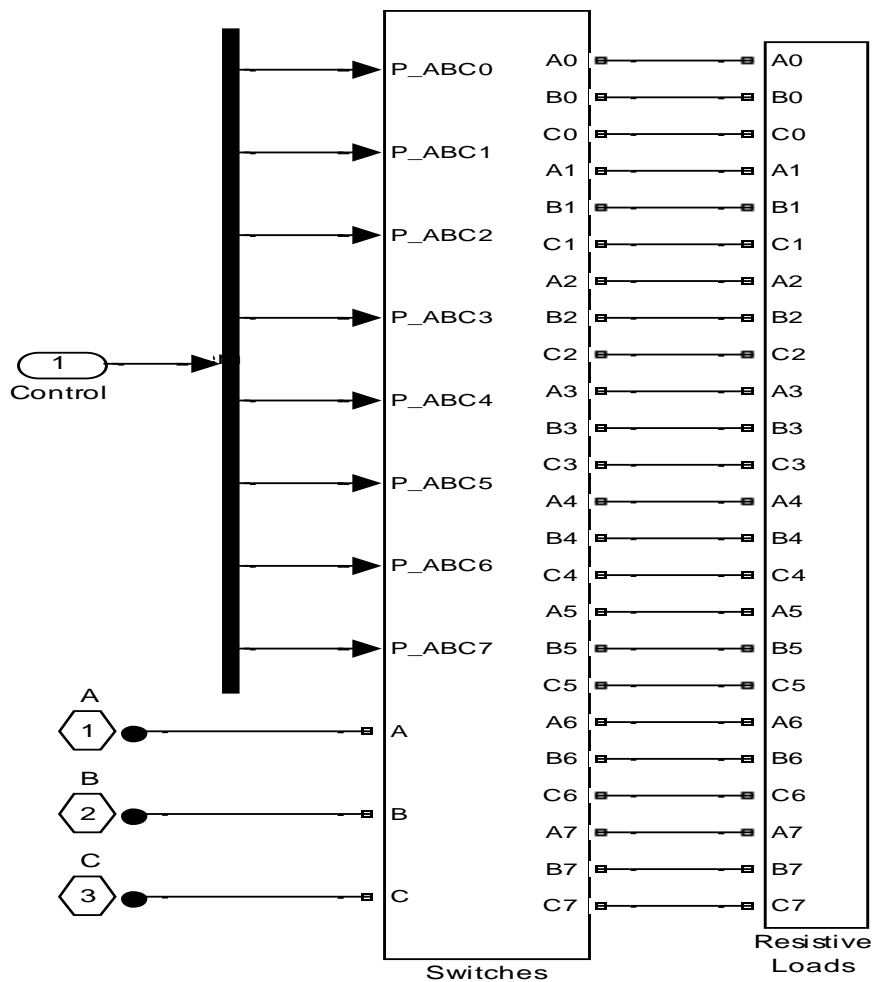


Figure 4.4: secondary loads switching process

4.3.3 Synchronous condenser

The synchronous machine is provided to support the wind turbine in case the wind speed is not enough for the generator to produce required power to supply the load. But in the present case the wind speed is assumed enough, above 10m/s. Thus the synchronous machine is not receiving any mechanical energy, rather is acting as condenser providing reactive power to support the asynchronous generator to meet the demand. In the present design the synchronous condenser has following configuration and parameters:

- Wye connected on internal neutral point.
- Mechanical input is set to zero
- Rotor type is a salient pole
- Power nominal: 200 MVA
- Line Voltage: 575 Volts
- Frequency: 60 Hz
- Stator resistance R_s (pu): 0,017
- Inertia coefficient: 1
- Friction factor: 0
- Pole pairs: 2

An excitation system is implemented using Institute of Electrical and Electronics Engineers (IEEE) type 1 synchronous machine voltage regulator combined with an exciter. As shown on Figure 4.5, the system uses dq components of the stator voltage measurement to calculate and supply the correct value excitation or field voltage (V_f) to be applied to the synchronous machine. All is done in accordance to the reference (V_{ref}) and in conjunction with the stabilization voltage from user-supplied power system stabilizer (V_{stab}). All measurements are per unit.

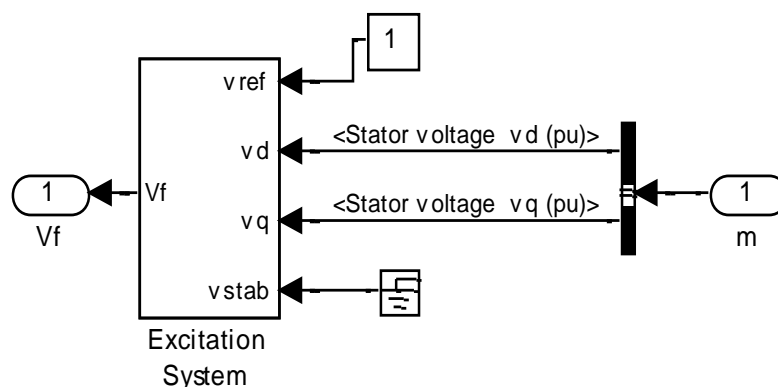


Figure 4. 5: synchronous condenser excitation system

4.3.4 Wind turbine

A wind turbine with characteristics shown in Figure 4.6 is used to drive an asynchronous generator at a speed of 1800 round per minute (rpm). In the present model, the wind speed is set at 10 m/s, so a control strategy is used to keep the speed of the asynchronous despite changes in wind speeds.

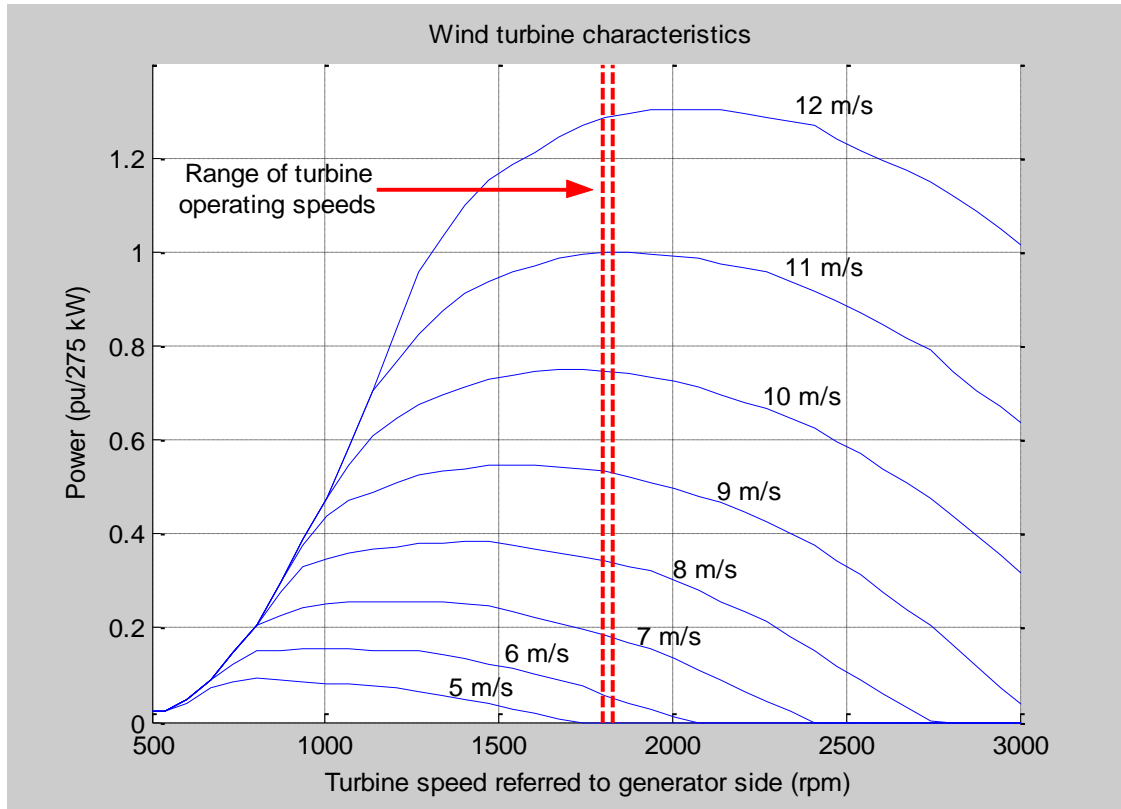


Figure 4.6: Wind turbine characteristics

The control strategy for this turbine consists in keeping the turbine, driving the asynchronous generator, to the rotational speed of 1800 rpm. At that speed the generator can produce enough power to meet the demand. As shown in Figure 4.7, the measurement of the turbine and the synchronous generator speeds w_{Turb} and w_{Asw} respectively, are taken. The values measured are then compared to the references. In case of low rotational speed of turbine and consequently the generator rotor speed; a gain is applied by controllers to the turbine to meet the 1800rpm. Otherwise, the switches are activated to the signal for turbine speed damping in case it tends to go higher than the set value. Thus, an appropriate mechanical torque T_m is constantly applied to the generator rotor.

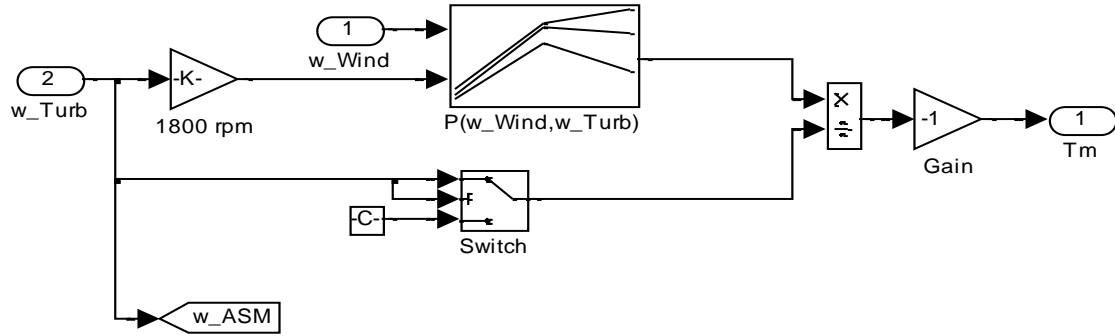


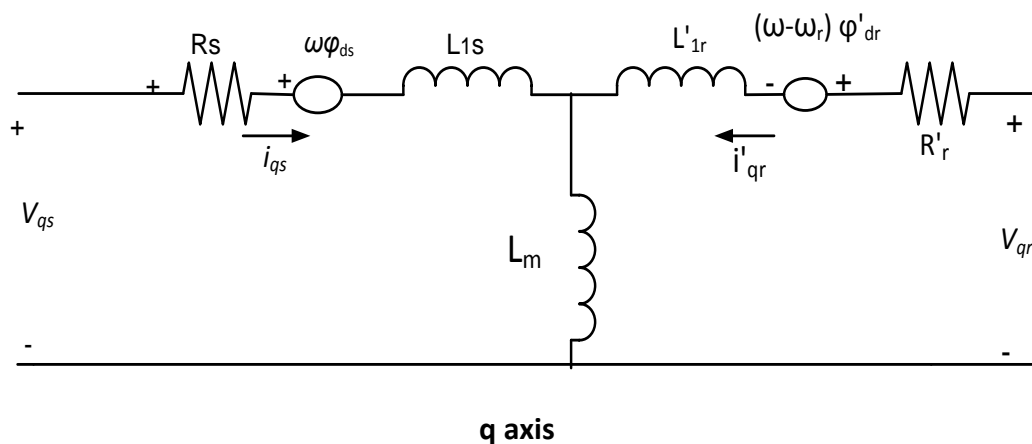
Figure 4.7: Wind turbine control diagram

4.3.5 Asynchronous generator

A squirrel cage rotor three phase synchronous machine was used. It produced 575 volts, 60 Hz at 1800 rpm and power around 150 MVA. With parameters shown in Table 4.1 below, the electric part of the machine is modelled in dq frame according to Figure 4.8. The machine received the mechanical power input from the turbine and run at constant speed. While the mechanical part or system was modelled according mathematical equation

Table 4. 1: Asynchronous generator parameters used

Parameter	Value
Nominal power (Pn)	150 MVA
Voltage (line –line)	575 V
Stator resistance (Rs) p.u	0.016
Stator inductance(Ls) p.u	0.06
Rotor resistance (Rr') p.u	0.015
Rotor inductance (Lr') p.u	0.06
Mutual inductance (Lm) p.u	3.5
Inertia constant H(s)	2
Friction factor F p.u	0
Pole pairs	2



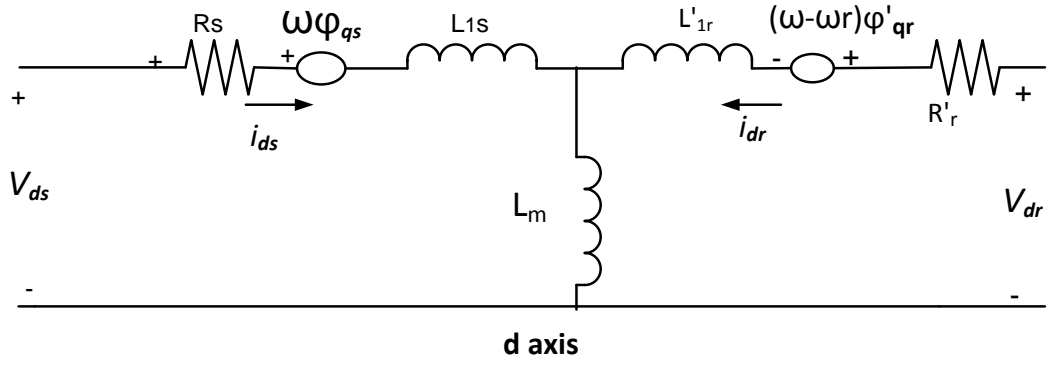


Figure 4. 8 : Asynchronous squirrel cage machine in dq model

As it is shown in Figure 4.8 of asynchronous machine electric model, all variables and parameters are referred to stator side. This is indicated by the prime signs in the machine equations given below. The use of dq model gives different parameters equations independently one to each, dq transformation theory is given in appendices .Thus; from this model the following equations are derived:

$$V_{qs} = R_s i_{qs} + \frac{d\phi_{qs}}{dt} + \omega\phi_{ds} \quad (4.1)$$

$$V_{ds} = R_s i_{ds} + \frac{d\phi_{ds}}{dt} - \omega\phi_{qs} \quad (4.2)$$

$$V'_{qr} = R'_r i'_{qr} + \frac{d\phi'_{qr}}{dt} + (\omega - \omega_r)\phi'_{dr} \quad (4.3)$$

$$V'_{dr} = R'_r i'_{dr} + \frac{d\phi'_{dr}}{dt} - (\omega - \omega_r)\phi'_{qr} \quad (4.4)$$

$$T_e = 1.5 p (\phi_{ds} i_{qs} - \phi_{qs} i_{ds}) \quad (4.5)$$

With:

$$\phi_{qs} = L_s i_{qs} + L_m i'_{qr} ; \quad \phi_{ds} = L_s i_{ds} + L_m i'_{dr} ; \quad \phi'_{qr} = L'_r i'_{qr} + L_m i_{qs}$$

$$\phi'_{dr} = L'_r i'_{dr} + L_m i_{ds} ; \quad L_s = L_{lr} + L_m ; \quad L'_r = L'_{lr} + L_m$$

and with mathematical model for the mechanical system given by the following equations :

$$\frac{d\omega_m}{dt} = \frac{1}{2H} (T_e - F\omega_m - T_m) \quad (4.6)$$

$$\frac{d\theta_m}{dt} = \omega_m \quad (4.7)$$

And where for both models:

ω = Reference frame angular velocity

ω_r = Electrical angular velocity

R_s, L_{ls} = Stator resistance and leakage inductance

L_m = Magnetizing inductance

L_s = Total stator inductance

V_{qs}, i_{qs} = q axis stator voltage and current

V_{ds}, i_{ds} = d axis stator voltage and current

$\varphi_{qs}, \varphi_{ds}$ = Stator q and d axis fluxes

ω_m = Angular velocity of the rotor

θ_m = Rotor angular position

p = Number of pole pairs

ω_r = Electrical angular velocity given by $(\omega_m \times p)$

θ_r = Electrical rotor position angular position given by $(\theta_m \times p)$

T_e = Electromagnetic torque

T_m = Shaft mechanical torque

J = Combined rotor and load inertia coefficient. Set to infinite to simulate

H = combined rotor and load inertia constant. Set to infinite to simulate locked

F = Combined rotor and load viscous friction coefficient

4.3.6 Power factor correction capacitor

Capacitor banks are installed in parallel with the turbine in order to assist it with the reactive power. For the power factor correction 10 Mvar capacitors were used, as the power factor was set to around 0.9, therefore there is a need for capacitors banks. They can be connected to the bus through the circuit breakers and could be controlled manually. On the other hand, a converter can be used instead to allow automatic control. As they are controlled using three different controllers, namely AC voltage, DC voltage and current regulators. The three controllers interact to provide the control signal to the converter connecting the capacitor banks to the bus.

4.4. The grid

The grid is represented by a Thevenin's equivalent model, on Figure 4.9, it consists of voltage source with series impedance, representing the lines impedance's parameters. The source is internally wye ground connected, running at 50 Hz and in swing mode. The source inductance is set to 62.23 mH and the source voltage output is 120 kV. The resistive and inductive parts of the impedance are determined from the grid angle. The voltage source models conventional power plant, that drives the grid and is taken as the reference for measurements.

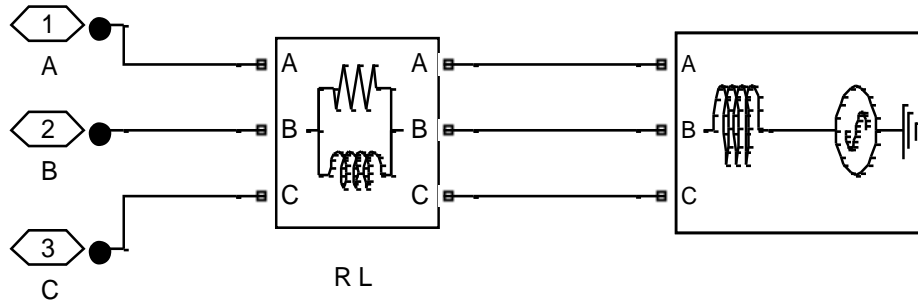


Figure 4. 9: Grid model

4.5. Converter transformer

The converter transformer serves two purposes: the first is the interface between the AC network and VSC, the second is to adjust the AC voltage level to a suitable level for the converters. The transformers may be of different designs depending on the power to be transmitted and possible transport requirements. Thus, the grid side converter transformers have the nominal voltage ratio of 100/120 kV as they interface the 100 kV VSC with the 120 kV grid. The transformers are sized at 200 MVA with leakage reactance of 15 pu.

4.6. Voltage Source Converters

Three-level bridge IGBT based converter was used for the VSC-HVDC transmission. Sine-triangle modulation switching frequency ratio of 27 was used to control the switches. Series RC snubber circuits are connected in parallel with each switch device. Thus 5 kΩ snubbed resistors are used in addition to the 1μF capacitances for this purpose.

Due to the pulse width modulation and high frequency switching of the converter, harmonics were generated all around the switching frequency and their multiples. The magnitude of harmonics is expressed in output Equation (4.8) by (Grahame & Thomas, 2003):

$$\begin{aligned}
 v_{an}(t) = & \frac{V_{dc}}{2} M \cos(\omega_0 t + \theta_0) + \frac{2V_{dc}}{\pi} \sum_{m=1}^{\infty} \frac{1}{m} J_0\left(\frac{m\pi}{2} M\right) \sin\left(\frac{m\pi}{2}\right) \cos\{m(\omega_c t + \theta_c)\} \\
 & + \frac{2V_{dc}}{\pi} \sum_{m=1}^{\infty} \sum_{\substack{n=-\infty \\ n \neq 0}}^{\infty} \frac{1}{m} J_n\left(\frac{m\pi}{2} M\right) \sin\left(\frac{(m+n)\pi}{2}\right) \cos\{m(\omega_c t + \theta_c) + n(\omega_0 t + \theta_0)\}
 \end{aligned}
 \tag{4.8}$$

with:

$v_{an}(t)$ = Instantaneous line to ground voltage

V_{dc} = Pole to pole dc voltage,

M = Modulation index

ω_c, ω_o = Fundamental and carrier frequencies

θ_o, θ_c = Phase angles of the fundamental and the carrier frequency at time, ($t=0$)

$J_i(\beta)$ = i -th order Bessel function of the first kind with the argument, β .

As it can be seen from the expression above; as m , the multiple number of switching frequency increases; the amplitude of harmonic components decreases. Thus, the harmonics near the first and second multiple of the switching frequency are greater in magnitude in comparison to the rest. Third harmonics are blocked by the converter transformer winding arrangements.

4.7. Filters

In order to comply with AC system or the grid code about harmonics, shunt filters were used. They were low rated in regards to the converter rating, because only the high frequency harmonics generated by PWM were treated. The AC harmonics mainly depends upon the:

- Type of modulation (e.g. single-phase or three-phase carrier based, space vector, etc.)
- Frequency index p = carrier frequency / modulator frequency (e.g. $p = 1350/50 = 27$)
- Modulation index m = fundamental output voltage of the converter / pole to pole DC voltage

As for the present model the principal harmonic voltages were generated at and around multiples of p . The shunt AC filters were 27th and 54th high pass totaling 40 Mvar.

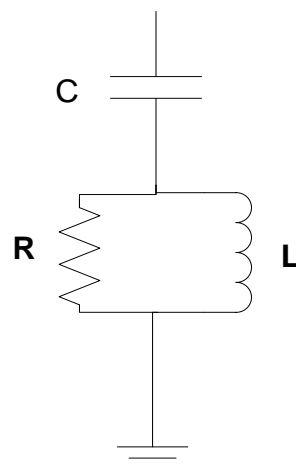


Figure 4. 10: AC high pass filter

Two filters, tuned at the 27th and 54th harmonic frequencies, were used at each of the two VSC-HVDC terminals in this test system. They both had the quality factors of 15, and they injected 18 and 22 Mvar power respectively. All the filters were three phases Y connected made

of capacitor, inductor and capacitance were calculated from these data. The frequency characteristics of these filters are shown in Figure 4.11 and Figure 4.12. It can be seen that the impedance of the filters reach its maximum peak at 50 Hz and thereafter decrease to its minimum value at 27th and 57th harmonics, which means that the components of the voltage signal with frequency beyond the fundamental they are channeled to ground through those filters and the components at fundamental frequency are the only ones flowing to the output.

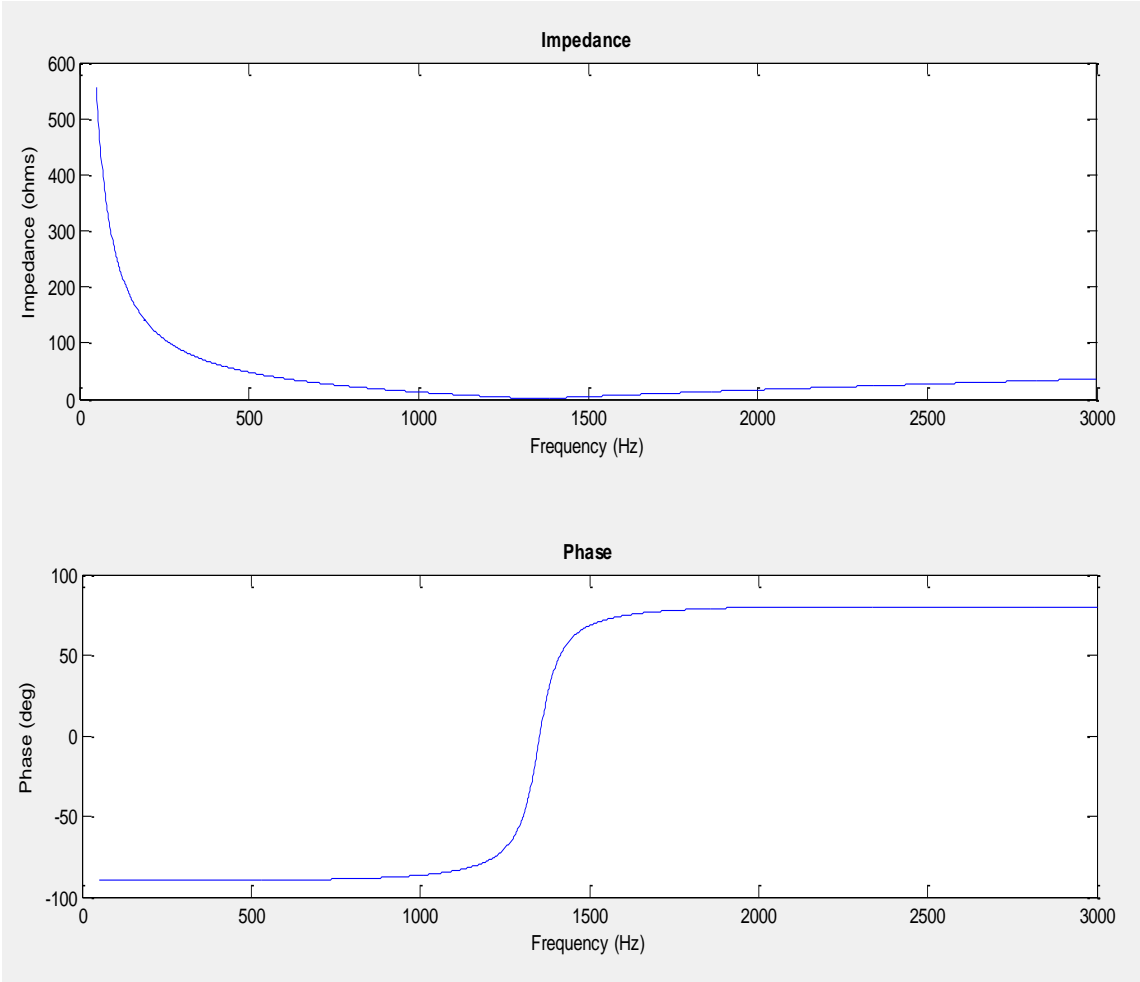


Figure 4. 11: High pass filter response frequency characteristics at 27th harmonic

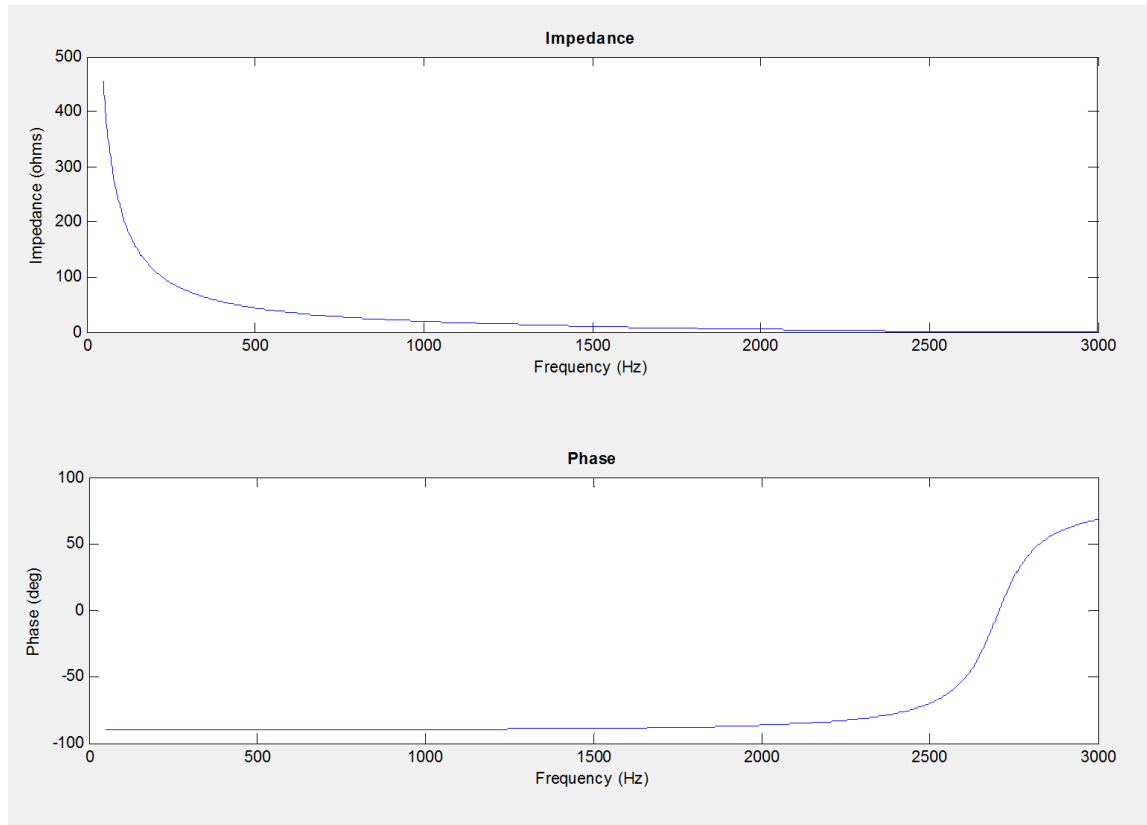


Figure 4. 12: High pass filter frequency response characteristic at 54th harmonics

4.8 DC Capacitors

In addition to AC side harmonics, the DC voltage and current have harmonics resulting from the PWM switching action. The DC side capacitors are important features of a VSC-HVDC system, besides maintaining the DC voltage, they also act as filters of the harmonics that appear in form of current or voltage ripples.

The design of the DC side capacitors took into a count the DC link voltage, the power handling capacity of the converter as well as the transient state of the system in case of a faults on AC side. In the latter, large power oscillations may rise between the AC side and DC side, which will result in overvoltage and stress on the converter.

The capacitor is sized in terms of its time constant; the necessary time for it to fully charge at nominal DC voltage by the rated current is given by equation 4.9. In our models 70 μ F capacitor was used.

$$\tau = \frac{C V_{dc}^2}{2Pn} \quad (4.9)$$

Where:

τ = Time constant

C = Capacitance

P_n = Nominal apparent power transmitted

V_{dc} = Nominal DC voltage

4.9 HVDC Cables

For the VSC-HVDC transmission usually cross linked polyethylene (XLPE) cables are used. For the present model the pi section cables are used, for power transmission rated at 200 MW and ± 100 kV dc voltage. A flowing current around 2 kA is expected. The cables have 13, 9 m Ω /km, 15.9 mH/km, capacitance of 23.1 μ F per km.

Different distances are used as the conception is of distributed power generation points connecting to the HVDC high way linking to the AC grid. As the DC voltage is the one transmitted only ohm losses are a concern in our model.

4.10 Converter control

The VSC-HVDC system has got two converters with the same design but working independently one from another, no communication is used between the sending and the receiving end for control purposes. They are able to control either the P and Q at station 1 or Udc and Q at station 2.

Figure 4.13 shows the overview diagram of the VSC-HVDC converter control system on the grid side.

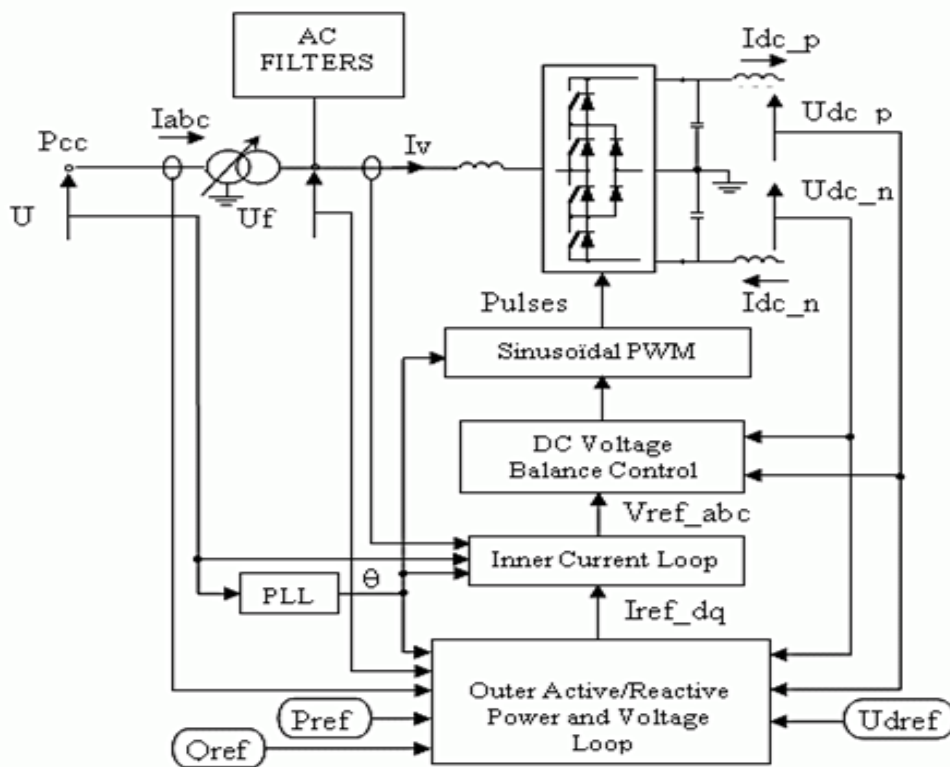


Figure 4. 13: VSC-HVDC converter control system

The vector control method is used, where Clark's transformations block transforms from rotating frame three-phase quantities to space vector components α and β . The measurement of the signal taken (U and I) are transformed such way that they will have the same reference frame as the signals on the secondary side of the transformer. The dq transformation is then applied to α and β in order to obtain axis "d" and axis "q" quadratic quantities (two axis rotating reference frame).

The phase locked loop block takes the system frequency and produces for the Clark's transformer block, the phases angles parameters which are $\sin \theta$ and $\cos \theta$. The fundamental of α component and the phase of the point of common connection (PCC) voltage (U_{abc}), are in phase with $\sin \theta$ during the steady state.

4.10.1. Outer Active and Reactive Power and Voltage Loop

The converter reference current vector (I_{ref_dq}), which is the input to inner current loop is evaluated by outer loop regulators contained in the active, reactive power and voltage loops. The control modes are: in the "d" axis, either the active power flow at the PCC or the pole-to-pole DC voltage; in the "q" axis, the reactive power flow at the PCC. There is a possibility of adding an AC voltage control mode at the PCC in the "q" axis.

In order to increase the time constant or the response speed, reactive power control regulator loop combines a PI control with a feedforward control. To avoid integrator wind-up, the following actions are taken: the error is reset to zero, when the measured PCC voltage is less than a constant value (i.e., during an AC perturbation); In case of limitation of the regulator output, the limitation error fed back to the integrator entry with positive sign. The AC voltage control override block, implemented with two PI regulators, will step aside the reactive power regulator to maintain the AC voltage at point of common connection within the predefined range, especially during the steady state.

The working principle of the active power control block is the same as of reactive power control block. An extra ramping block ramps the power order towards the defined value with an adjusted rate when the control is de-blocked. In case the converter is blocked, the value of the ramp is reset to zero. The DC voltage control override block, based on two PI regulators, will override the active power regulator to maintain the DC voltage within a secure range, especially during a perturbation in the AC system of the station controlling the DC voltage.

A PI regulator is used within DC voltage control regulator block. The latter is enabled when the Active Power Control block is disabled. The block output provides to the converter current vector "d" component, a reference value, for the current reference limitation block.

The current reference calculation block transforms the active and reactive power references, calculated by the P and Q controllers, to current references according to the measured (space vector) voltage at the filter bus. The current reference is estimated by dividing the power

reference by the voltage (up to a minimum preset voltage value). Moreover, the current reference vector is limited to a maximum acceptable value by the equipment by the current reference limitation block. In power control mode, equal scaling is applied to the active and reactive power reference when a limit is imposed. While in DC voltage control mode, higher priority is given to the active power when a limit is imposed for an efficient control of the voltage.

4.10.2. Inner current loop

In current loop control block, an AC current control tracks the current reference vector d and q components using the feed forward scheme for a fast control of the load current variations and faults. Thus, fault currents do not exceed the references. The idea is to know the values of the U_{dq} vector voltages in order to calculate which voltage values the converter should have. This is achieved by adding the voltage drops due to currents through impedance between the U and the PWM-VSC voltages. Calculations are made using state equations that reproduce VSC currents dynamics and currents through AC filters are not taken into account. A decoupling of dq components is done for obtention of independent first order plants model. The two independent first order models are used with the proportional integral (PI) converter current feedback to reduce the error to zero in steady state. The output of the AC current control block is the unlimited reference voltage vector V_{ref} in dq .

In process of generating the voltage reference, the actual DC voltage and the maximum peak value of the fundamental bridge phase voltage in relation to the DC voltage were considered. In the three-level NPC with carrier based pulse width modulation (PWM) that we were using, the ratio between the maximum fundamental peak phase voltage and the DC total voltage is equal to 0.816. Thus, the converter is able to generate up to $1/0.816$ or 1.23 p.u when the modulation index is . However, the reference voltage limitation block prevents the reference voltage vector to go beyond 1, as no over modulation is needed.

4.10.3. DC voltage balance control

The balance between the DC positive and negative voltages, during the steady state is kept by the DC voltage balance control. However, small differences can occur, result of the changes of converter active or reactive current. Also, the nonlinearity and lack of precision in switching of PWM switch bridge voltage. Moreover, the imbalance between the circuit impedance may cause the deviations between pole voltages.

The difference between pole voltages is determined by the midpoint current. As it is shown in Figure.4.14 and by the equation 4.10, the midpoint current I_{d_0} determines the upper and lower DC voltages difference U_{d_0}

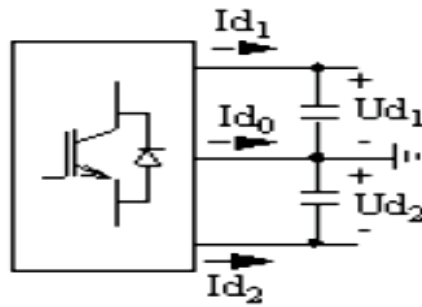


Figure 4. 14: DC voltages and currents of a three level bridge

$$Id_0 = (Id_1 - Id_2) = -C \frac{d}{dt} (Ud_1 - Ud_2) = -C \frac{d}{dt} (Ud_0) \quad (4.10)$$

By varying the conduction times of the switches in pole, it is possible to change the average of the midpoint current and have a control over the difference voltage Ud_0 . It is possible to reduce to zero a positive difference ($Ud_0 \geq 0$) by increasing the amplitude of the reference voltage that generates a negative DC midpoint. This has to be done at the same time as the amplitude of the reference voltage that generates a negatives midpoint is reduced. This is achieved by adding an offset signal to the sinusoidal reference voltage. In fact, the bridge voltage is subject to distortions which are limited by the fact that the control is done slowly. In order to achieve a good performance this control should be done in the station controlling the DC voltage.

4.11 Solar power plant

4.11.1 Introduction

A solar power plant with 65MW power capacity is considered. The plant is made out with the association of solar panels to achieve the required output. The configuration of the plant is according to Figure 4.15

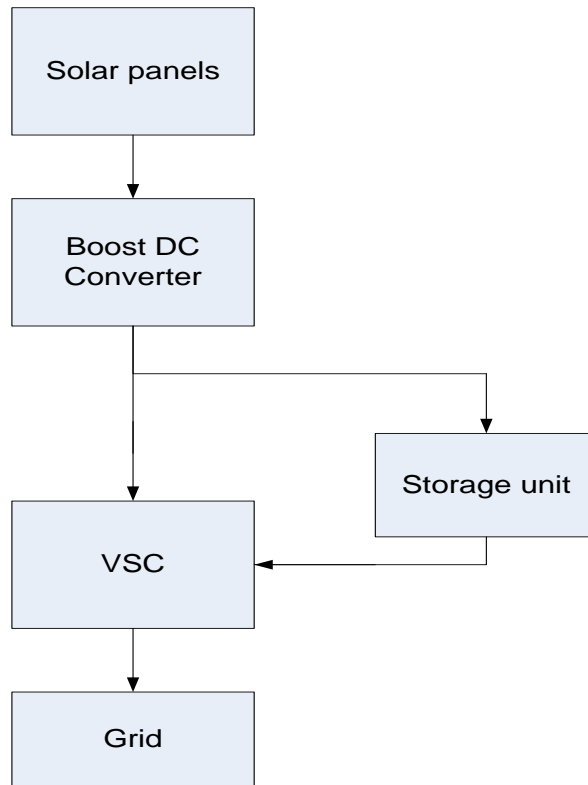


Figure 4. 15: Solar Park connected to grid

The power plant consists of following main components:

- solar panels
- charge controller
- storage unit and a
- boost converter

4.11.2 Solar panels

Solar panels are implemented using the amorphous solar cells. For our design, the solar cells are modeled in Simulink using the electrical model. According to the model in Chapter 3, where solar cell electrical model is made as a parallel combination of a current source, two exponential diodes and a parallel resistor, R_p , that are connected in series with a resistance R_s . The output current I is given by:

$$I = I_{ph} - I_s \cdot (e^{(V+I \cdot R_s)/(N \cdot V_t)} - 1) - I_{s2} \cdot (e^{(V+I \cdot R_s)/(N_2 \cdot V_t)} - 1) - (V+I \cdot R_s)/R_p \quad (4.11)$$

I_s and I_{s2} are the diode saturation currents, V_t is the thermal voltage, N and N_2 are the quality factors (diode emission coefficients) and I_{ph} is the solar-generated current.

The quality factor varies for amorphous cells, typically ranges between 1 and 2. The amount of solar energy that reaching the cells is expressed as irradiance, I_r (light intensity) in W/m^2 falling onto the cell. The solar-generated current I_{ph} , is given by $I_r \cdot (I_{ph0}/I_{r0})$ where I_{ph0} is the measured solar-generated current for irradiance I_{r0} . The values of different parameters are shown in Table 4.2 below:

Table 4. 2: solar cells parameters

Parameters	Value	Unit
Diode saturation current , I_s	1e-6	A
Diode saturation current , I_{s2}	0	A
Solar-generated current for measurements, I_{ph0}	7.34	A
Irradiance for measurement, I_{ph0}	1000	W/m^2
Quality factor, N	1.5	-
Quality factor, N2	2	-
Series resistance, R_s	0	Ohms
Parallel resistance, R_p :	infinity	Ohms

4.11.12 Controller

A controller of generated voltage by the solar park is implemented by electronics devices. The controller is of paramount importance for any solar power systems with storage unit. The controller function is to regulate the power flowing from the solar panels to the storage units. The overcharging will reduce the lifespan of the storage unit, which is in our case superconducting magnetic energy storage (SMES). The overcharging of the latter may result in more damage not only for the unit but also for the personnel working around it.

The basic operation that does the controller is to monitor the storage unit voltage and disconnect it once fully charged. The actual controllers, far different from the older ones that were using mechanical relay to disconnect or connect the storage units, they use pulse width modulation (PWM).

The uses of pulse width modulation (PWM) permits a slow reduce of the power amount applied to the storage unit as it gets closer and closer to fully charged level. This method allows less stress on the unit during the charging and can keep the storage unit in a fully charged state indefinitely.

In summary, beside the main function of regulating the power flowing to storage unit in order to avoid the overcharging and prevention of reverse current flow, the controller is due to:

- To halt the battery when fully charged
- Disconnect the storage unit when discharged
- Monitoring the storage unit output voltage and the state of charge

Giving alarm at the occurrence of fault condition

Detecting whenever no power is coming from the solar panels, disconnect the storage unit and prevent a reverse current.

4.11.13 Storage unit

In our model, the storage unit used is a superconducting magnetic energy storage (SMES) unit. As it was developed in Chap 3, SMES have got high power storage density and with this method of storage; fast charge and discharge are possible. This high dynamic that permits response that range of milliseconds is the main advantages. Compared to the ordinary batteries, the SMES can withstand tens of thousands of charging cycles without losing their storing capacity, thus the life cycle is greater.

In the design, the super magnetic energy storage is feed by the boost converter. During the discharge, which is thought to happen during the event of no power is provided by the solar panels; power is delivered to the grid side through an HVDC-VSC converter. Beside the advantages of Superconducting magnetic energy storage, as shown in (Ana, et al., 2013) its association with the VSC-HVDC permits a good power quality injected into the grid.

4.11.14 Boost converter

1. Introduction

A boost converter is a dc to dc converter that has an output dc voltage greater than its input dc voltage. It is categorised among switching mode supply and it is composed with more less two power electronics switches and one energy storage element .The switching control is performed by pulse width modulation (PWM).

Boost converter shown on Figure 4.16, produces an output which is greater than the input V_{in} . The working principle consists in switching on and off the converter for a certain period of time, according to the load requirement. We can say that the actual converter has two modes of function: the ON mode and OFF mode. Both modes topologies are shown in Figure 4.17.and Figure 4.18, while the characteristic of the two modes duty cycle against time is shown on Figure 4.19

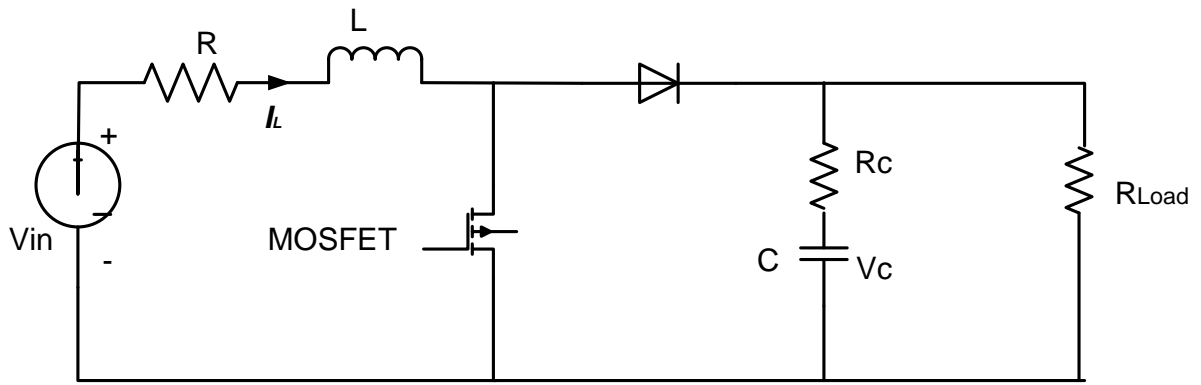


Figure 4. 16: DC-DC boost converter topology

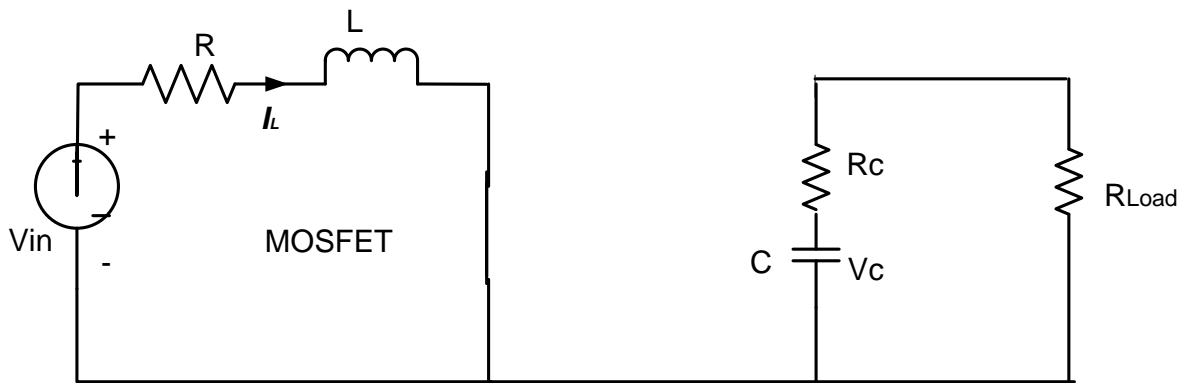


Figure 4.17: DC-DC boost converter ON mode topology

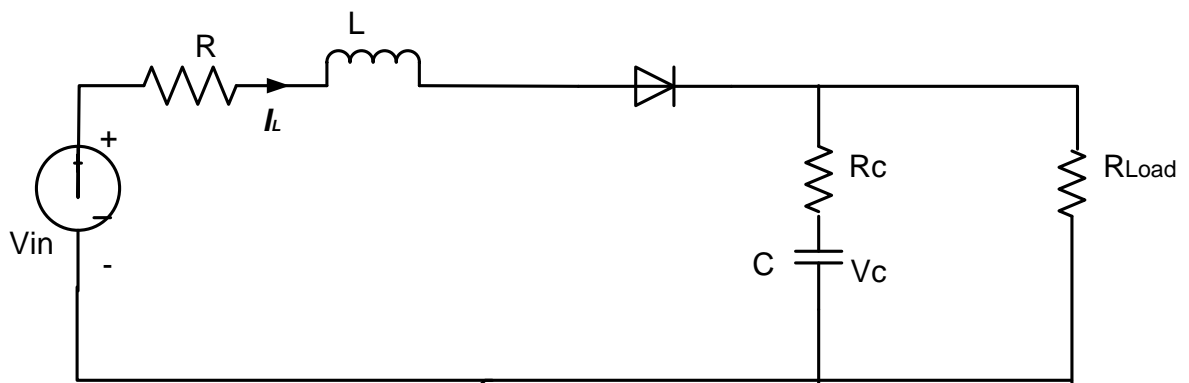


Figure 4.18: DC-DC boost converter OFF mode topology

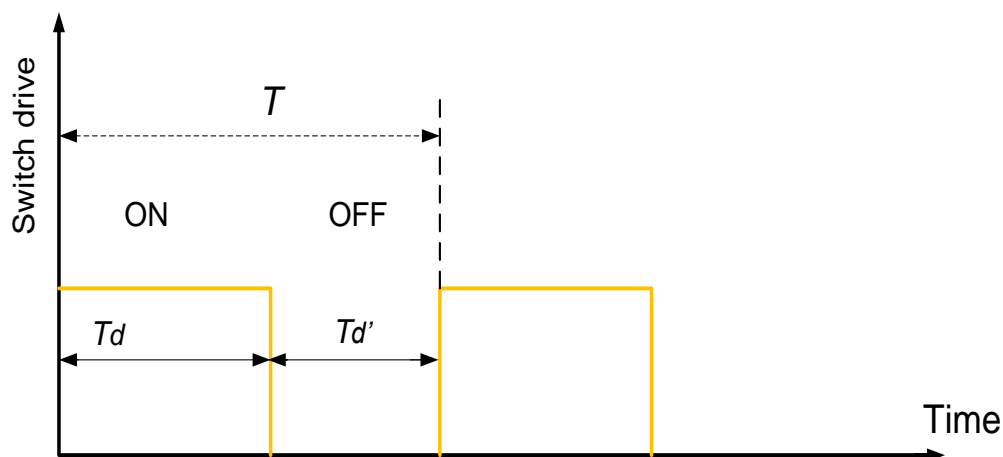


Figure 4. 19: ON and OFF modes time duration

The DC-DC boost converter model on Figure 4.16 is considered as ideal. Therefore, we consider the voltage drop as zero during the time the switch is ON. On other hand, we consider that there is no current flowing during the time the switch is OFF and that voltage drop across the switch is at maximum. The diode, considered as the ideal one, has zero voltage drops during the conducting state and zero current flowing during the reverse-bias mode. The switching of the diode is considered as instantaneous, no time delay during the switching ON and OFF. The capacitor and the inductor are considered as being lossless.

The circuit responses are periodic, which implies that the current is periodic. It has the same value at the start and the end of the switching cycle. The net inductor current increase over a cycle is zero. A different value, on-zero, would suggest that the average inductor current has to be either increased or decreased and then the inductor current is in a transient state and that is not periodic.

The ON and OFF switching sequences are performed at fixed frequency. We consider T as the time period corresponds the switching fixed frequency, while the duty cycle is D . Thus during the ON mode, the switch is closed or on for a period equal to DT . For the OFF mode, the switch is off or opens for a time interval equal to $(1-D) T$.

The inductor current is continuous and greater than zero. As the capacitor is large, the time constant RC is large as well such that changes in capacitor voltage during both modes ON and OFF are considered as none while calculating the change in inductor current and the average output voltage. The latter is considered to be constant as well as the input voltage V_s .

2. Analysis of the ON mode

During the ON mode the converter switch is closed. Figure 4.17 represents the equivalent circuit of the converter during the ON mode. As the switch is closed the source voltage V_{in} is applied across the inductor causing the rise of inductor current at a rate depending on input voltage V_{in} and the inductance L . This condition is described by the differential equation below

$$L \frac{di}{dt} = V_{in}(t) \quad (4.12)$$

For constant voltage source constant, the rise of inductor current is positive and remains so, as long as long there is no saturation into the inductor. Thus equation (4.12) may be written as

$$\frac{di}{dt} = \frac{V_{in}(t)}{L} \quad (4.13)$$

For the ON mode, the switch still ON for period of time DT during one cycle. Then DT can be taken as the total ON time for the switch, which makes equation (4.13) to be written as equation (4.14) expressing the net increasing in inductor current when the switch is ON.

$$\Delta i = \frac{V_{in}(t)}{L} (DT) \quad (4.14)$$

3. Analysis of OFF mode

Figure 4.18, shows the off mode circuit topology. During the off mode the switch is open and voltage across the inductor, for an output voltage V_o , is given by equation (4.15) below:

$$V_L = V_{in} - V_o \quad (4.15)$$

Having in mind that for a dc-dc boost converter the output voltage is greater than input voltage, equation (4.15) would be negative as well as the rate of rise of inductor current given by equation (4.16). Thus, if we consider the switch to be kept OFF for a time period equal to $(1-D)T$, then the change in inductor current can be calculated using equation (4.17)

$$\frac{di_L}{dt} = \frac{V_{in} - V_o}{L} \quad (4.16)$$

$$di_L = \frac{V_{in} - V_o}{L} (1 - D)T \quad (4.17)$$

Where for, recall :

V_{in} = the input voltage

V_o = the output voltage

L = the inductance

D = duty circle

T= period

di_L = change in inductor current.

From equation (4.17), we see that the value of change in inductor current is negative. This is due to the fact that the output voltage V_o is greater than the input voltage V_{in} . Knowing that the net change of inductor current over the cycle period is zero, therefore the sum of net changes in inductor current given by equations (4.14) and (4.17) is zero. Thus,

$$\frac{V_{in}(t)}{L} (DT) + \frac{V_{in}-V_o}{L} (1 - D)T = 0 \quad (4.18)$$

By rearranging the equation (4.18) we have:

$$V_o = \frac{V_{in}}{1-D} \quad (4.19)$$

Since the inductor current is a periodic function of time, $i_L(t)$, and the net change in inductor current is zero ; The net voltage across the inductor over cycle is zero also. Therefore using equation (4.18), in order for the equation to satisfy the zero condition we should have the following equation:

$$V_{in} * DT + (V_{in} - V_o) * (1 - D)T = 0 \quad (4.20)$$

From equation (4.19), we can see that for the output voltage to be greater than the input, the characteristic of a boost converter should be comprised between 0 and 1. In other words, $0 < D < 1$. Hence the output voltage has the lowest value when the D is equal to zero, which is equal to the input voltage. The maximum output voltage is obtained with D equal to 1, which makes the output theoretically infinity. In reality the D is varied between 0 and 0.9 for the maximum output. The characteristic of the boost converter, conversion ratio vs. the duty cycle, inductor voltage and current waveforms are shown on below on Figure 4.20 and Figure 4.21 respectively. For the voltage and current waveforms, only steady states for both the input and output are considered.

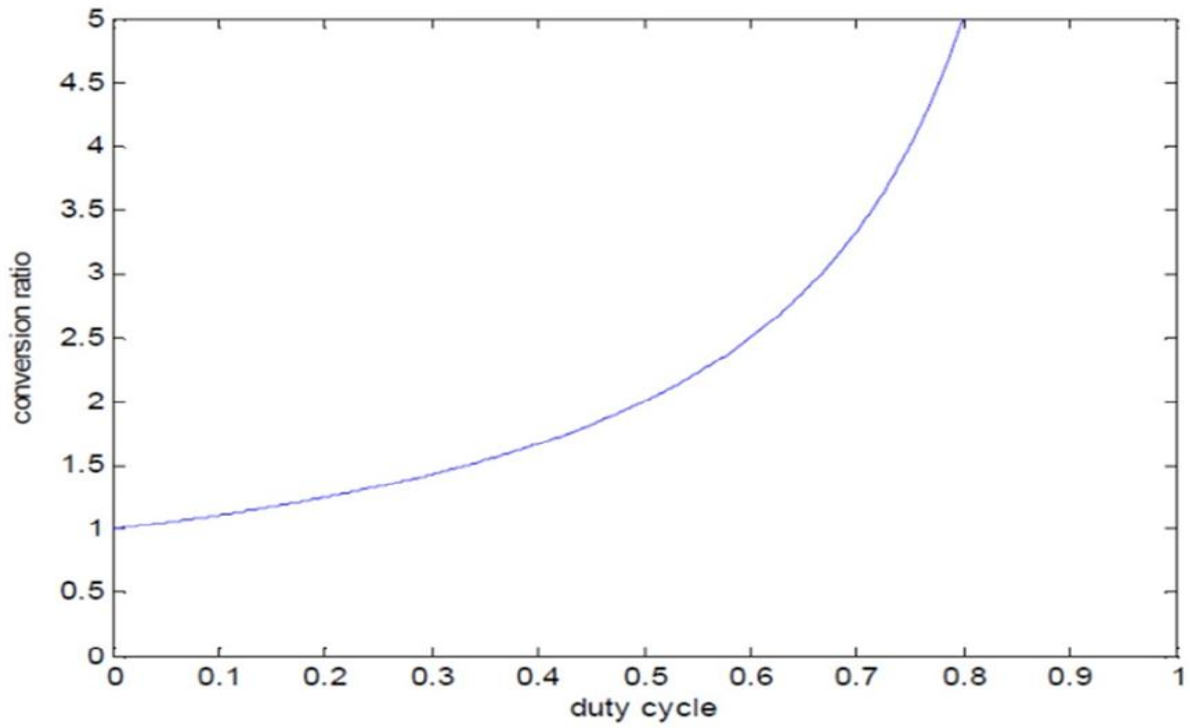


Figure 4. 20: DC-DC boost converter characteristic

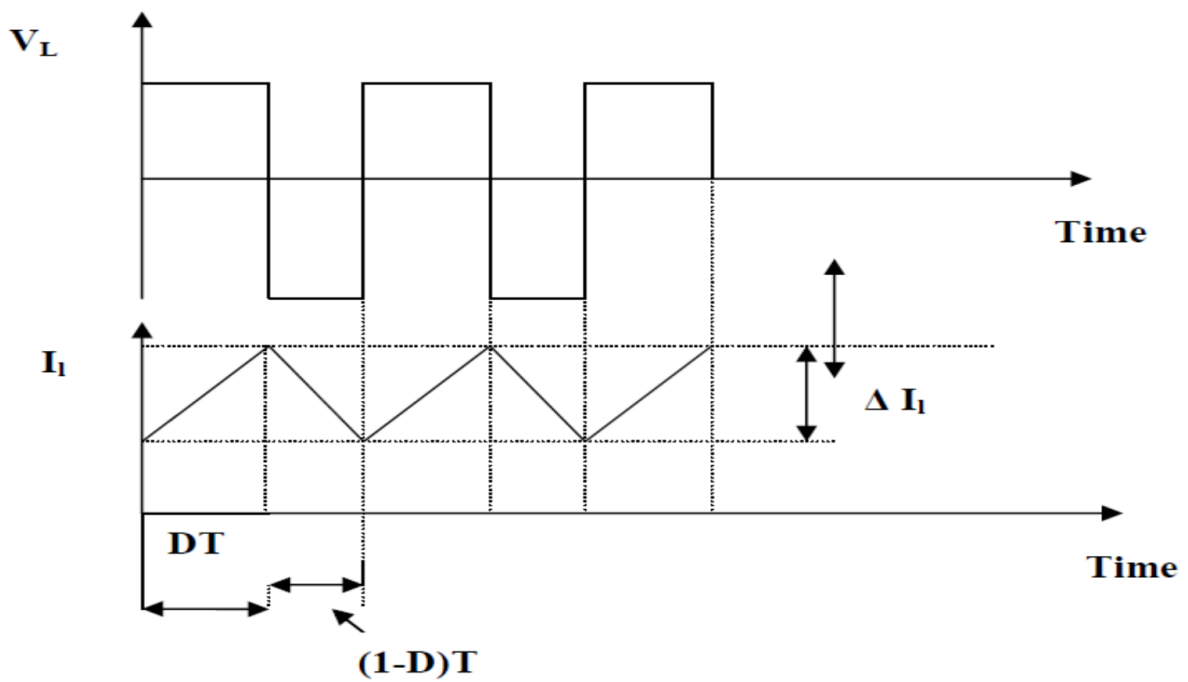


Figure 4. 21: Inductor steady state voltage and current waveform

4. ON mode output voltage ripples

During the OFF mode, Figure 4.18, the load is directly connected to the supply. In the same time the capacitor is charged at the load voltage level. Same as the inductor current, the net capacitor voltage is zero over the cycle. When the boost converter reverses back from OFF mode to the ON mode, the load is supplied by the capacitor all along the ON mode period. As it can be seen from Figure 4.17 of ON mode, during this period the capacitor discharges into the load at supply voltage level and recharge again during the ON mode period. As long as the capacitor is involved, peak to peak ripples in output voltage will rise even though small for a good designed circuit.

The capacitor is charged through the inductor by the input voltage, which will make that the current charging the capacitor to be larger than the load current. Referring to the boost converter topology on Figure 4.16 the current through the capacitor can be expressed by Equation (4.21) below:

$$i_c = C \frac{dV_o(t)}{dt} \quad (4.21)$$

During the charging time or during OFF mode period, the capacitor voltage increases meaning that the rise of capacitor voltage is positive. During the ON mode the capacitor is discharging its energy through the load. The voltage across it, is decreasing and the current is negative as it is flowing out. However, with respect to Figure 4.16, the output voltage remains positive then shall be the current, the explanation would be that the output current is the negative of the capacitor current. The change in output voltage is small, assumption that the load current remains constant during the ON mode period holds. Therefore, the capacitor current is given by following equation:

$$i_{C(t)} \approx \frac{V_o}{R_{Load}} \quad (4.22)$$

Even though the capacitor current being constant, time related linear variations in voltages are still there. Keeping in my mind that we refer the time t as the ON mode period, that period is equal to DT . Then, the expression of the peak to peak ripples in output voltage can be written as shown by equation (4.23):

$$\Delta V_o = i_c \times (DT) = -\frac{V_o}{R} \times (DT) = -\frac{DV_o}{fR} \quad (4.23)$$

Where, the f switching frequency replaces T period through the $1/f$ formula. Capacitor voltage and current waveforms are shown on Figure 4.22, where the ripples in output voltage are magnified for the demonstration purpose but in practical they are small.

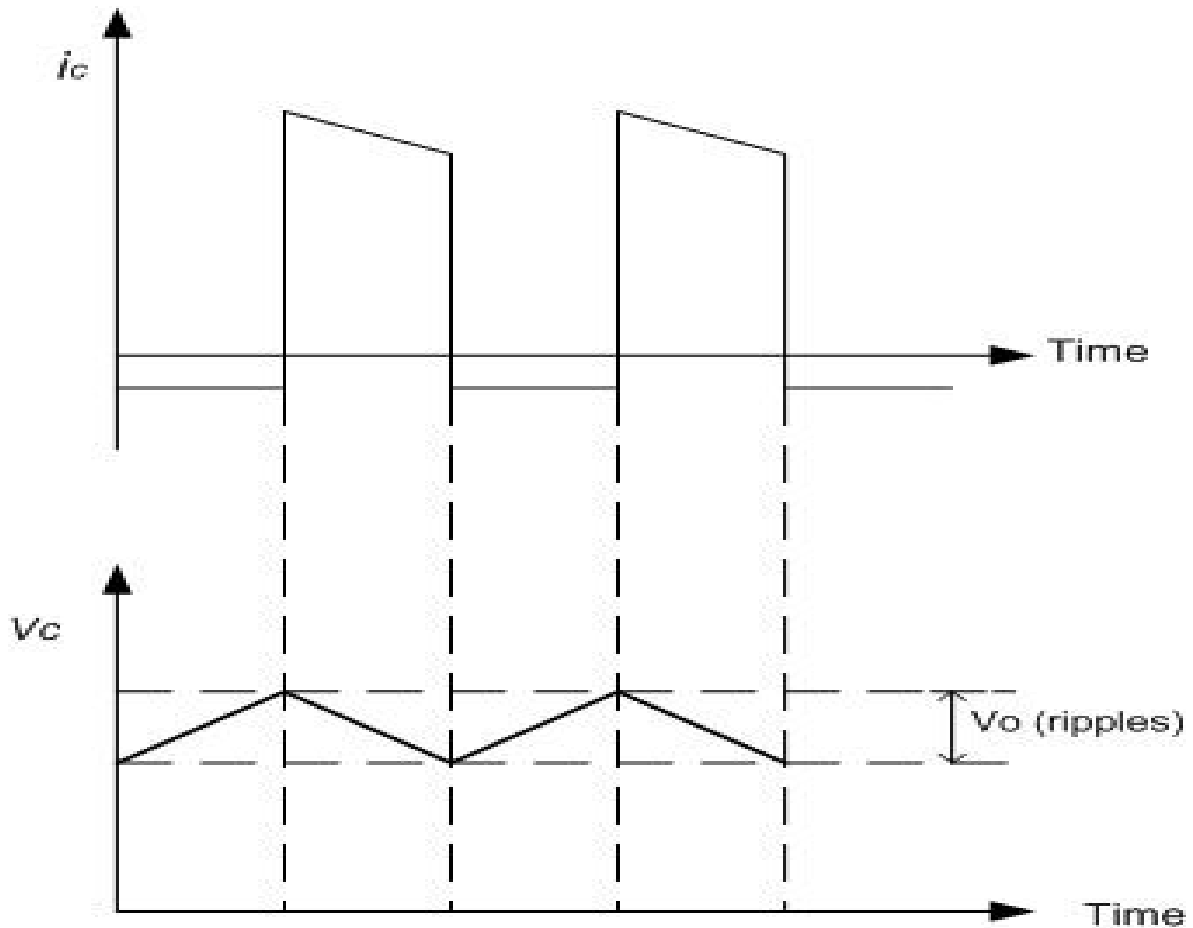


Figure 4. 22: DC-DC boost converter capacitor current and voltage waveforms

5. OFF mode inductor current

During the OFF mode, as it is shown on Figure 4.18, the supply voltage is applied to the load through the inductor L. Thus the average input current may be taken as equal to the average load inductor current. By ignoring the output voltage ripple, the power drawn by the load can be equaled to the supplied input power. The power dissipated through the load resistor is given by:

$$P_o = \frac{(V_o)^2}{R_{load}} \quad (4.24)$$

Having seen that the inductor average current I_L is same as the input average current, then input power can be calculated using equation (4.25) below:

$$P_{in} = V_{in}I_L \quad (4.25)$$

by equaling both equations (4.24) and (4.25) we get the inductor average current given by

$$I_L = \frac{(V_o)^2}{V_{in} R_{load}} \quad (4.24) \quad \text{and Knowing that} \quad I_o = \frac{V_o}{R_{load}} \quad (4.25)$$

By inserting equation 4.19, conversion ratio, and the equation (4.25) into (4.24) we get the inductor current in form of equation (4.26):

$$I_L = \frac{I_o}{1-D} \quad (4.26)$$

Equation (4.26) shows the average inductor current, with assumption that the current across the inductor is continuous. However the current is changing or varying all along the cycle, oscillating between maximum and minimum values. Those values are given by the expression of inductor average current and the net increase in inductor current as given by the equation (4.17). Thus,

$$I_{max} = I_L + \frac{\Delta I_L}{2} \quad (4.27)$$

And

$$I_{min} = I_L - \frac{\Delta I_L}{2} \quad (4.28)$$

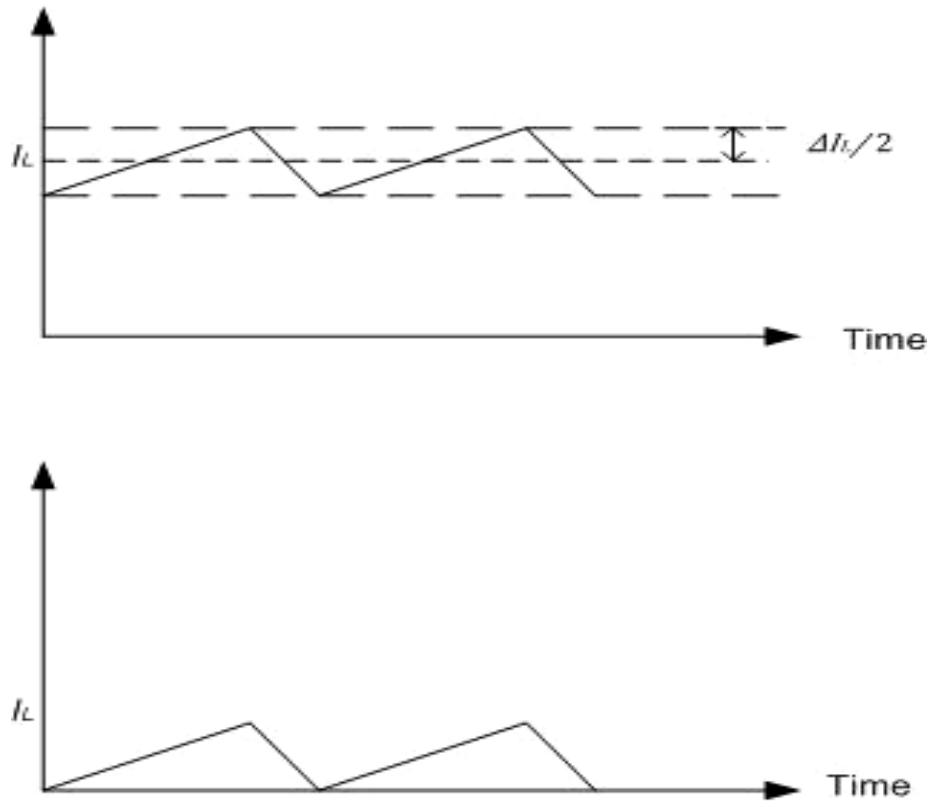


Figure 4. 23: Inductor currents for continuous conduction and boundary condition mode

Figure 4.23 shows the maximum and the minimum of inductor current .it can be seen that as the load resistor increases, the inductor average current decreases. However the net change of inductor current does not change, as it can be seen from equation (4.26) it is not related to the load resistor.

In order to have a continuous conduction, the condition given by equation (4.29) below has to be satisfied. Whereas for conduction at the boundary of the continuous conduction mode and for discontinuous conduction and equation (4.28) must be fulfilled.

$$I_L > \frac{\Delta I_L}{2} \tag{4.29}$$

$$I_L = \frac{\Delta I_L}{2} \tag{4.30}$$

I_L may be expressed using the expression from equation(4.19) of average output voltage V_o expressed in terms of input voltage V_{in} , by inserting in equation(4.26) we have a following expression:

$$I_L = \frac{V_{in}}{(1-D)^2 \times R_{load}} \quad (4.31)$$

The maximum current I_{max} can be expressed by equation (4.32) below, inserting equation (4.31) into equation (4.27), we obtain

$$I_{max} = \frac{V_{in}}{(1-D)^2 \times R_{load}} + \frac{(DT)V_{in}}{2L} \quad (4.32)$$

Same as above, the I_{min} will be given by equation (4.33) after the reinserting the equation (4.31) into equation (4.28). Then we get:

$$I_{min} = \frac{V_{in}}{(1-D)^2 \times R_{load}} - \frac{(DT)V_{in}}{2L} \quad (4.33)$$

by now , we can express the condition for continuous condition , in terms of Equation (4.32) and (4.33) ,thus equation (4.29) may be rewritten as

$$\frac{V_{in}}{(1-D)^2 \times R_{load}} > \frac{(DT)V_{in}}{2L} \quad (4.34)$$

And by rearranging equation (4.34) and having in mind $1/T$ equals the switching frequency f we get

$$f > \frac{D \times R_{load} \times (1-D)^2}{2L} \quad (4.35)$$

From equation (4.34) we can conclude that, by assuming that only one parameter is varied at time, the behavior of the circuit is as follows:

The discontinuous of the circuit is observed whenever the switching frequency is decreased, the duty cycle decreased, increasing of the load and when inductance is of low value.

During the discontinuous conduction, the voltage across the inductor is zero all along that part of the cycle. We assume the time the switch is ON as D_1T and D_2T as the time when the switch is off, which corresponds to the time of conduction of the diode. Figure 4.24 below shows the waveforms of inductor current and voltage during the discontinuous conduction.

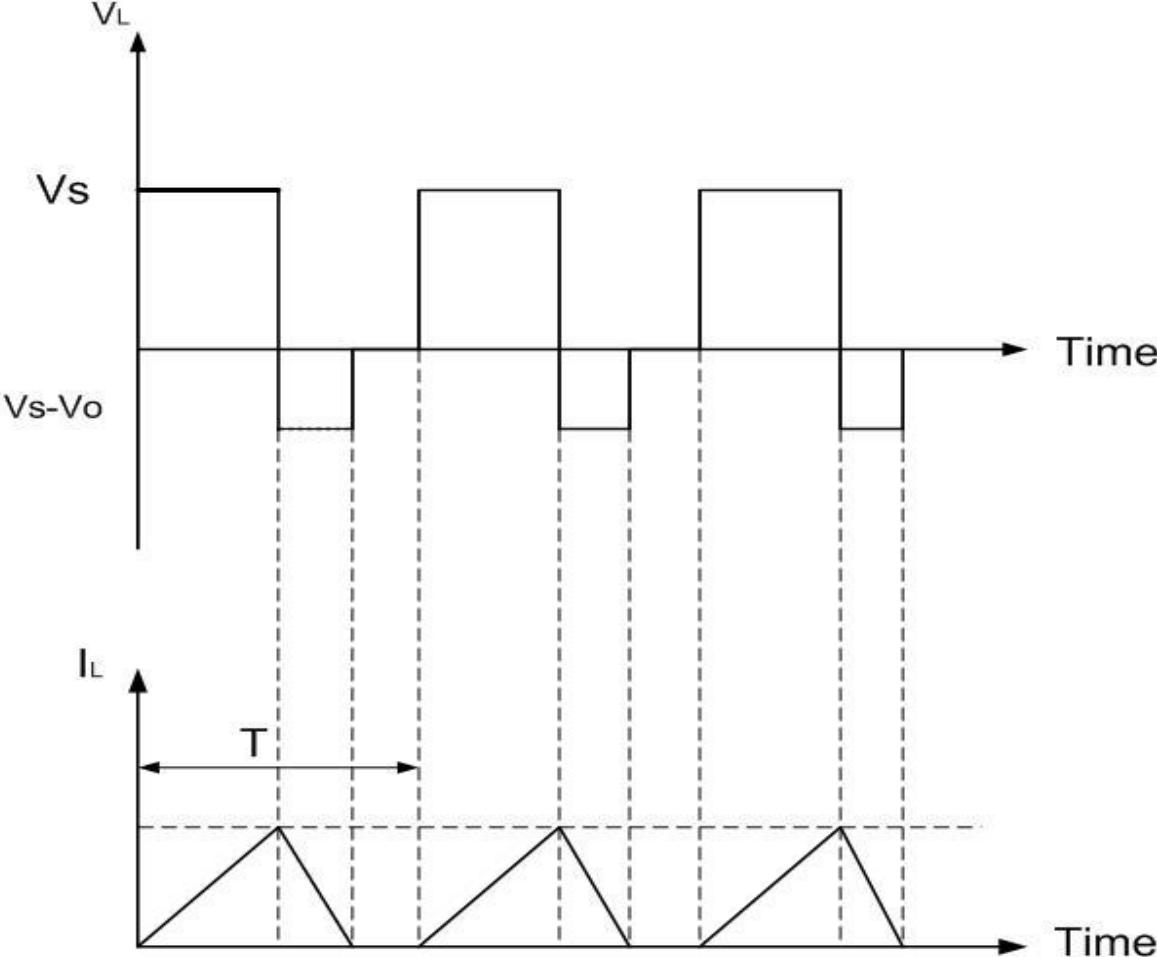


Figure 4. 24: Inductor voltage and current waveforms during the discontinuous mode

As it can be seen from the graph with reference to the Figure 4.24, the duty cycles $D_1 + D_2$ are less than 1. Knowing that the net change in inductor current is zero over a cycle,so it is for net voltage associated to it, is zero. Thus using the D_1 and D_2 , duty cycle of the switch and diode duty cycle respectively, we can write as follows:

$$(D_1T)V_{in} + (V_{in} - V_o)D_2T = 0 \tag{4.36}$$

This after rearrangements will give us the equation of output voltage:

$$V_o = V_{in} \times \frac{(D_1+D_2)}{D_2} \quad (4.37)$$

Thus the output voltage is can be calculated in function of duty cycles ,knowing the switch duty cycle D_1 the challenge is to find the D_2 duty cycle of diode as it depends on other circuit parameters. However, it can be calculated using the power balance concept and by assuming the circuit ideal. Let consider the average input current and output current being I_{in} and I_o respectively, then we have according to power balance concept:

$$V_{in} I_n = V_o I_o \quad (4.38)$$

By replacing V_o in equation (4.38) by its value from equation (4.36) we get:

$$I_{in} = I_o \frac{(D_1+D_2)}{D_2} = \frac{V_o}{R} \times \frac{(D_1+D_2)}{D_2} = \frac{V_{in} (D_1+D_2)^2}{R D_2} \quad (4.39)$$

The inductor being in series with the source, we may say that the average input current is same as the average inductor current. Thus if we assume the peak inductor current to be ΔI_L and the time period for the flow of current equals the total conduction time of the inductor and the diode:

$$I_{in} = \Delta I_L \frac{(D_1+D_2)}{D_2} \quad (4.40)$$

Comparing (4.39) to (4.40) gives us the following equation:

$$\Delta I_L \frac{(D_1+D_2)}{D_2} = \frac{V_{in} (D_1+D_2)^2}{R D_2} \quad (4.41)$$

And knowing from equation (4.14) that $\Delta i_L = \frac{V_{in}(t)}{L} (D_1 T)$ which is equal to

$$\Delta I_L = \frac{D_1 V_{in}(t)}{fL} \quad (4.42)$$

By substituting equation (4.42) back into equation (4.41) we get,

$$\frac{D_1}{2fL} = \frac{(D_1+D_2)}{(D_2)^2 \times R} \quad \text{That can be rewritten after the arrangements as}$$

$$D_2 = \frac{fL}{R \times D_1} \times \left[1 + \sqrt{1 + \frac{2R(D_1)^2}{fL}} \right] \quad (4.43)$$

From equation (4.43) it can be seen that the diode duty cycle D_2 is proportional to the other circuit parameters such as load resistor R , inductance L , and duty cycle D_1 and the switching frequency f . Having the diode duty cycle, the diode average current can be calculated using the equation (4.41) below

$$I_D = \Delta I_L \frac{D_2}{2} \quad (4.44)$$

The average diode can also be expressed in terms of input and output voltage, this achieved by expressing the diode current as average load current and by replacing ΔI_L with its value given by the equation (4.42) :

$$\frac{V_o}{R} = \frac{V_{in} D_1 D_2}{2fL} \quad (4.45)$$

Then,

$$D_2 = \frac{2fL}{RD_1} \times \frac{V_{in}}{V_{on}} \quad (4.46)$$

Knowing, from equation (4.36), that it can be rewritten as

$$\frac{V_o}{V_{in}} = 1 + \frac{D_1}{D_2} \quad (4.47)$$

By substituting the value of D_2 given by equation (4.46) into (4.47) we get an expression

$$\frac{V_o}{V_{in}} = 1 + \frac{R(D_1)^2}{2fL \times \frac{V_o}{V_{in}}} \quad (4.48)$$

The equation (4.48) after rearrangements can be written as

$$\left(\frac{V_o}{V_{in}}\right)^2 - \frac{V_o}{V_{in}} = \frac{R(D_1)^2}{2fL} \quad (4.49)$$

The conversion ration equation (4.49) is solved as second order equation, the ratio taken as the unknown, and then we get solution as:

$$\frac{V_o}{V_{in}} = \frac{1}{2} \times \left[1 + \sqrt{1 + \frac{2R(D_1)^2}{fL}} \right] \quad (4.50)$$

From equation (4.50) above, we can see that the ration is proportional to the other circuit parameters: inductance, switching frequency, and duty cycle and load resistor. The critical load resistor is given by equation (4.51) below:

$$R_{critical} = \frac{2fL}{D_1 \times (1-D_1)^2} \quad (4.51)$$

4.12. Summary

In this chapter the testing system for integration of Independent Power Providers (IPP) to grid using VSC-HVDC as interface is provided. Models for every IPP and each system components are developed as well as parameter values. A discussion is made on converter control, converter transformer and boost converter design calculations are provided.

CHAPTER FIVE

VSC-HVDC IN APPLICATIONS FOR INDEPENDENT POWER PROVIDER, SIMULATIONS RESULTS

5.1 Introduction

The grid integration of Independent Power Providers (IPPs) using High Voltage Direct Current – Voltage Source Converter (VSC-HVDC) simulations results are presented in this chapter. As described in chapter 4, considered IPPs are that use conventional power plant, wind farm and solar park. For each IPP, two scenarios are considered: The first scenario is normal working conditions after the grid integration and the second scenario is abnormal working conditions with symmetrical faults on grid side. Through those conditions analysis are performed.

Simulations are performed using Matlab/Simulink software, where the symmetrical faults on grid side are implemented by lines to ground faults and the grid is implemented by a programmable voltage source.

The Independent Power Providers (IPPs) involved in these simulations are referred to as IPP1 for the conventional power plant, IPP2 for wind farm and IPP3 for solar park. They are connecting to the Alternating Current (AC) grid through VSC-HVDC transmission system.

5.2 Integration of the conventional power plant (IPP1) through VSC-HVDC

5.2.1 Normal conditions

A conventional power plant (IPP1) is integrated to the grid using a VSC-HVDC interconnection. The arrangement is given in Figure 5.1; The IPP1 consists of 120 kV, 200 MVA, 50 Hz and is transmitting to the grid which is operating at 120 kV, 60Hz and a load of 100 MW is connected between them.

Per unit (p.u) measurement system is used for easier analysis of the results.

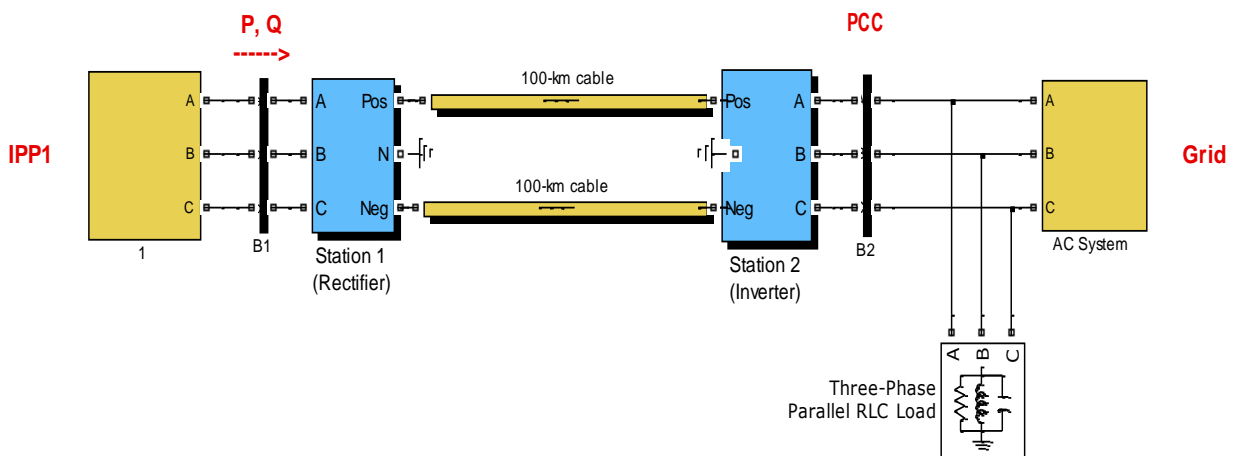


Figure 5. 1: IPP 1 connection to the grid

The system start from zero off set reaches the steady state. Steps were applied in a sequence manner on both reference of active P_{ref} and Q_{ref} reactive power of the rectifier. Measurements are taken on both side at sending and receiving end, the responses are shown in Figure 5.2 and Figures 5.3 respectively. Base power is set at 200 MW for active power (P), base voltage at 120 kV and 200 MVAR for base reactive power (Q).

From the Figure 5.2 we see that at $t=1.5$ s, a decrease onto the active power reference, plotted in red, is introduced by the application of a -0.1 p.u. step. The decrease of active power reference reflects on the line voltage transmitted (U_{meas}) that decreases from 1 p.u to 0.9 p.u, after 0.3 seconds the power stabilizes voltage goes back to the rated value.

In similar way steps are applied to the reactive power reference at $t=2.0$ s; a negative 0.1 step is applied to the reactive power reference (Q_{ref}) in red. The generated reactive power (Q_{meas}), plotted in blue, follows the reference and a decrease of 0.1 P.U is observed.

The change in transmitted reactive power does not affect the transmitted active power. From that a decouple of reactive and active power response is achieved.

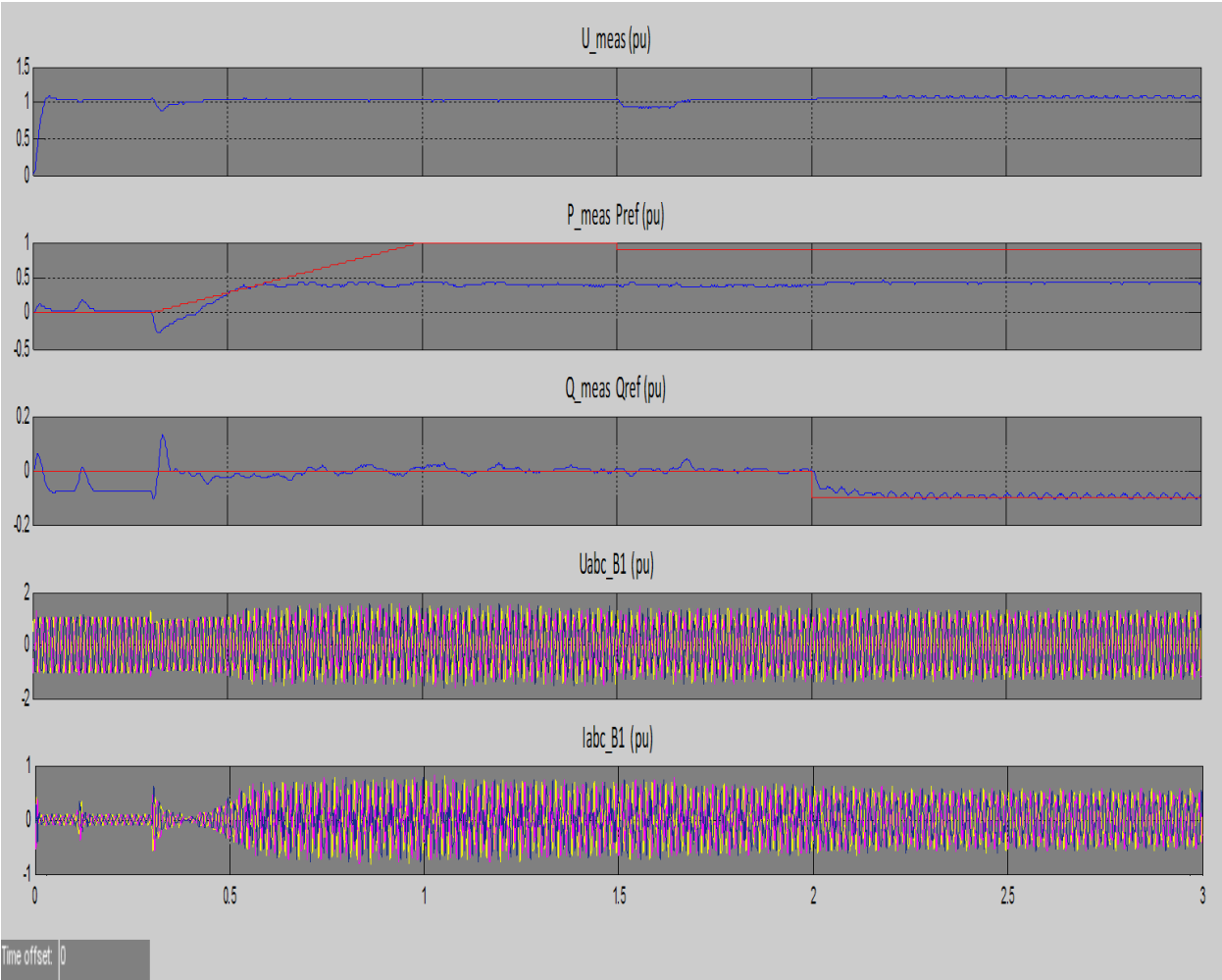


Figure 5. 2: Measurement taken at IPP1 station during normal conditions

At bus B2 the Point of common connection (PCC) with the grid or at the transmission end side the measurements results are shown in the Figure 5.3 below. Measurements are taken using same base parameter, per unit system (p.u), as for the IPP sending end measurement. At t=0.5 sec after the initialization, the system reaches the steady state. From the measurement, it is observed that the sudden small change in voltage from the sending side does not affect the transmitted voltage (U_{meas}) or power (P_{meas}) at point of common connection (PCC). Transmitted three phase voltage (U_{abc_B2}) and Currents (I_{abc_B2}) remains stable. .

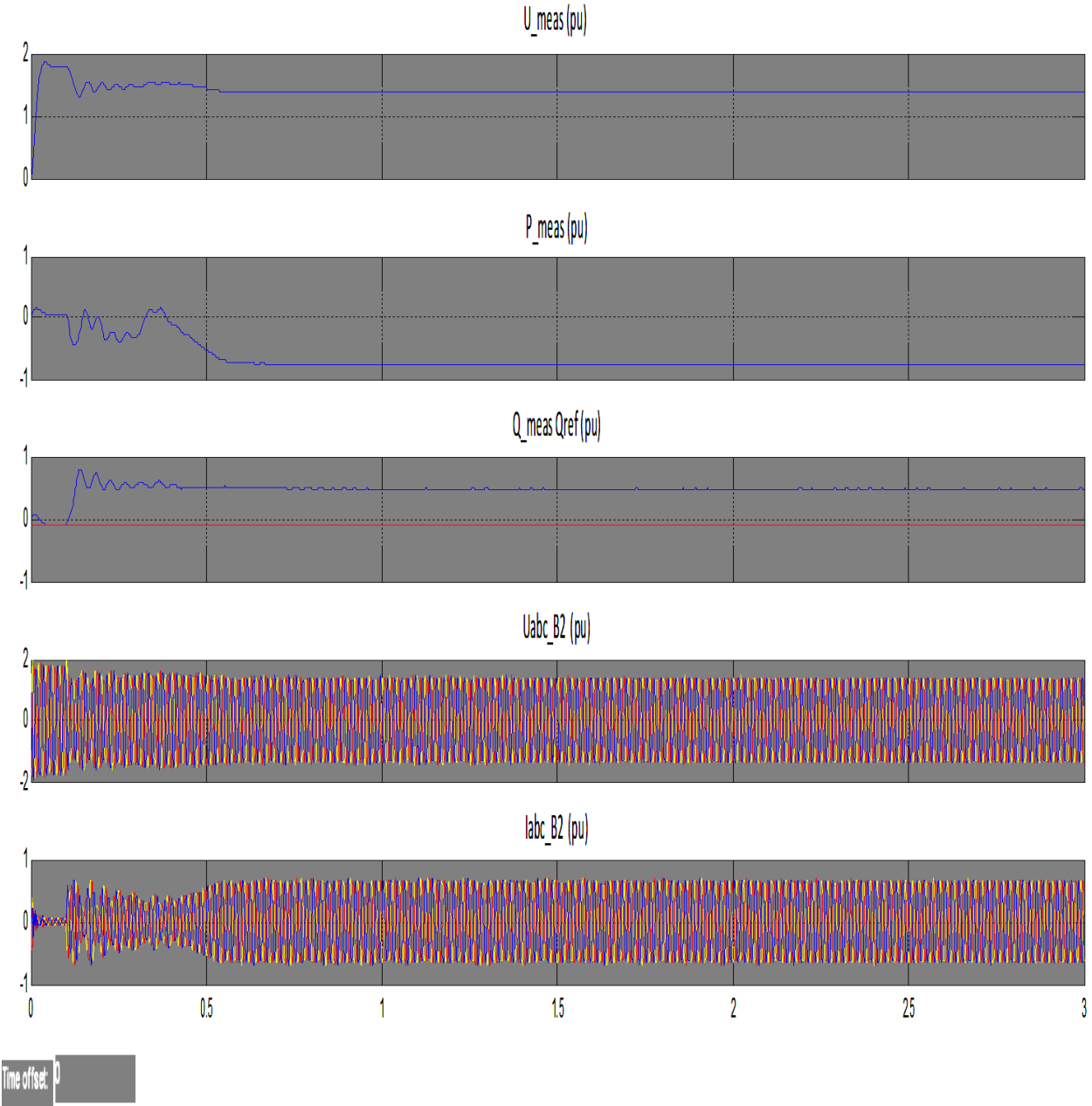


Figure 5. 3: Measurement taken at grid side station 2 during the normal condition

5.2.2. Abnormal conditions

Abnormal conditions were simulated with the help of the model on Figure 5.4; with the same parameters as in the model for normal conditions, the abnormal conditions are implemented by disturbances. Minor and severe disturbances are introduced by voltage steps and three phase lines to ground faults on the grid side. Line to ground faults are implemented by the fault block that closing and connecting the lines to ground.

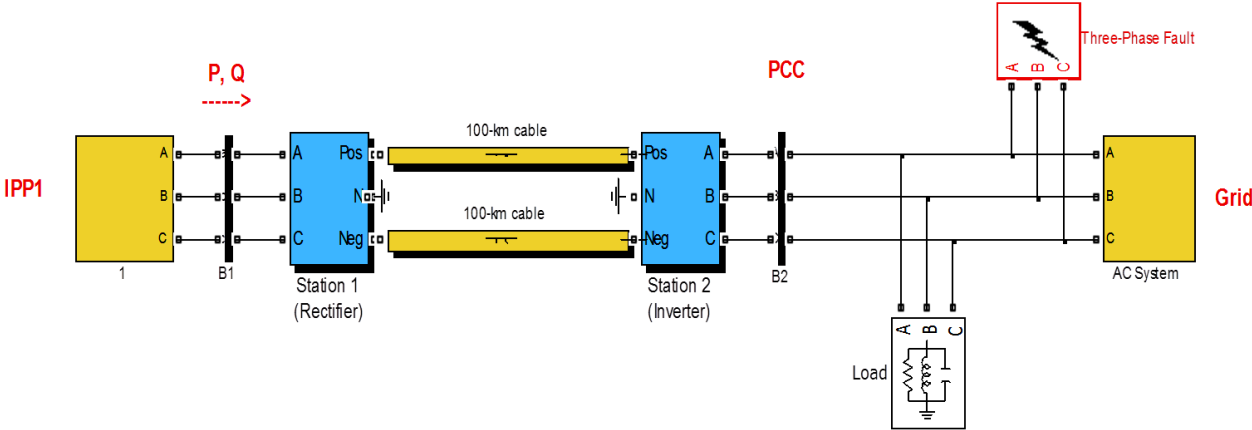


Figure 5. 4: IPP1 connection to grid, fault testing model

A minor disturbance is achieved by a negative voltage step with a magnitude of 0.1 p.u., which is introduced after 1.5 second for a period of 0.14 seconds to the IPP side. After the recovery of the system, at t= 2.0 seconds a severe disturbance in the form of lines to ground fault is introduced by the three phase faults block on the grid side for a period of 0.12 seconds. Results of the measurements taken at IPP bus station and at the point of common connection (PCC) are shown on Figure 5.5 and Figure 5.6 respectively.

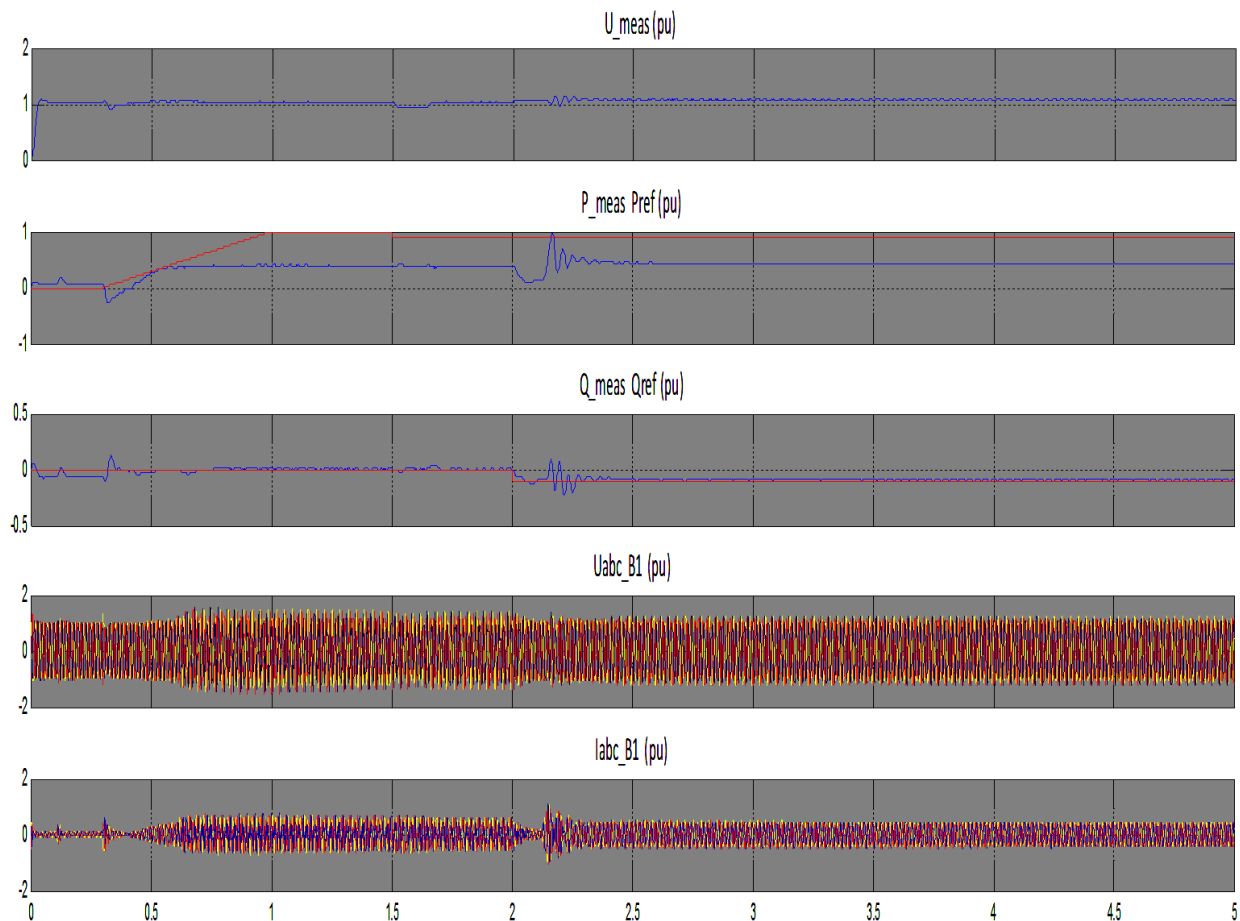


Figure 5. 5: Measurement at IPP1 station during the faults

From Figure.5.5 above we can see that at $t=2.0$ when the line to ground faults occurs on grid side, at the IPP1 bus station the power sent drop by 0.3 p.u during the 0.12 s of the disturbance. The power sent will return to its pre disturbance values around at $t=2.3$ s, the recover take around 0.2 s. Meanwhile the three phase voltage transmitted is less affected, no significant change occurs and an increase of 0.1 p.u is observed on the voltage of the converter. The IPP1 is isolated from the fault on the grid while still connected to it as required by South African grid code discussed in Chapter 3.

On the other side of the transmission end, at the point of common connection of the IPP1 and the grid, a voltage drop to zero is observed at the during the duration of the fault. As it is shown on Figure 5.6, the active and reactive powers as well as the voltage on converter go to zero during the time of fault. However, the current I_{abc} is not so much affected unless an overshoot at the restart of the transmission after the fault clearance.

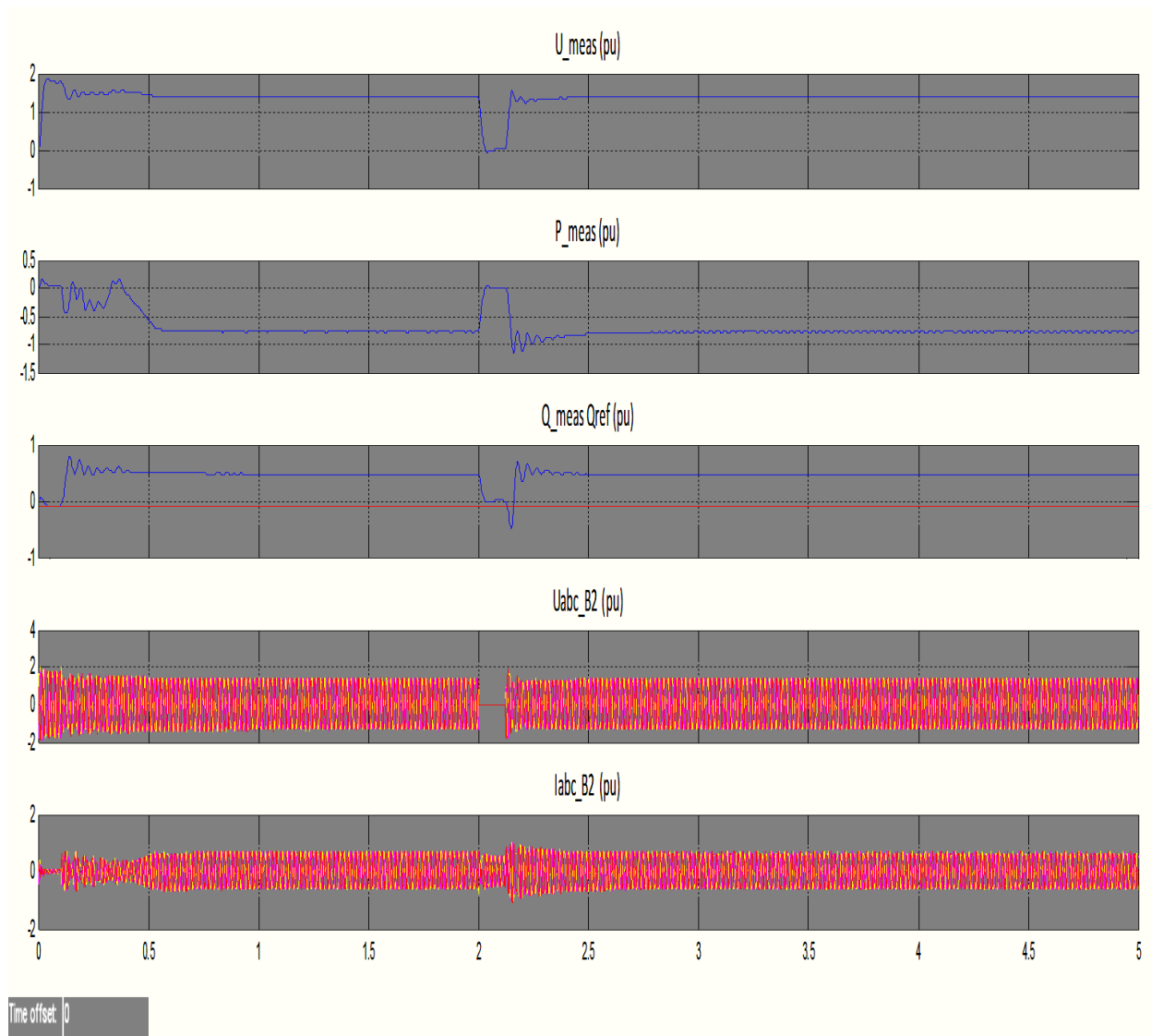


Figure 5. 6: Measurement taken at grid side station 2, during fault condition

5.3 integration of the wind power plant (IPP2) through VSC-HVDC

5.3.1 Introduction

Simulation results of the wind park, producing 135MW at 120 kV 60Hz, supplying power to a 120 KV 50 Hz grid through an HVDC-VSC connection are shown in this section. Three conditions were simulated using Simulink, the normal working conditions, the fault conditions and grid side frequency disturbances. The grid is implemented by a programmable voltage, while the wind farm an asynchronous wind turbine is used.

5.3.2. Normal condition

For the normal working conditions, the wind farm is set to transmit power to the grid where a load is connected, as shown on Figure 5.7. The system is set to start and reach study steady

state. Steps were applied to the reference of the grid voltage source, to evaluate the behaviour on the sending side, the wind farm.

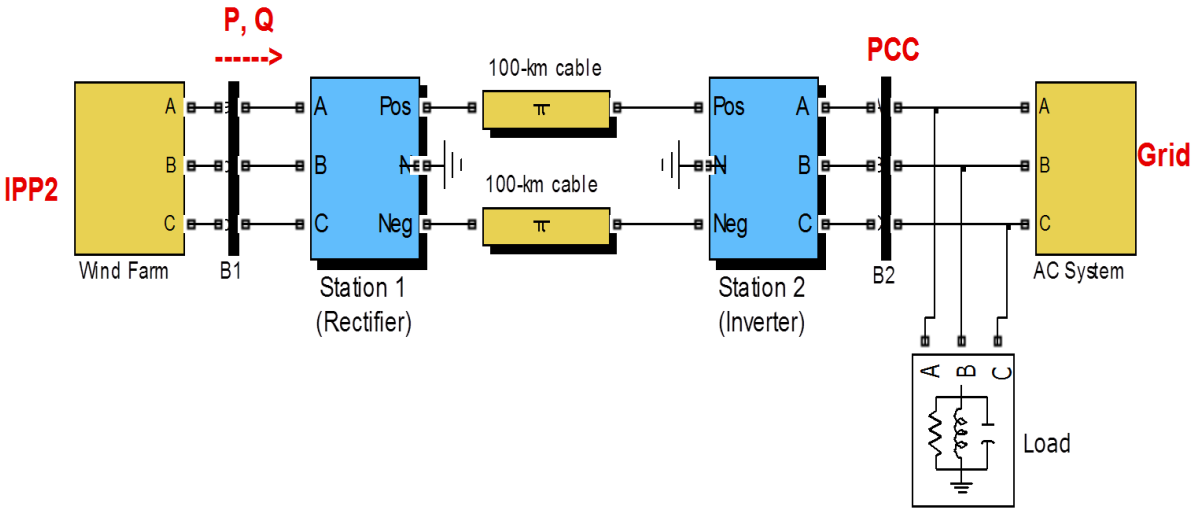


Figure 5. 7: IPP2 connection to grid

The grid side measurements are shown on Figure 5.8. The measurements taken are per unit and based on three phase voltages. The voltages are in per unit system where 120kV is the base voltage while 200 MW is the base power. The simulation start at zero offset, the system reaches the steady after 1 s. The active power delivered by the grid is around 1 p.u. At t = 2.0 s, a 0.2 p.u voltage sag from the grid side of is introduced for a period of 200 ms. The perturbation from the grid reflects on IPP2’s active power measured (P_meas), reactive power measured (Q_meas), currents (Iabc_meas) and converter dc voltage (U_meas). During the simulations converter control system of both sides were assumed not communicating.

For voltage sag on grid side, we can see that the grid is trying to recover its stability by increasing the reactive power that is draining from the IPP2, as the discussed in Chapter 3 section 3.24, on power system stability, the reactive power participate to the voltage stabilisation. Hence during the disturbance, the IPP2 through the HVDC-VSC on grid side try to increase the reactive power and decrease the active power transmitted to grid.

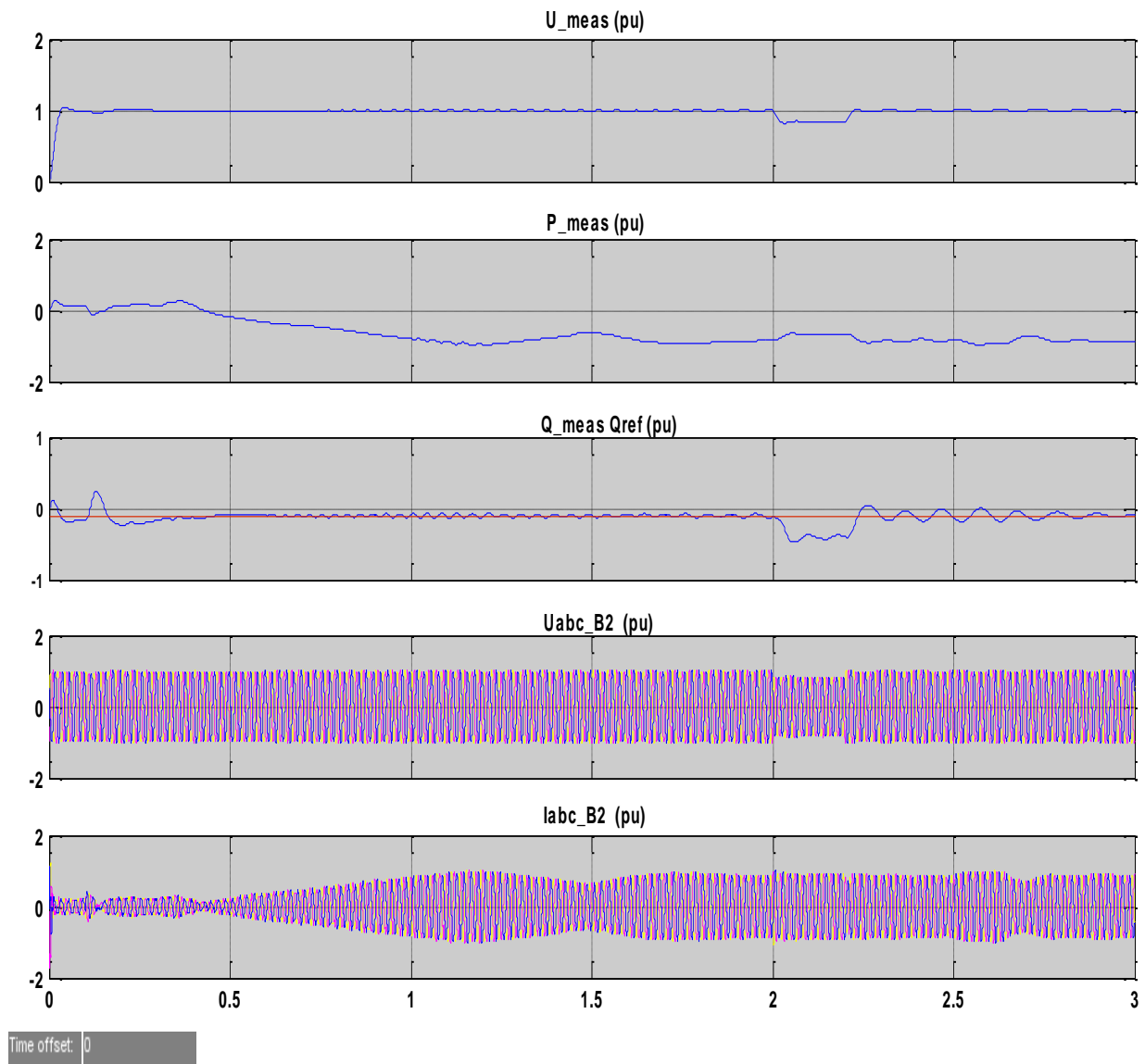


Figure 5. 8: Measurements taken at grid side, station 2 during the normal condition

Measurements are performed onto IPP2 side station to see how the IPP2 is being affected by the grid perturbations; results are shown on Figure 5.9. From it we can see that the average power is delivered is around 1 per unit, with 200MVA power base and 120 kV as base for voltage measurements. The IPP2 start from zero offset reaches the steady after 1 s. At $t = 2.0$ s when a voltage sag occurs on grid side, on IPP2 side station little increase of voltage U_{meas} while a little oscillations in reactive power (Q_{meas}) and in active power (P_{meas}) are observed for a period equal to 140 ms. They, instantaneously return to the normal values after the sag passed. No significant changes occur in the I_{abc} currents waveforms same as for the U_{abc} three phase voltages.

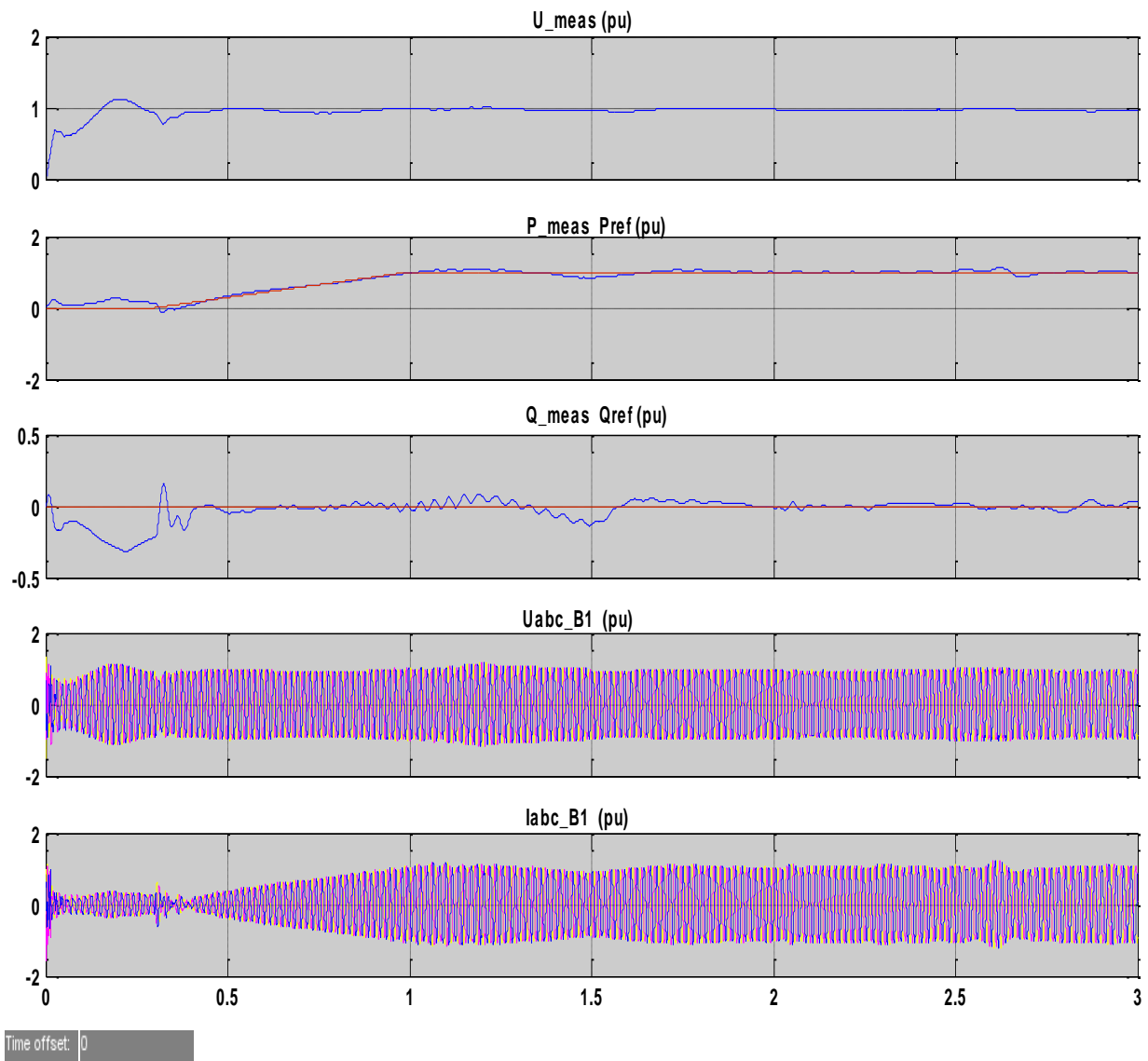


Figure 5. 9: Measurement taken at IPP2 side station during the normal condition

Besides the voltage sag, frequency variations on grid side were also introduced to see the behaviour of IPP2 to that changes, hence a negative step of 3 Hz were introduced at $t = 1.5$ s for a duration of 210 ms. The measurement results of both the IPP2 side and grid side at the point of common connection are shown on Figure 5.10 and 5.11 respectively

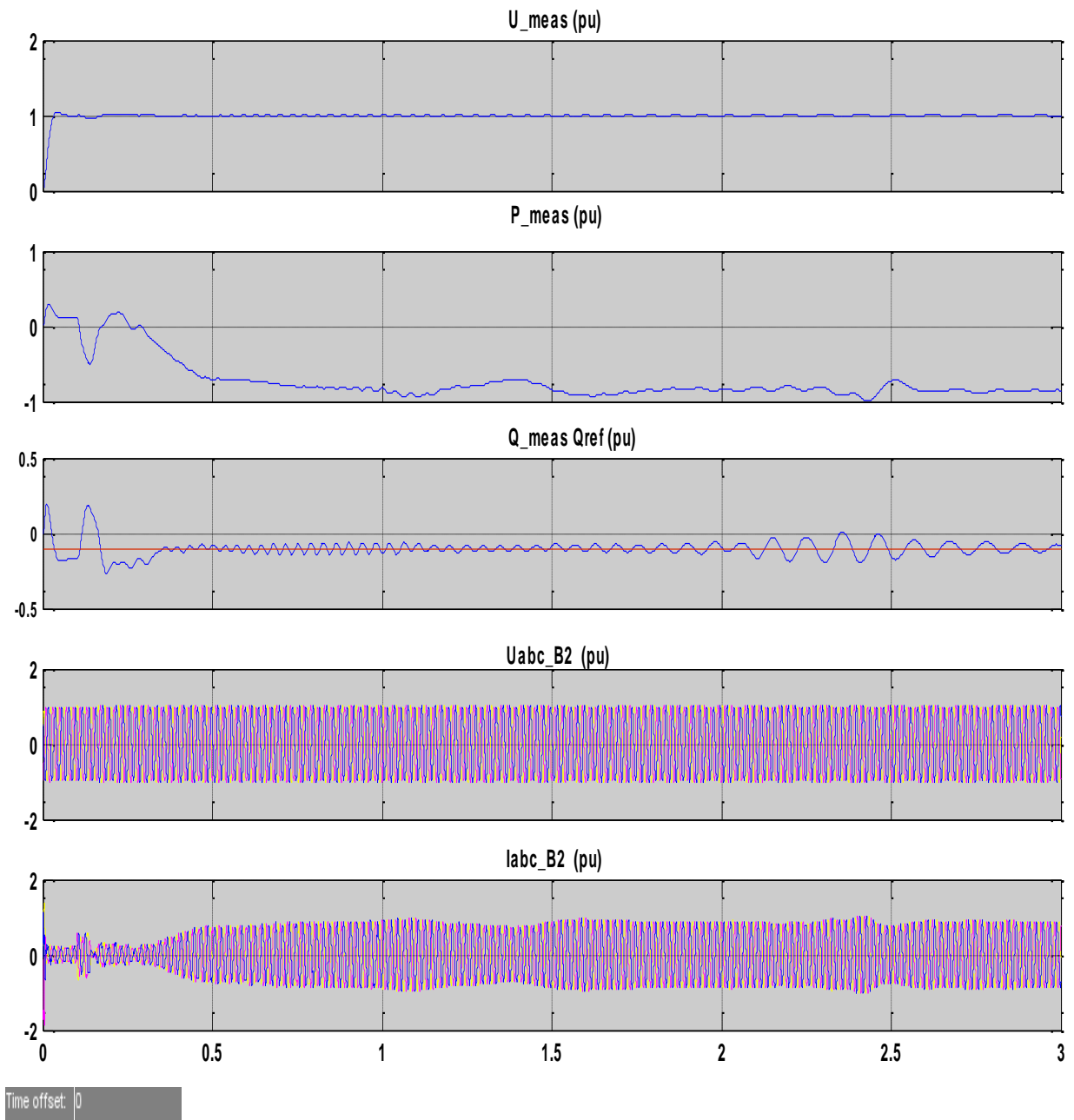


Figure 5. 10: Measurement taken at station 2 during grid side frequency variation

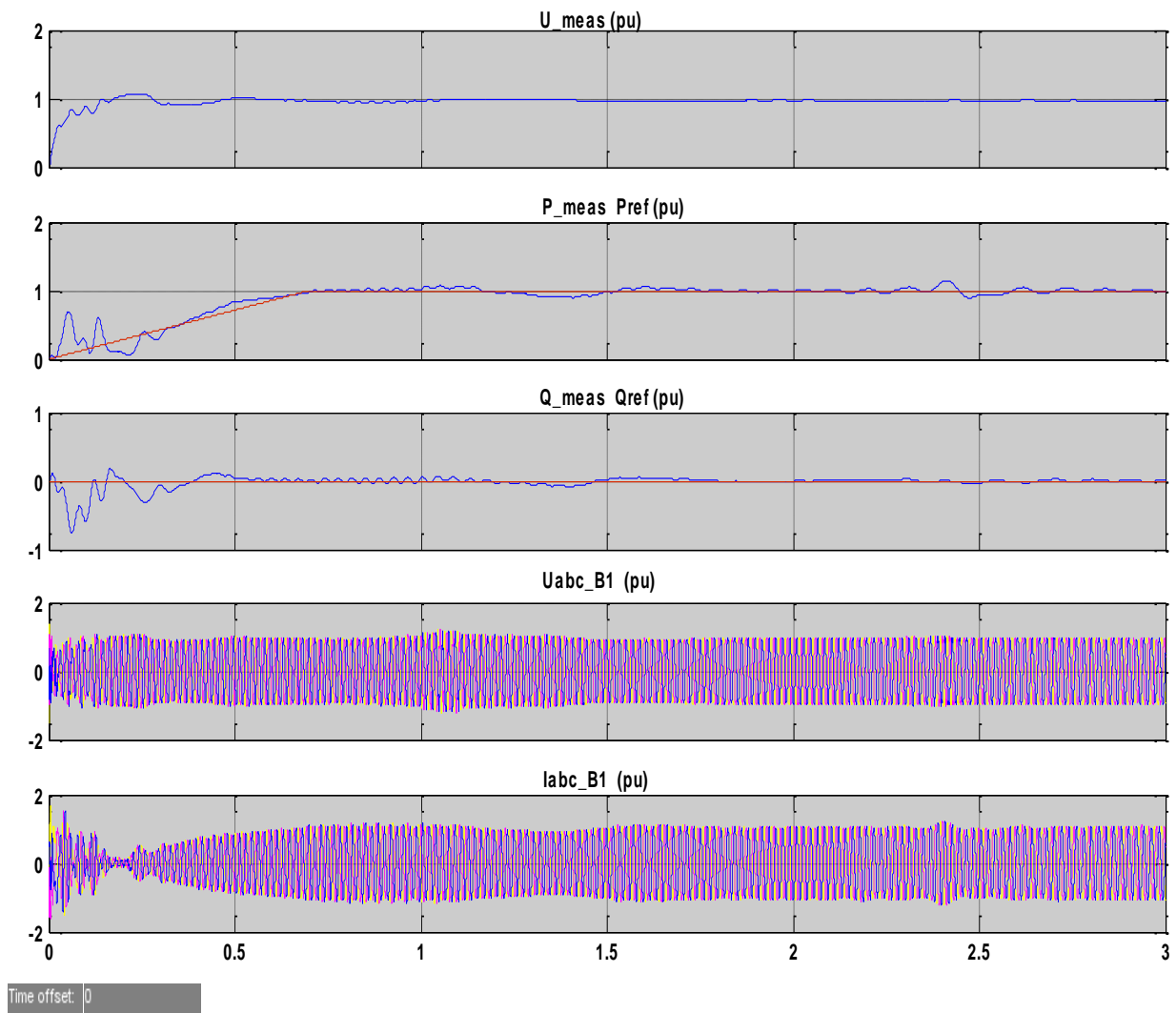


Figure 5. 11: Measurement taken at IPP2 station 1 during the grid side frequency variations.

5.3.3 Abnormal conditions

The simulations for the abnormal conditions on grid to which IPP2 is connected through HVDC-VSC link, is implemented using the model on Figure 5.12. As in previous simulations the wind farm (IPP2) is transmitting power to the grid but a fault is introduced on grid side and implemented by a three phase fault block in our model.

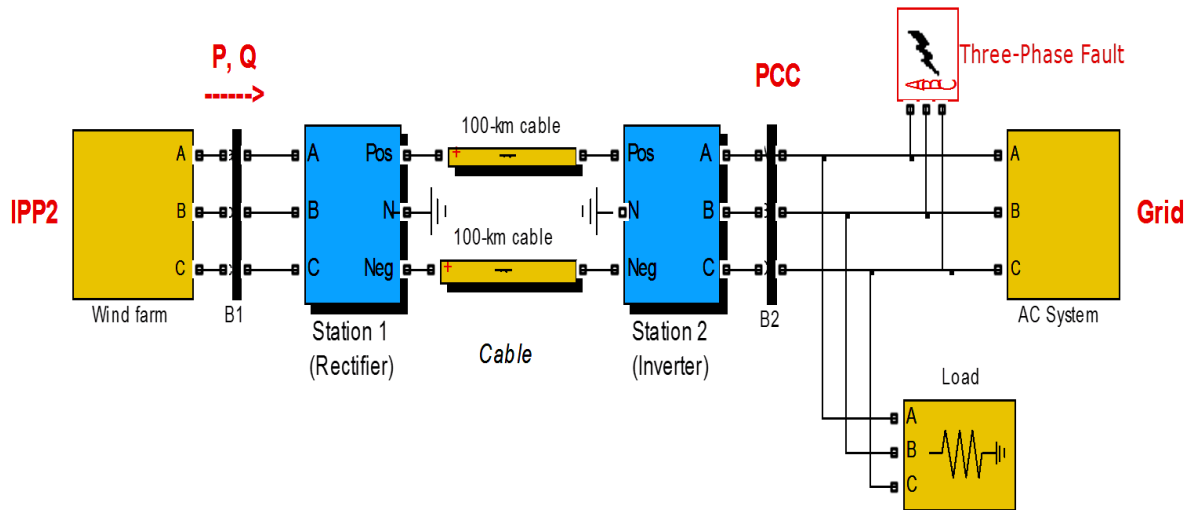


Figure 5. 12: IPP2 connection to grid, fault testing model

The system is set to start at zero offset and reaches study state after 1 second. After 2 seconds, a three phase short circuit is introduced making the voltage on grid side to drop to zero. As it can be seen from Figure 5.13 of measurements made at station 2 on point of connection, the grid powers active and reactive also drop. A high short circuit current is observed all along the fault period which is 200 milliseconds. The period is longer than what is stated by the NERSA regulation and grid code discussed in this thesis in Chapter 3 section 3.5; the idea is that knowing the behaviour of the model for longer period it will be easier to know for a short period.

Measurements taken on IPP2 side are shown on Figure 5.14. Where it can be seen that, the occurrence of fault on grid around 2 s, does affect the IPP2. The transmitted current and active power drop significantly around zero. On other hand reactive power increases to compensate the voltage drop on grid side. The phase voltages on IPP2 side are slightly affected by small fluctuations. With this response, IPP2 via HVDC-VSC ride through capability is proven. As the VSC-HVDC act as a buffer then isolates the fault from the grid to propagate to the other side of the network.

Beside the three phase fault, a sudden jump in phase is simulated. Considered as an abnormal condition on the same level as the three phase fault by the regulation authorities, a step phase shift of 40 degrees is introduced on the grid side at $t = 2$ s for a period equal to 210 ms. The model on Figure 5.12 was used with fault block disabled. Results of measurements taken on grid and on IPP2 station side during that sudden phase jump are shown on Figure 5.15 and 5.16 respectively. Per unit system is used, where the base power is 200 MW and base voltage is set at 120 kV. All simulations were done on 3 seconds period range.

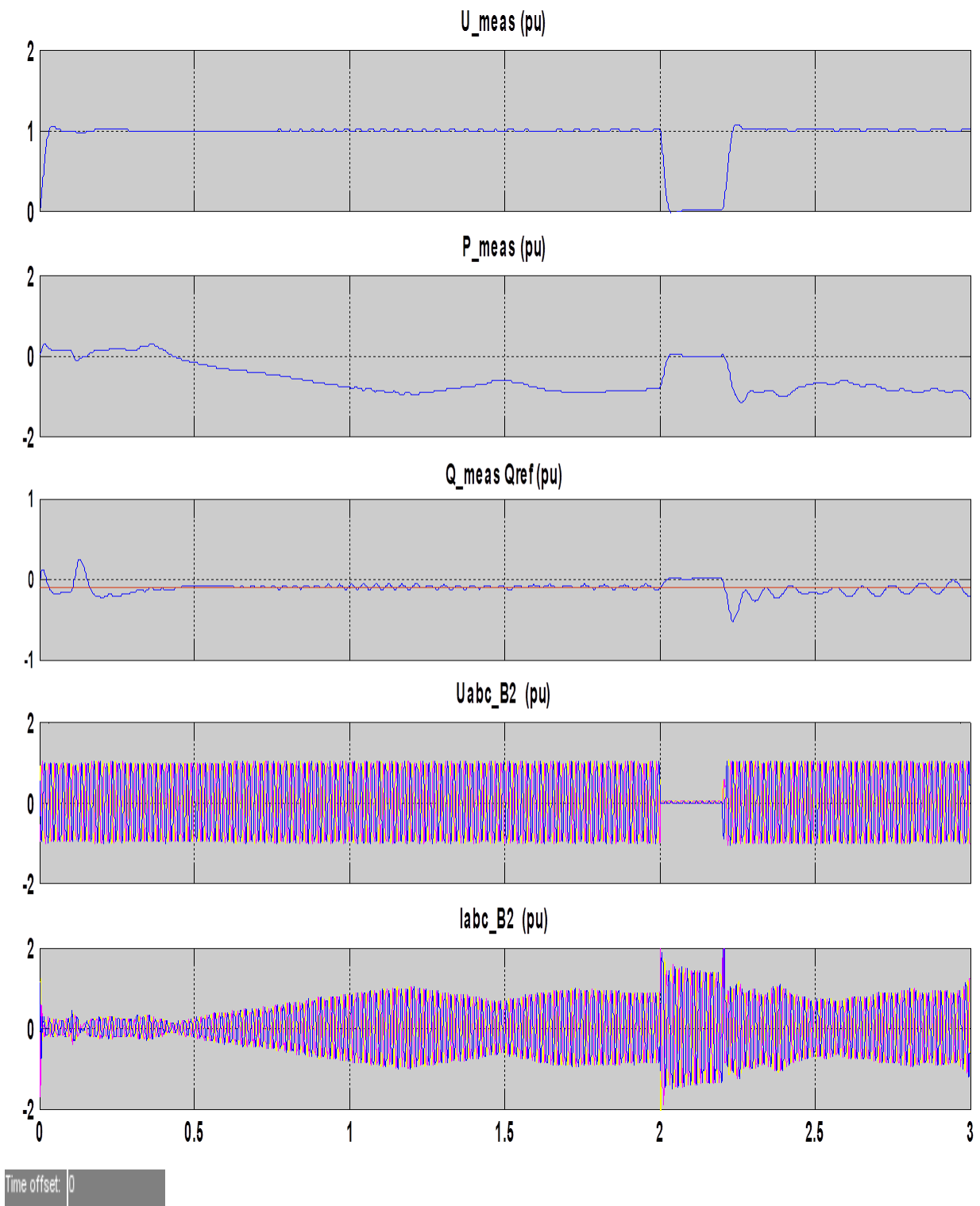


Figure 5. 13: Measurement taken at station 2 during three phase fault on grid side

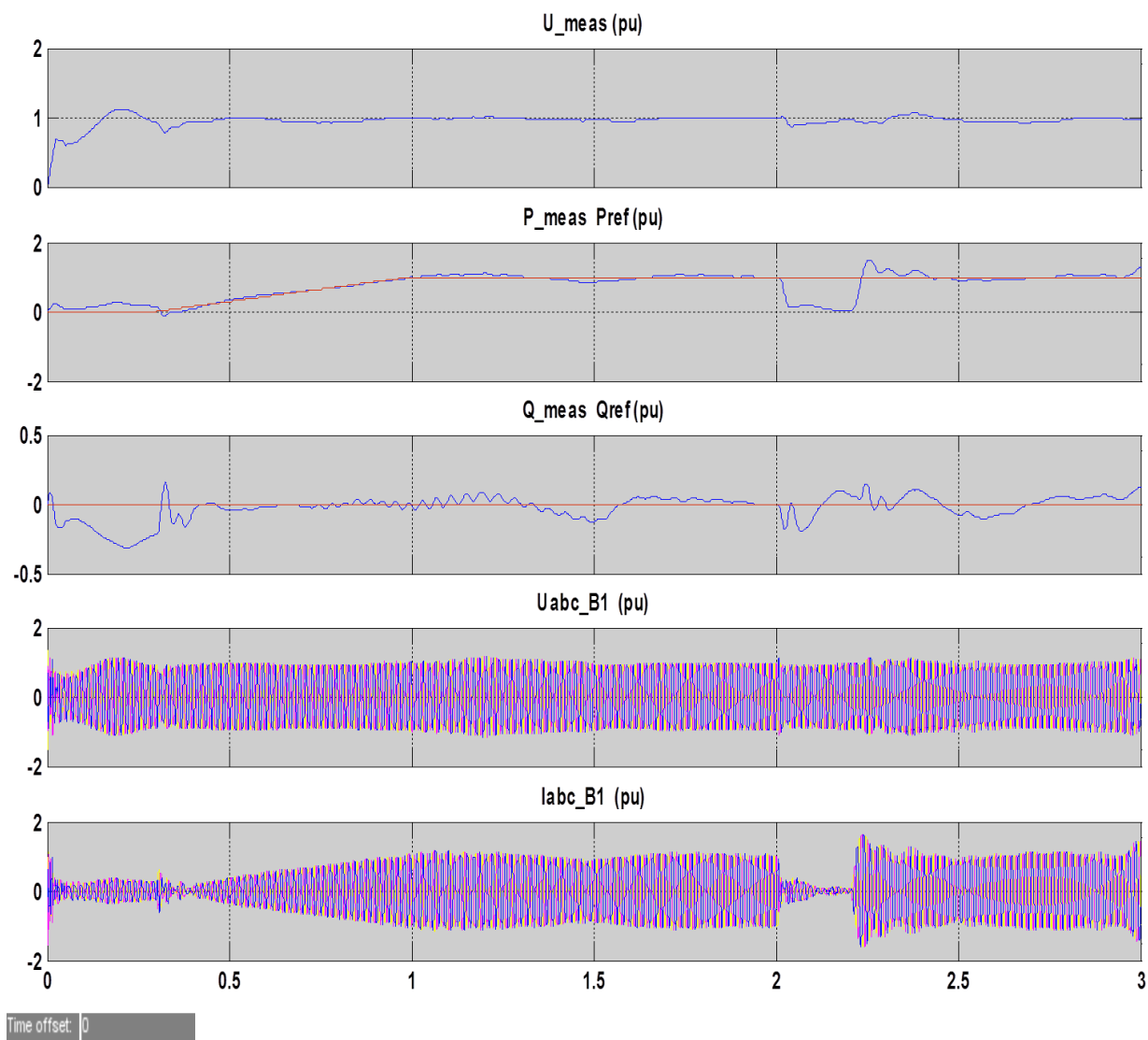


Figure 5. 14: Measurement taken at IPP2 station during three phase fault on grid side

From Figure 5.15 and Figure 5.16, we can see that during a grid sudden phase shift of 40 degrees; the active power (P_{meas}) on grid side slightly decreases, while the reactive power is subject of oscillations with peaks jumping from the negative side to positive. The oscillations are also observed in three phase currents (I_{abc}) all along the disturbance period. On other hand the three voltages (U_{abc}) are not affected.

The jump in phase angle is felt on IPP2 side. As it can be seen from Figure 5.16, an increase in active power transmitted by the IPP2 to the grid is observed, while small oscillations in reactive power and peaks in transmitted currents can be seen during the disturbance period. Voltages at IPP2 sending end are not affected.

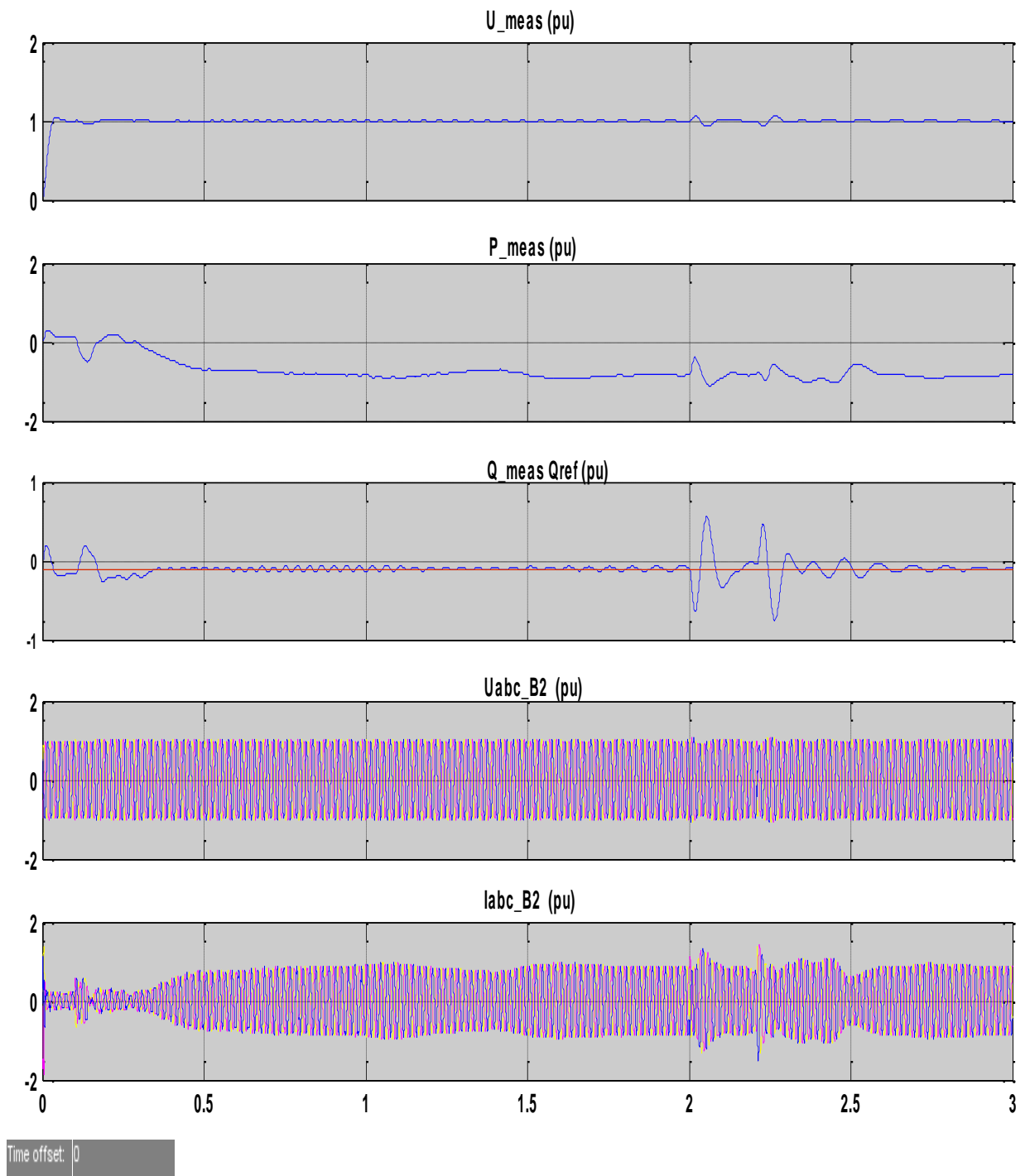


Figure 5. 15: measurement taken at station 2 during the grid side phase angle jump

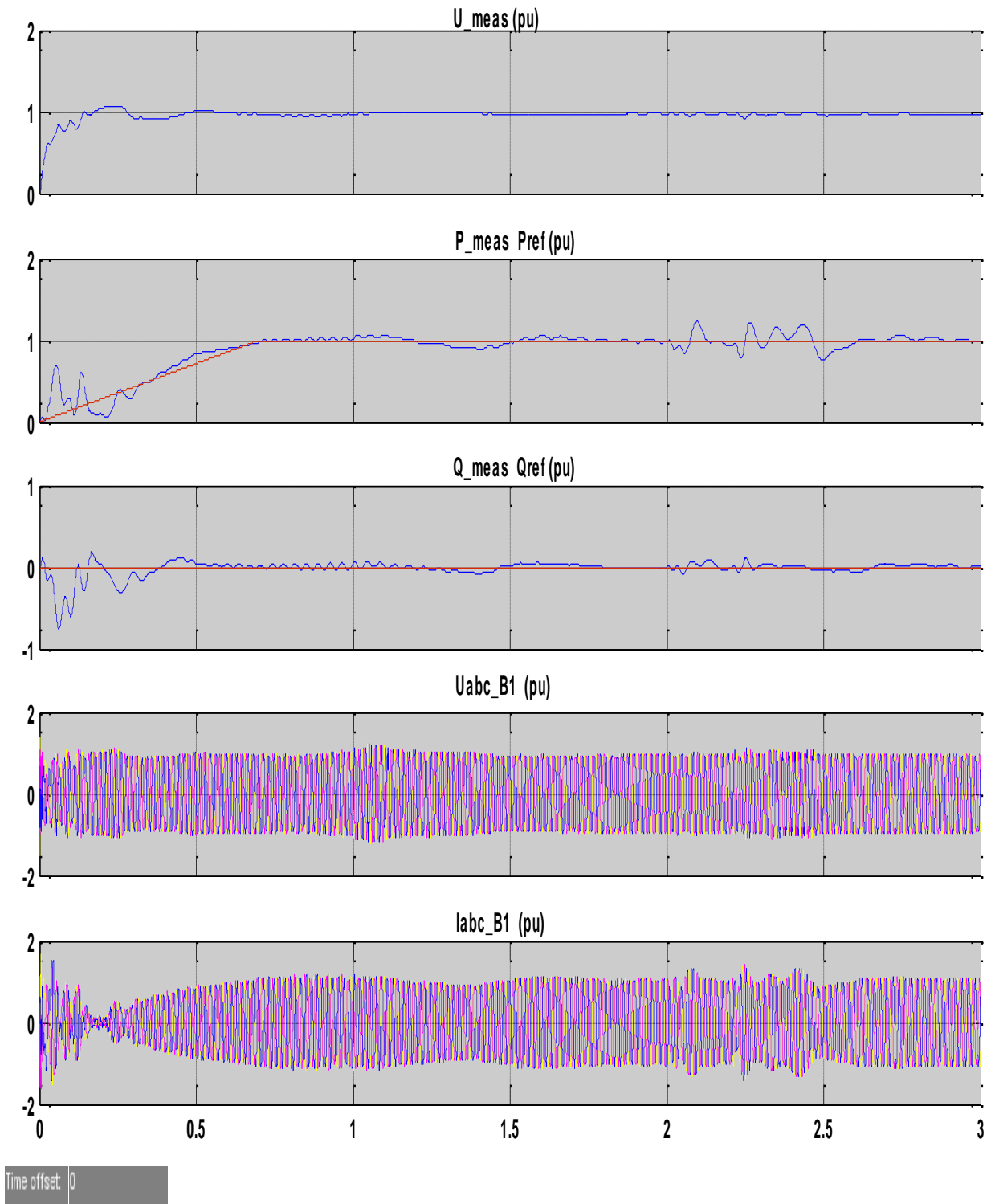


Figure 5. 16: Measurement taken at IPP2 station 1 during grid side phase angle jump

5.4 Integration of solar power plant (IPP3) through VSC-HVDC

5.4.1. Introduction

Simulations results of the solar park, producing and transmitting 60 MW to a 120 kV 50 Hz grid through an HVDC-VSC connection is shown in this section. The power produced by the solar park is converted using the boost converter to the required level for transmission to the HVDC-VSC system, accordingly to the design presented in Chapter 4 section 4.11. Three conditions were simulated using Simulink, the normal working conditions, the fault conditions and grid side frequency disturbances. The grid is implemented by a programmable voltage, while the solar park is implemented by DC sources.

5.4.2. Normal working conditions

For the normal working conditions, the solar is set to transmit power to the grid where a load is connected, as shown on Figure 5.17. The system is set to supply a 10 MW load connected at grid. A negative step is introduced onto grid side, emulating any sudden voltage sag that may temporary occur during the normal working condition. Measurements are taken at station 1 and station 2 on the point of common connection (PCC).

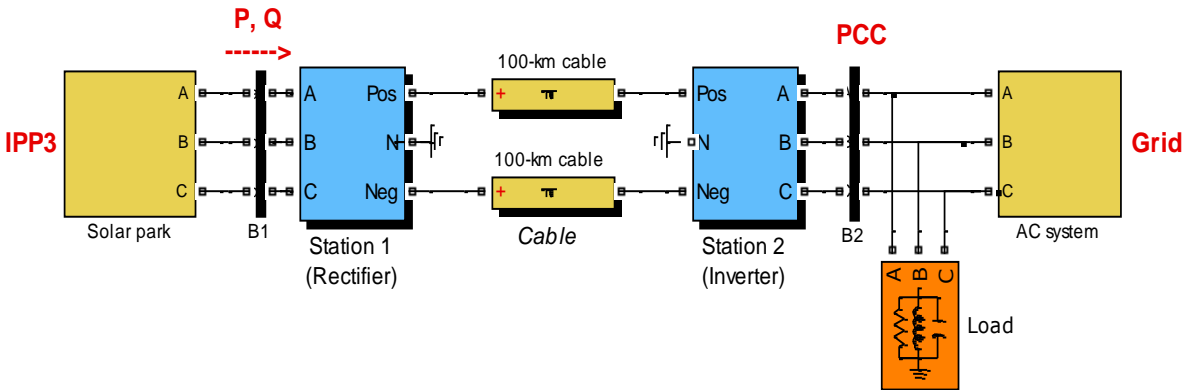


Figure 5. 17 : IPP3 connection to the grid

Results of measurements taken on station 2 on grid side are shown in Figure 5.18. The measurements taken are per unit and three phase voltages based. The base power is 200 MW and base voltage is 120kV. The system starts at zero off set, the active power (P_{meas}) delivered to the grid with a load connected, is 0.2 p.u while measured reactive (Q_{meas}) drained by the load is 0.1. As it can be seen from measured phase voltage (U_{meas}), a voltage drop of 0.15 p.u occurs at $t = 1.8$ s for a duration of 400 ms. The drop of grid voltage cause as well 0.1 p.u drop in active power and sudden increase by 0.2 p.u in reactive power drawn by the grid from the IPP3 for the duration of the phase voltage drop.

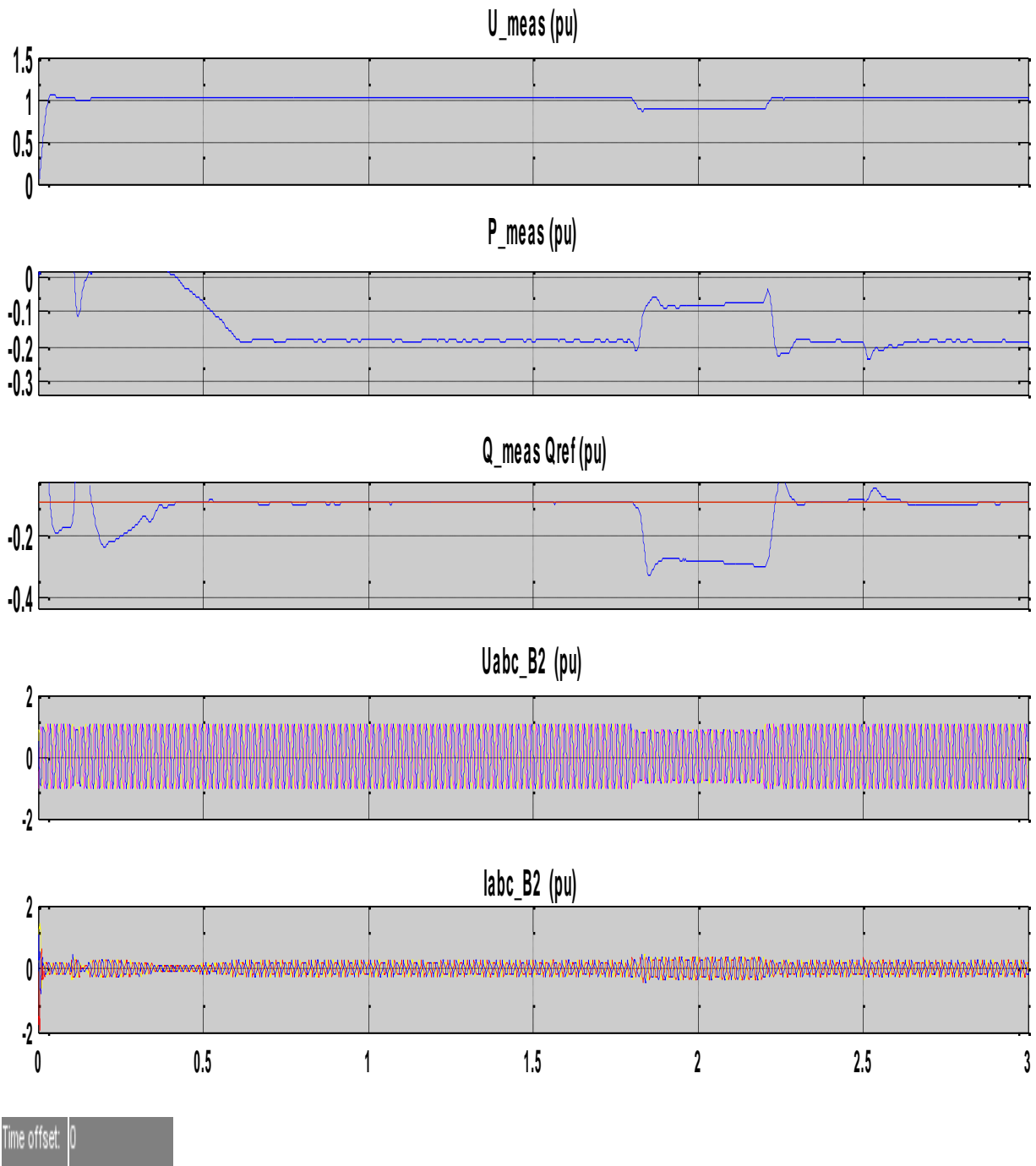


Figure 5. 18: Measurements taken at station 2 on grid side

Figure 5.19 shows the results of the measurements taken at the IPP3 sending station, where the transmitted active power (P_{meas}), reactive power (Q_{meas}), phase voltage (U_{meas}), three phase voltage (U_{abc}) and the currents (I_{meas}) are expressed in per unit measure. With the base power set at 200 MW, base voltage at 120 kV, we see that the active power transmitted is 0.2 p.u. while the reactive power is nearly zero. The system starts at zero off set and reaches the steady state after 0.5 s. At $t = 1.8$ s, when a negative step voltage is introduced to the grid side, the disturbance doesn't affect the IPP3 side.

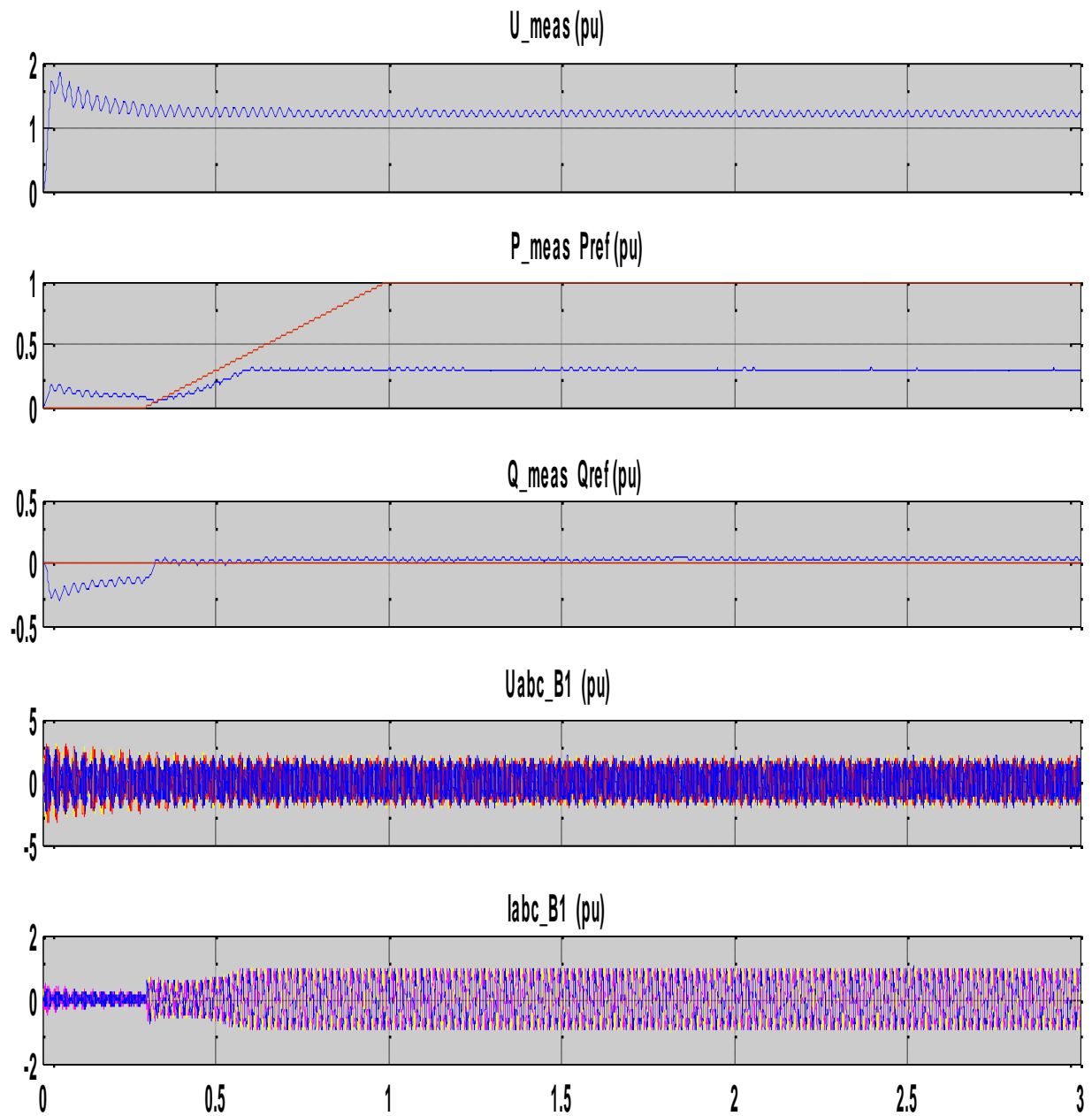


Figure 5. 19: Measurement taken at IPP3 on station

5.3.3 Abnormal conditions

The simulations for the abnormal conditions on grid to which IPP3 is connected through HVDC-VSC link, is implemented using the model on Figure 5.20 below. As in previous simulations the solar park (IPP3) is transmitting power to the grid, where a fault is introduced and implemented by a three phase fault block in our model.

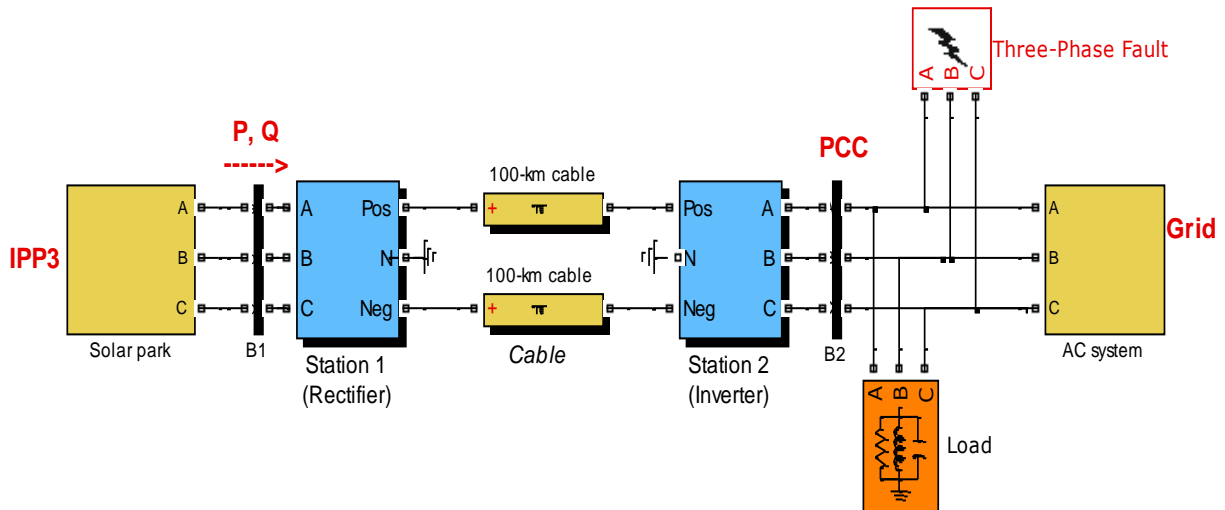
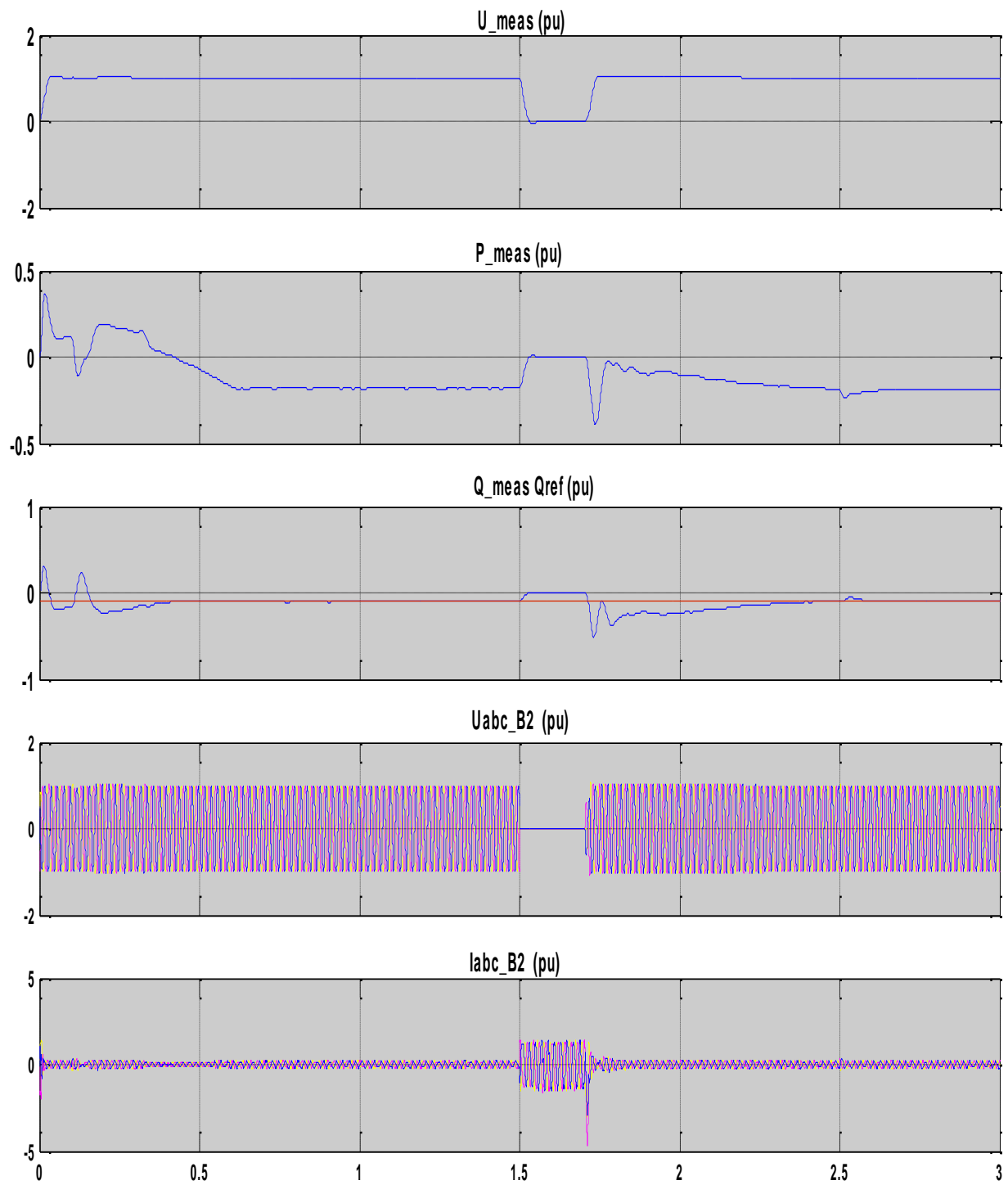


Figure 5. 20: IPP3 connection to grid, fault testing model

The system is set to start at zero offset and reaches study state around 0.8 s. A three phase short circuit is introduced, at $t = 1.5$ s, making the voltage (U_{meas}) on grid side to drop to zero. As it can be seen from Figure 5.21 of measurements made at station 2 on point of connection (PCC), the grid side active power (P_{meas}) and reactive (Q_{meas}) also drop. A high three phase short circuit currents (I_{abc}) are observed all along the fault period which is 200 ms. After the fault clearance at $t = 1.7$ s, the system has a recovered its pre fault condition at $t = 2.5$ s. Measurements results are shown in per unit system with base voltage set at 120 kV and 200 MW as base power.

The results of measurements taken on IPP3 side are shown on Figure 5.22. where it can be seen that the occurrence of fault onto the grid at $t = 1.5$ s, does affect the IPP3 side for all along the fault period. The transmitted power (P_{meas}) drops to 0.1 p.u, fluctuation appears in transmitted reactive power (Q_{meas}) and the three phase currents (I_{abc}) drop to 0.5 p.u while transmitted voltages (U_{abc}) are not affected.

After fault clearance on grid the side, the IPP3 side recover pre-fault condition at $t = 2$ s. Thus, 0.3 s after fault clearance.



Time offset: 0

Figure 5. 21: Measurement taken at IPP3 station 2 during three phase fault on grid side

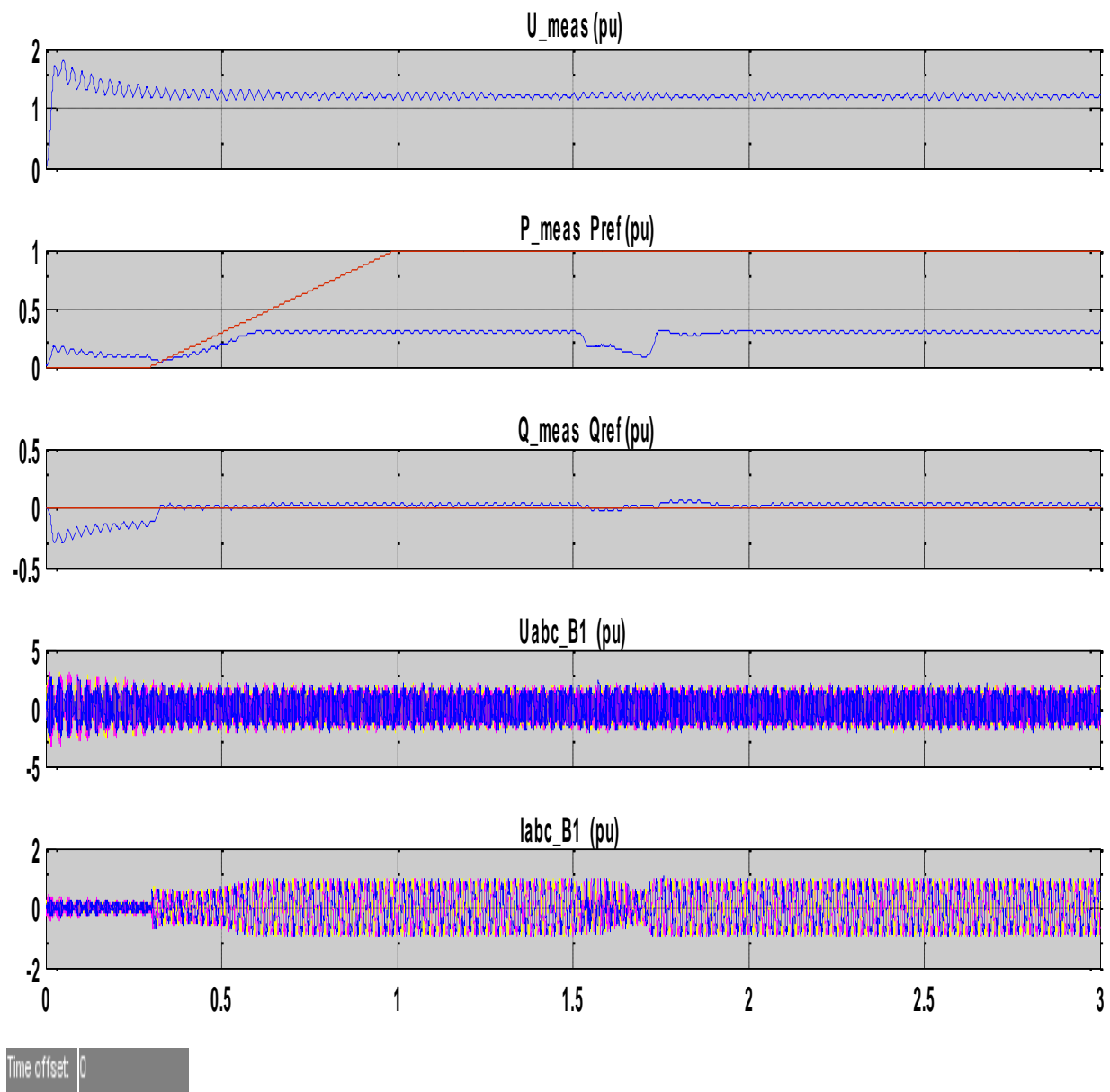


Figure 5. 22: Measurement taken at station 1 on IPP3 side during the fault on grid

A sudden jump in phase was considered as an abnormal condition on the same level as the three phase fault by the regulation authorities, a step phase shift of 40 degrees is introduced on the grid side at $t = 2$ s for a period equal to 210 ms. As in previous simulations in integration of IPP2, the three phase fault model on Figure 5.20 was used with fault block disabled. Results of measurements taken on grid and on IPP2 station side during that sudden phase jump are shown on Figure 5.23 and 5.24 respectively. Per unit system is used, where the base power is 200 MW and base voltage is set at 120 kV. All simulations were done on 3 s period range.

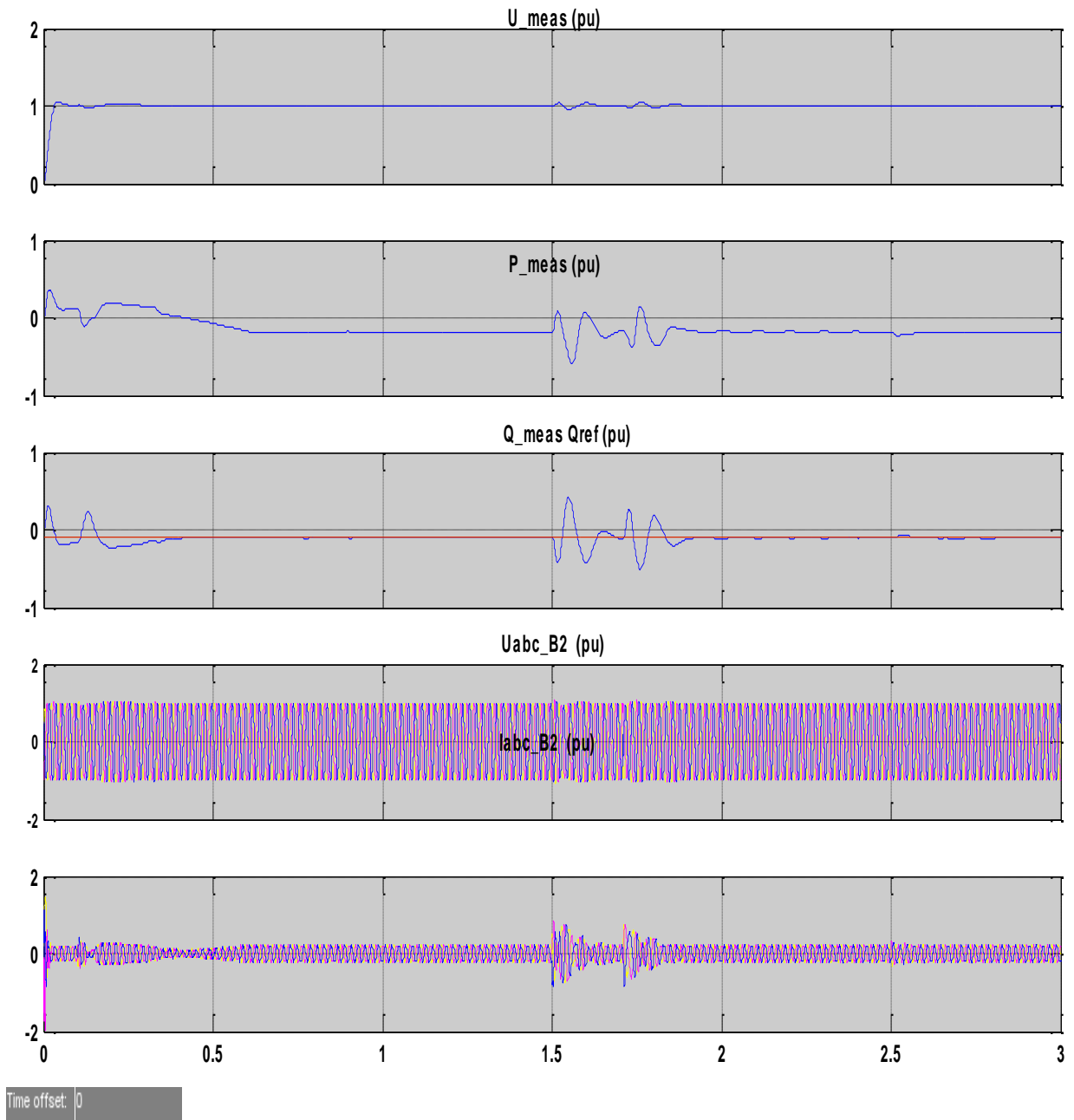


Figure 5. 23: Measurement taken at IPP3 station 2 during grid side phase angle jump

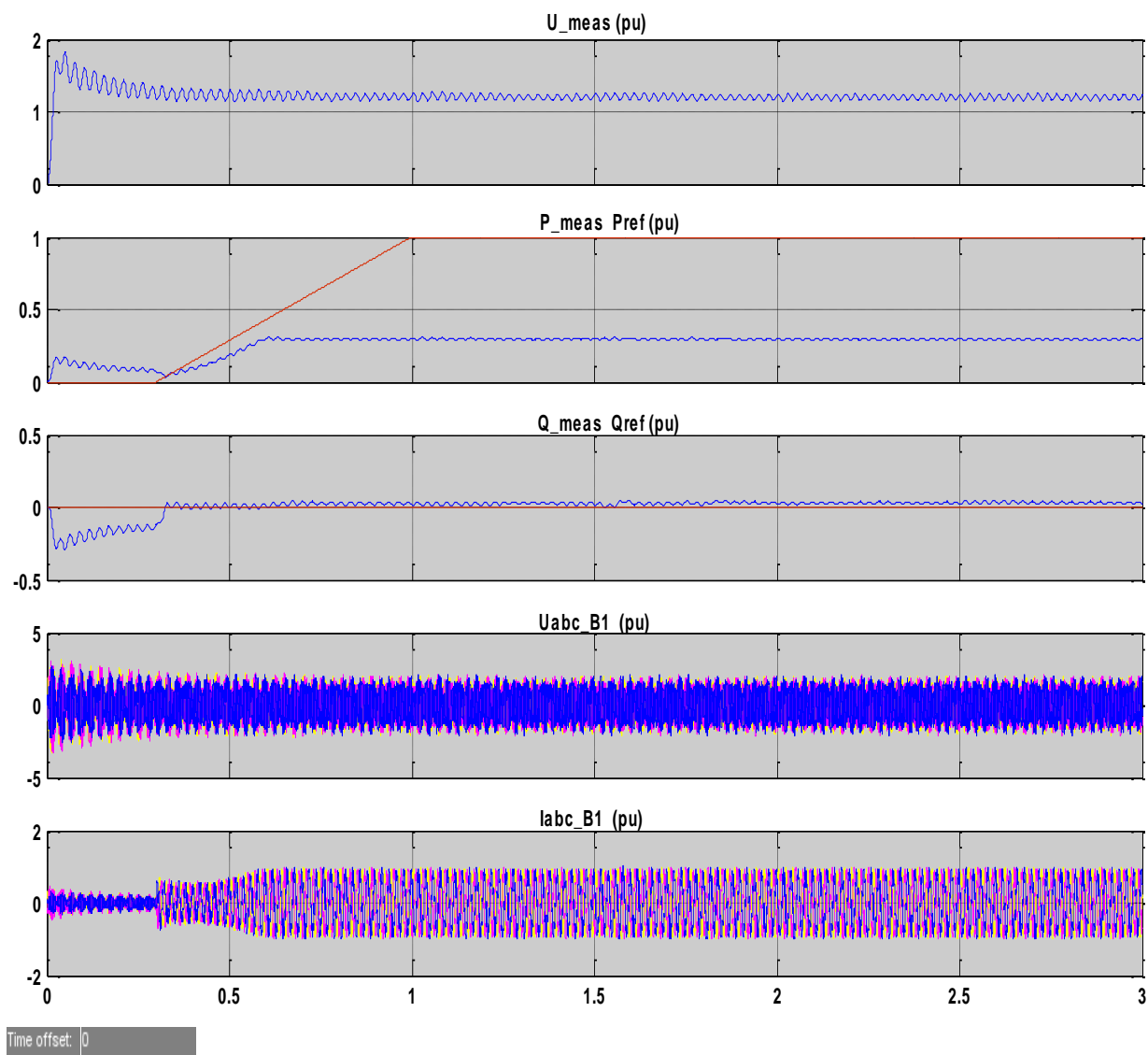


Figure 5. 24: Measurement taken at IPP3 station during grid side phase angle jump

5.5 Summary

IPPs integration to grid through VSC-HVDC simulations results have been presented in this chapter. For each of three IPPs considered, various scenario of working condition have been performed. Normal working condition and grid side fault condition simulations have performed for the study of the behaviour of IPPs. Grid three phase short circuits and phase angle jump are done, measurements taken at both side namely IPP side and grid side are shown. Consequent analyses are presented.

CHAPTER SIX

CONCLUSION AND RECOMMENDATION

6.1 Conclusion

In South Africa the level of penetration of the renewable energies through the Independent Power Provides (IPP), is increasing. It is necessary to analyze and evaluate the interaction of those sources with the power system grid. Interconnecting those IPPs power influences the performance of the power system in the light of stability, reliability, and quality.

The intermittence of those renewable based IPPs, their distributed locations and the requirements by the regulating authority make the integration of those IPPs a challenge. In this thesis HVDC-VSC transmission system is proposed for the distributed IPPs grid interconnection. Three IPPs were considered namely conventional power plant, wind farm and a solar park. Simulations in Matlab/Simulink were conducted for analyzing the performance of the system during the normal and fault working conditions.

The IPP1 grid integration simulations results show good interactions with the grid in terms of voltage, power quality and control. During normal working conditions, exchange of reactive power was observed with the grid. During fault condition onto the grid, IPP1 is isolated from the fault propagation through HVDC-VSC. In return the IPP1 is participating into stabilization of the grid by increasing the active and reactive power sent to the grid.

The IPP2 grid integration, through HVDC-VSC system simulations, results show a successful integration with power generated according to the grid load demand. A full support by the IPP2 to the grid during the fault condition is observed all along the disturbances without being affected itself by the fault.

The IPP3 integration simulations results, as previous IPPs, show the successful integration. During the normal working conditions, the IPP3 is providing the active power and little reactive power. This is compensated by the capability of VSC-HVDC system to decouple reactive and active such that at the grid side required power is delivered. During the fault condition at grid side, The IPP3 maintains the transmitted voltages and same time reducing active power. Meanwhile due to the nature of IPP3, which is a solar park, only active power is produced. The VSC-HVDC grid connected IPPs fault ride through capability as required by the regulation authorities has been demonstrated.

With the use of VSC-HVDC system as interface for the integration of three IPPs considered in this thesis, it has been observed that despite the difference in their technologies all those IPPs behaves similar during the normal working conditions and that they are able to support the grid during fault.

The grid integration of IPPs using VSC-HVDC is proven to be an efficient and good method for both the grid and the IPPs.

The nature of IPPs or the renewable energy sources technologies that it is used influences the support that those IPPs might give to the grid. Among the three IPPs, the wind farm in isolated network is the best for the grid support .It doesn't need to draw reactive power from the grid to operate as it is generated on site. For the solar park, an additional storage system like superconducting magnetic energy storage can be used in conjunction with a VSC-HVDC just for grid support in terms of reactive power.

6.3 Future work

In this thesis, we have been looking at the system behavior in general during the grid side disturbances. As future work it should be interesting to analyze:

- The system behaviour during faults on IPPs side.
- Protection system performance.
- The VSC-HVDC system converter faults and their impacts on the grid would be an interesting case to study.

The actual trends in power system is smart grids and the idea of HVDC grid is becoming more and more reality, thus a study of IPPs connected to an HVDC grid is of great importance. Fault analysis, system protection and system stability studies of such system should be conducted in future works.

REFERENCES

- Abbey, C., 2007. *Protection coordination planning with distributed generation*, Varennes , Quebec: CETC.
- Abhijit, C. & Halder, S., 2011. *Power system analysis operation and control*. 3rd ed. New Delhi: PHI Learning Private Limited.
- Acha, E., Agelidis, V., Anaya-Lara, O. & Miller, T., 2002. *Power electronic control in power systems*. 1st ed. oxford: Newnes.
- Ackerman, T., 2005. Chap 6 . comparison of technical interconnection regulations. In: *Wind Power in Power Systems*. s.l.:John Wiley & Sons, Ltd, pp. 121-134.
- Adrian, T., Remus, T., Frede, B. & Marco, L., 2005. *Synchronization methods for three phase distributed power generation systems - An overview and evaluation*. Recife, IEEE, pp. 2474 - 2481 .
- Amirnaser & Iravani, &., 2010. Classification of converters. In: *Voltage sourced converters in power system: Modeling, Control, and Applications*. Hoboken, New Jersey: John Wiley & Sons, p. 12.
- Ana, R., Francisco, H., Emilio, J. B. & Francisco, J. R., 2013. Analysis and performance comparison of different power conditioning systems for SMES-based energy systems in wind turbines. *Energies*, Volume 6, pp. 1527-1553.
- Andersen, B., Xu, L., Horton, P. & Cartwright, R., 2002. Topology for VSC transmission. *Power engineering journal*, June , 16(3), pp. 142-150.
- Anders, G., 1996. *Design of direct-driven permanent-magnet generators for wind turbines*, Göteborg: Chalmers University of Technology.
- Andrzej, T. M., 2010. *Introduction to modern power electronics*. 2nd ed. New Jersey: Wiley.
- Antoni, G. et al., 2010. State of the art on high temperature thermal energy storage for power generation. Part 1—Concepts, materials and modellization. *Renewable and Sustainable Energy Reviews*, Volume 14, pp. 31-55.
- Arrillaga, J., Liu, H. Y., Watson, N. & R., 2007. *Flexible Power Transmission: The HVDC Options*. West sussex: John Wiley & Sons Ltd.
- Asplund, G., 2004. *Sustainable energy systems with HVDC transmission*. Denver , Colorado, IEEE, pp. 2299-2303.

- Asplund, G., Carlsson, L. & Tollerz, \., 2003. 50 years of HVDC Part1. *ABI Review*, 4.
- Bacon, R. & Besant, J., 2001. Global electric power reform, privatization, and liberalization of the electric power industry in developing countries. *Annual Review of Energy and the Environment*, November, Volume 26, pp. 331-359.
- Bahrman, M. & Brian, K., 2007. The ABCs of HVDC Transmission Technology. *IEEE power & energy magazine*, 5 (2), p. 40.
- Benato, R., Marelli, M., Ambogrio, O. & Ernesto, Z., 2010. Harmonic behaviour of HVDC cables. *Transmission and distribution conference and Exposition, IEEE PES*, 19-22 April, Issue Power energy, industrial applications, pp. 1-9.
- Bianchi, F., De Battista, H. & Mantz, R., 2008. Optimal gain-scheduled control of fixed-speed. *IET Renewable Power Generation*, 2(4), pp. 228-238.
- Bidyadhar, S. & Raseswari, P., 2013. A Comparative Study on Maximum Power Point Tracking Techniques for Photovoltaic Power Systems. *IEEE TRANSACTIONS ON SUSTAINABLE ENERGY*, January, 4(1), pp. 89-98.
- Bimal, B. K., 2000. *Power electronics and variable frequency drives: technology and applications*. 1st ed. Delhi: Standard publishers distributors.
- Bindeshwar, S. et al., 2012. Multi-level inverter: a literature survey on topologies and control strategies. *International Journal of Reviews in Computing*, 31 July. Volume 10.
- Blaabjerg, F. & Chen, Z., 2006. In: *Power electronics for modern wind turbines*. s.l.:Morgan & Claypool, pp. 11-20.
- Blaabjerg, F., Remus, T., Marco, L. & Adrian, V., 2006. Overview of control and grid synchronization for distributed power generation systemns. *IEEE transactions on industrial electronics*, 53(5), pp. 1398-1409.
- Boom, R., 1991. *Superconductive magnetic energy storage for electric utilities , a review of 20 years wisconsin program*. New jersey, IEEE, pp. 1-4.
- Bose, B., 2002. *Modern power electronics and AC drives*. Upple Saddle river, NJ: Prentice-Hall.
- Boxwell, M., 2010. In: *Solar Electricity Handbook- 2010 Edition*. s.l.:Greestream publishing 2010, pp. 15-18.
- Burton, T., Sharpe, D. & N. Jenkins, a. E. B., 2001. *Wind Energy Handbook*. s.l.:John Wiley & Sons,.

- Castellano, 2010. Solar cell manufacturing. In: *solar panel processing*. Philadelphia: Old city publishing.Inc & Edition des archives contemporaine.Ltd, p. 27.
- Castellano, R., 2010. In: *Solar panel processing*. Philadelphia; Paris: Old city publishing.Inc & Editions des archives contemporaines.Ltd, pp. 5-10.
- Chan-Ki, K., Vijay, K. S., Gil-Sooang & Seong-Joo Lim, S.-J. L., 2009. *HVDC Transmission:power conversion applications in power systems*. Singapore: Wiley & Sons.
- Chaudhary, S., Teodorescu, R. & Rodriguez, P., 2008. *Wind Farm Grid Integration Using VSC Based HVDC Transmission - An Overview*. Antlata, IEEE.
- Chen, Z., 2005. *Issues of connecting wind farms into power systems*. Dalian, IEEE, pp. 1-6.
- Clark, H., Robert, L., Divan, D. & T.A, L., 1994. *Comparison of multilevel inverters for static var compensation*. Denver,CO, IEE, pp. 921-928.
- Colak, I., Ersan, Kabalci & Ramazan, B., 2010. Review of multilevel voltage source inverter topologies and control schemes. *Energy Conversion and Management*, September, pp. 4-5.
- David, M. & Camm, E. H., 2012. *Power Quality Standards for Utility Wind and Solar Power Plants*. Orlando, IEEE, pp. 1-3.
- DGS, 2005. In: *Planning and Installing Solar Thermal Systems: A Guide for Installers,architects and engineers*. s.l.:James and james (Science Publishing), p. 162.
- Eduardo, L., 1994. In: *Solar electricity:Engineering of photovoltaic system*. seville: Progensa, pp. 59-65.
- EERE, 2011. *Energy Efficiency&Renewable Energy*. [Online]
Available at: http://www1.eere.energy.gov/wind/wind_how.html
[Accessed 16 July 2012].
- EL-Shimy, M., Badr, M. & RASSEM, O., 2008. *Impact of large scale wind power on power system stability*. Aswan, IEEE, pp. 630 - 636 .
- Ernesto, Z., 2009. *HVDC transmission cable systems: state of the art and future trends*. Orlando, Prysminian powerlink, pp. 1-46.
- Europacable, 2011. *An introduction to High Voltage Direct Current (HVDC)*, Brussels: Europacable.

- Farmer, R., 2001. Power system dynamics and stability. In: L. Grisby, ed. *The electric power engineering handbook*. s.l.:CRC Press LLC.
- Fereidoon, P. S., 2010. Solar energy:the largest energy resource. In: *Generating electricity in a carbon constrained world*. s.l.:Elsevier, pp. 279-282.
- Florin, I., Poul, S., Anca-Daniela, H. & Frede, B., 2005 . *Grid connection of active stall wind farms using a VSC based DC transmission system*. Dresden, s.n., p. 10.
- Frede, B. & Chen, Z., 2006. *Power electronics for modern wind turbines*. 1 ed. s.l.:Morgan & Claypool publisher.
- Gianluigi, m., 2013. *Advanced technologies for future transmission grids*. london: Springer.
- Goodrich, F. & Andersen, B., 1987. The 2000 MW HVDC link between England and France. *Power engineering journal*, March, 1(2), pp. 69-74.
- Grahame, D. ,. H. & Thomas, A. L., 2003. *Pulse Width Modulation for Power Converters: Principles and Practice*. New Jersey: John Wiley & Sons.
- Grauers, A., 1996. Efficiency of three wind energy generator systems. *IEEE Trans. Energy Conversion*, 11(3), pp. 650-657.
- Grigsby, L., 2007. Power system stability and control. In: *Electric Power Engineering Handbook*. 2nd ed. s.l.:Taylor & Francis Group, I.I.C.
- Guan, c. ,. & James, C., 1996. Phase locked loop techniques a survey. *IEEE transactions on industrial electronics* , 43(6), pp. 609-615.
- Guanjun, D., Guangfu, T., Zhiyuan, H. & Ming, D., 2008. *New Technologies of Voltage Source Converter (VSC) for HVDC Transmission System Based on VSC*. Pittsburgh, PA, IEEE, pp. 1-8.
- Hansen, D. A., 2005. Wind Power in Power systems. In: A. Thomas, ed. *Generators and Power Electronics for Wind Turbines*. stockholm: Wiley, pp. 53-77.
- Hao, L., Lewin, P., Swingler, S. & Bradley, C., 2010. *Leak detection for self-contained fluid filled cables using regression analysis*. san diego, IEEE, pp. 1-5.
- Harnefors, L., Bongiorno, M. & Lundberg, S., 2007. Input-admittance calculation and shaping for controlled voltage-source converters. *IEEE transaction on industrial electronics* , 54(6), pp. 3323-3334.

- Hau, E., 2006. In: *Wind Turbines: Fundamentals, Technologies, Application, Economics*. 2nd Edition ed. Berlin: Springer, pp. 68-71.
- Heinrich, H., 2012. In: *Photovoltaics System Design and Practice*. West Sussex: John Wiley and Sons., pp. 264-266.
- Himanshu, J., Bruce, A. M. & Hans, K. H., 2012. *Comparison of Wind Farm Topologies for Offshore Applications*. San Diego, IEEE, pp. 1-8.
- Horiuchi, T. & Kato, Y., 1974. Japan prepares HVDC techniques to meet domestic need. *Energy Int.*, 30 June, 11(1), pp. 13-14.
- Hough, T. P., 2006. In: *Solar Energy: New Research*. s.l.: Nova Science Publisher, p. 311.
- Hyong, S. & Dylan, D.-c. L., 2010. *Review on Wind Turbine Generators and Power Electronic Converters with Grid-Connection Issues*. Christchurch, s.n., pp. 1-6.
- Inigo, M. D. A. et al., 2007. Connection requirements for wind farms: A survey on technical requirements and regulation. *ScienceDirect: Renewable and Sustainable Energy Reviews*, 11(8), pp. 1858-1872.
- Jamieson, P., 2011. *Innovation in Wind Turbine Design*. West Sussex: Wiley.
- Jie, Y., Jianchao, Z., Guangfu, T. & Zhiyuan, H., 2010. *Characteristics and Recovery Performance of VSC-HVDC DC Transmission Line Fault*. Chengdu, IEEE, pp. 1-4.
- Jin, Y., John, E. J. & O'Reilly, J., 2010. Multiterminal DC wind farm collection grid internal fault analysis and protection design. *IEEE Transactions on Power Delivery*, October, 25(4), pp. 2308-2318.
- Johnsson, G. L., 1985. *Wind Energy Systems*. Englewood Cliffs, N.J, USA: Prentice-Hall.
- Jovanovic, M. G., 2009. Sensorless and sensorless speed control methods for brushless doubly fed reluctance motors. *IET*, 3(6), pp. 503 - 513.
- Jovic, D., 2003. Phase Locked Loop Systems for FACTS. *IEEE Transactions on Power Systems*, 18(3), pp. 1116-1124.
- Ju, W., Jian, X., You, G. & Jian G., Z., 2007. *Theory and Applications of Superconducting Magnetic Energy Storage*, Chengdu, China: University of Electronic Science and Technology of China. Sydney, Broadway, NSW, Australia: Faculty of Engineering, University of Technology.

- Kahn, MTE., Ogbonnaya, I. & Edward, C., 2008. *CONCISE HIGHER ELECTRICAL ENGINEERING*. Cape Town: Juta & Company Ltd.
- Kala, m. & Sadrul, u., 2007. *Comparative evaluation of HVDC and HVAC transmission systems*. s.l.:IEEE.
- Kanamaru, Y. & Amemiya, Y., 1991. Numerical analysis of magnetic field in superconducting magnetic energy storage system. *IEEE transaction on magnetics*, September, 27(5), pp. 3935-3938.
- Kashif, I. & Zainal, S., 2013. A review of maximum power point tracking techniques of PV system for uniform insolation and partial shading condition. *Renewable and Sustainable Energy Reviews*, March, Volume 19, p. 475–488.
- Kazmierkowsk, M. P. & Malesani, L., 1998. Current control techniques for three-phase voltage-source PWM converters: A survey. *IEE transaction on industrial electronics*, 45(5), pp. 691-703.
- Khatir, M. et al., 2009. Performance Analysis of a Voltage Source Converter (VSC) based HVDC Transmission System under Faulted Conditions. *Leonardo Journal of Sciences*, July-December, Issue 15, pp. 33-46.
- Kichartz, T., 2009. In: *Generalized Detailed Balance Theory of Solar Cells*. Aachen: Forschungszentrum Julich, pp. 33-36.
- Kjell, E., 2001. Operational experience of HVDC light. *AC-DC Power Transmission*.
- Krauter, S. C., 2006. *Solar electric power generation - Photovoltaic energy system*. s.l.:Springer.
- Kundur, P., 1994. introduction to stability problem. In: N. Balu & M. Lauby, eds. *Power system stability and control*. s.l.:McGraw Hill Inc, pp. 17-40.
- Larruskain, D. M., Mazon, A. I., Zamora, A. O. & J.Monasterio, 2005. *Transmission and distribution networks: AC versus DC*. Marbella, Spain, s.n.
- Lord, R. & Bule, A. M., 1991. coil protection for the 20.4 MWh SMES/ETM. *IEEE transactions on magnetics*, 27(2), pp. 1716-1719.
- Luisa, F. C. et al., 2012. Review of SolarThermal Storage Techniques and Associated Heat Transfer Technologies. *Proceedings of the IEEE*, 100(2), pp. 525-538.
- Makoto, s. & Takaai, I., 1999. An evaluation of the inlet flow for a cable in conduit conductor by rapid heating. *Cryogenics*, Volume 39, pp. 939-945.

Marian, P. K., Ramu, K. & Frede, B., 2002. *Control in Power Electronics: Selected problems*. San diego,USA: Elsevier.

Markvart, T., 1994. solar cells. In: *Solar electricity*. West Sussex: John Wiley & Sons Ltd, pp. 21-43.

Marzinotto, M. & Mazzanti, G., 2011. A procedure for space charge measurements in full size HVDC extruded cables. *Annual report conference on electrical insulation and dielectric phenomena (CEIDP)*, 16-19 October. pp. 804-807.

Mathew, S., 2006. History of wind energy. In: *Wind Energy Fundamentals, Resource Analysis and Economics*,. Berlin Heidelberg: Springer, p. 2.

Mazzoldi, F., Taisne, J., Martin, C. & Rowe, B., 1989. Adapation of the control equipment to permit 3-terminal opterion of HVDC link between Sardinia, Corsica and mainland Italy. *IEEE, Power Delivery*, April, 4(2), pp. 1269-1274.

Michael, A. & Phoivos, D., 1988. State-of-the-Art Carrier PWM Techniques: A Critical Evaluation. *IEEE TRANSACTIONS ON INDUSTRY APPLICATIONS*,, March/April, 24(2), pp. 271-280.

Momoh, J. & El-Hawary, M., 1999. Electric systems, dynamics, and stability with artificial intelligence applications. In: *Electric systems, dynamics, and stability with artificial intelligence applications*. s.l.:Marcel Dekker Inc.

Müfit, A. et al., 2011. *Aspects of wind power plant collector network layout and control architecture*. Fredericia, Denmark, Energinet.dk, pp. 46-52.

Mukund, R., 2006. *Wind and solar power systems :design analysis and operation*. 2nd ed. New york: Taylor and Francis group & CRC press.

Muller, S., Deicke, M. & De Doncker, R. W., 2002. Doubly fed induction generator systems for wind turbines. *IEEE Industry Application Magazine*, May/June, 8(3), p. 26– 33.

Nayar, C. V., Islam, S. M. & Hari, S., 2001. Power Electronics for Renewable Energy Sources. In: H. R. Muhammad, ed. *POWER ELECTRONICS HANDBOOK*. san diego: Academic press, p. 560.

Neacsu, D. O., 2001. SPACE VECTOR MODULATION –An Introduction Tutorial at IECON2001. *The 27th Annual Conference of the IEEE Industrial Electronics Society*, pp. 1583-1592.

NERSA, 2012. *GRID CODE REQUIREMENTS FOR WIND ENERGY FACILITIES CONNECTED TO DISTRIBUTION OR TRANSMISSION SYSTEMS IN SOUTH AFRICA*, s.l.: NERSA.

NERSA, 2012. Grid connection code for renewable power plants (RPP) connected to the electricity transmission system or distribution system in south africa. November. Volume version 2.6.

NI, 2012. *National instrument*. [Online]

Available at: <http://www.ni.com/white-paper/7230/en#toc1>

[Accessed 13 July 2012].

Ninomiya, A. & Sakaniwa, K., 1989. Detection of superconducting magnets using ultrasonic wave. *IEEE transactions on magnetic*, Volume 25, pp. 1520-1523.

NREL, 2010. *Energy analysis*, Colorado: s.n.

Owen, P., 2009. *The history of high voltage direct curret transmission*. Dunedin, NZ:

http://www.ipenz.org.nz/heritage/conference/papers/Peake_O.pdf.

Padiyar, 2005. converter faults and protection. In: *HVDC Power Transmission System: Technology and System Interactions*. New Delhi: New age internationa (P) publisher Ltd, p. 97.

Padiyar, 2005. smoothing reactor. In: *HVDC Power Transmission systems technology and system interactions*. new delhi: New age international (P) Ltd, Publishers ,, p. 14.

Padiyar, K., 2007. *FACTS controllers in power transmission and distribution*. 1 ed. Bangalore: New age international publishers.

Padiyar, K., 2007. Pulse width modulation for voltage source converters. In: *FACTS controllers in power transmission and distription*. Bangalore: New age international(P) Limited, Publishers, pp. 507-521.

Padiyar, K., 2008. *FACTS controllers in power transmission and disribution*. Bangalore: New age international publishers.

Padiyar, K., 2008. FACTS controllers in power transmission and distribution. In: *FACTS controllers in power transmission and distribution*. Bangalore: New age international limited publishers, pp. 188-192.

- Patel, H. & Hoft, R., 1974. Generalized techniques of harmonic elimination and voltage control in thyristor inverters: Part II-Voltage control Techniques. *IEEE Transactions on Industry Applications*, Volume 10, pp. 666-673.
- Paul, B., 2005. *Power Generation Technologies*. Burlington: Newnes/Elsevier.
- Paulo, F. et al., 2001. Energy storage systems for advanced power applications. *Proceedings of IEEE*, December, 89(12), pp. 1744-1756.
- Pena, R., Clare, J. C. & Asher, G. M., 1996. "Doubly fed induction generator using back-to-back PWM converters and its application to variable speed wind-energy generation. *IEEE Power Electronics Application proceedings*, 143(3), p. 231–241.
- Piotr, B., 2008. Energy Storage Systems. In: S. Ryszard & B. Grzegorz, eds. *Power electronics in smart electrical energy networks*. London: Springer, pp. 269-302.
- Polinder, H., De Haan, S., Dubois, M. R. & Sloopweg, J. G., 2005. "Basic operation principles and electrical conversion systems of wind turbines. *European power electronics and drives Journal (EPE)*, 15(4).
- Prasad, D. K. & Snow, D. M., 2005. In: *Designing with Solar Power: A Source Book for Building Integrated* victoria, Australia: Image Publishing group Pty Ltd and Earthscan, p. 26.
- Qahraman, B., Gole, A. & Fernando, I., 2006. *Hybrid HVDC Converters and Their Impact on Power System Dynamic Performance*. Montreal, IEEE.
- Qiong-zhong, C., Michel, D. & Olivie, r. B., 2011. *Control and simulation of doubly-fed induction generator*. Brussels, s.n.
- Ragheb, M., 2009. [Online]
Available at:
<https://netfiles.uiuc.edu/mragheb/www/NPRE%20475%20Wind%20Power%20Systems/Control%20of%20Wind%20Turbines.pdf>
[Accessed 17 July 2012].
- Rakibuzzaman, S. et al., 2012. Influence of Large scale PV on voltage stability of Sub transmission system. *International journal on Electrical Engineering and Informatics*, March, 4(1), pp. 148-160.
- Rechsteiner, R., 2008. *Wind Power in Context –A clean Revolution in the Energy Sector*, Basel, Switzerland: Energy Watch Group / Ludwig-Boelkow-Foundation.

Robert, G. E., 2001. *Power system harmonics ,A Reference Guide to Causes, Effects and Corrective Measures*. [Online]

Available at: http://literature.rockwellautomation.com/idc/groups/literature/documents/wp/mvb-wp011_-en-p.pdf

[Accessed 18 June 2012].

Roberto, C., Marco, L., Marta, M. & José, R., 2011. Overview of Multi-MW Wind Turbines and Wind Parks. *IEEE TRANSACTIONS ON INDUSTRIAL ELECTRONICS, VOL. 58, NO. 4, APRIL 2011*, April, 58(4), pp. 1081-1095.

Roberto, C. & Sharma, R., 2000. High Voltage Direct Current(HVDC) Transmission systems technology review.pp. 2-4.

Rodríguez, J. et al., 2002. Multilevel Inverters: A Survey of Topologies,Controls, and Applications. *IEEE TRANSACTIONS ON INDUSTRIAL ELECTRONICS*,, AUGUST, 49(4), pp. 724-738.

Rodríguez, J. et al., 2007. Multilevel Voltage-Source-Converter Topologies for Industrial Medium-Voltage Drives. *IEEE TRANSACTIONS ON INDUSTRIAL ELECTRONICS*, December, 54(6), pp. 2930-2945.

Sahali, Y. & Ferrah, M., 2003. Selective Harmonic Eliminated Pluse width Modulation techniques (SHE-PWM) applied to the three level inverter/converter. *IEEE International Symposium*, Maarch, 2(Industrial Electronics), pp. 1112-1117.

Sathyajith, M., 2006. In: *Wind Energy Fundamentals,Resource Analysis and economics*. Berlin: Springer, p. 11.

Schettler, F., Huang, H. & Christl, N., 2000. *HVDC transmission systems using voltage sourced converters-design and applications*. s.l., IEEE.

Schutz, D., Jahn, M. & Pfeifer, T., 2008. grid integration of Photovoltaic and fuel cells. In: s. Ryszard & B. Grzegorz, eds. *Power electronics in smart electrical energy network*. s.l.:Springer, p. 376.

Serrano, I. L., 1993. The modern space-phasor theory, part I: Its coherent formulation and its advantages for transient analysis of converter-fed AC machines. *European Transactions on Electrical Power*, March/April,.3(2).

Shao, S., Abdi, E. & McMahon, R. A., 2009. *Dynamic analysis of the Brushless Doubly-Fed Induction Generator during symmetrical three-phase voltage dips*. Taipei, s.n., pp. 464 - 469 .

Sheng, J. , & Vassilios, G., 2010. Review of DC System Technologies for Large Scale Integration of Wind Energy Systems with Electricity Grids. *Energies*, 3(10), pp. 1303-1319.

Shri, h. J. et al., 2012. Voltage Source Converter Based HVDC Transmission. *International Journal of Engineering Science and Innovative Technology (IJESIT)*, September. 1(1).

Siemens, 2005. *Siemens*. [Online]

Available at: http://www.siemens.com/sustainability/pool/en/environmental-portfolio/products-solutions/power-transmission-distribution/hvdc_proven_technology.pdf

[Accessed 13 6 2012].

Solar Energy International, 2004. In: *Photovoltaics: Design and Installation Manual : Renewable Energy Education*. canada: New society publishers, p. 48.

SolarCatskills, 2011. [Online]

Available at: <http://www.solarcatskills.com/about-solar/>

[Accessed 18 July 2012].

squidoo, 2012. [Online]

Available at: <http://www.squidoo.com/vertical-wind-turbines>

[Accessed 18 July 2012].

Svensson, J., 1998. "Grid-connected voltage source converter," *Ph.D. dissertation*, Gothenburg, Sweden: Chalmers Univ. Technol..

Thomas, A., 2012. *wind power in power systems*. 2nd ed. west sussex, UK: wiley.

Thresher, R. & Laxson, A., 2006. *Advanced Wind Technology: New Challenges for a New Century*. Athens, Greece, National Renewable Energy Laboratory, US DoE, pp. 5-6.

Tomas, M., 1994. In: *Solar electricity*. s.l.:John wiley and Sons, pp. 92-99.

Turnbull, G., 1964. Selected harmonic reduction in static dc-ac inverters. *IEEE Transactions on Communication and Electronics*, Volume 83, pp. 374-378.

Tushar, G. K. & Mark, P. A., 2011. In: *Energy Resources and Systems: Renewable Resources, Volume 2*. New York: Springer, pp. 102-104.

TVA, 2011. *Tennessee Valley authority*. [Online]

Available at: http://www.tva.gov/greenpowerswitch/wind_diagram.htm

[Accessed 18 July 2012].

Twidell, J. & Gaudioisi, G., 2009. Chap 6. wind farm power connection. In: T. Ackerman, ed. *Offshore wind power*. 1 ed. London: Multi-Science publishing, pp. 109-114.

Vijay, v. & Ayyanar, R., 2012. *Grid Integration and Dynamic Impact of Wind Energy*. new york: Springer.

Volker, 2009. *articles:Solar thermal power plants Technology Fundamentals*. [Online] Available at: <http://www.volker-quaschnig.de/articles/fundamentals2/index.php> [Accessed 15 July 2012].

Wang, J. & Li, G., 2009. Economic Comparison of Different Collector Networks for Offshore Wind Farms. *Dianli Xitong Zidonghua/Automat. Electric Power System*, pp. 99-103.

Wang, Y., Wu, C., Liao, H. & Xu, H., 2008. *Study on Impacts of Large-Scale Photovoltaic Power Station on Power Grid Voltage Profile*. Nanjing, DRPT.

Wikipedia, 2012. *wikipedia*. [Online] Available at: http://en.wikipedia.org/wiki/Compact_Linear_Fresnel_Reflector [Accessed 15 July 2012].

Wikipedia, 2012. *wind farm*. [Online] Available at: http://en.wikipedia.org/wiki/Wind_farm [Accessed 18 July 2012].

Willi, C. & Johnsen, D. T., 2006. *Analysis of requirements in selected grid codes*, s.l.: Technical University of Denmark.

Xuesong, Z., Bin, L. & Youjie, M., 2012. A review on Superconducting Magnetic Energy Storage. *Advanced material research*, December, Volume 614-615, pp. 825-828.

Yazdani, D., Majid, P. & Alireza, B., 2009. *Three-phase grid synchronization techniques for grid connected converters in distributed generation systems*. Seoul, IEEE, pp. 1105-1110.

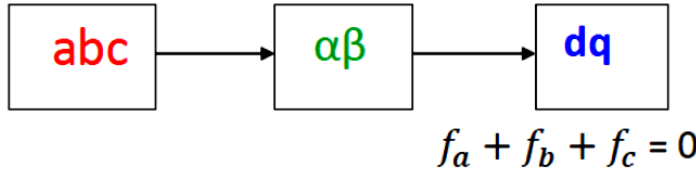
Yuan, K. W., Shao, H. T. & Ming, Y. ., 2013. Accommodating High PV Penetration on the Distribution System of Kinmen Island. *Energy and Power Engineering*, July, Volume 5, pp. 209-214.

Zhang, L., Harnefors, L. & Nee, H.-P., 2010. Power synchronization control of grid-connected voltage source converters. *IEEE Transactions on Power Systems*, May, 25(2), pp. 809-820.

Zhang, W., 1994. Active DC filter for HVDC systems. *Computer applications in Power, IEEE*, 7(1), pp. 40-44.

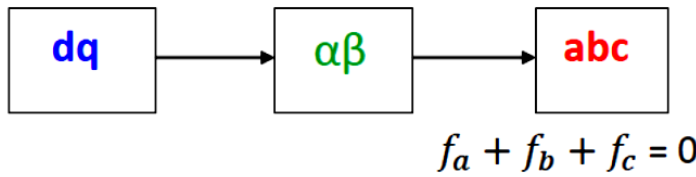
Zhenyu, Y., Arefeen, M. & Issa, P., 1997. *A Review of Three PWM Techniques*. New Mexico, IEEE, pp. 257-261.

dq Transformations



$$\begin{bmatrix} f_\alpha \\ f_\beta \end{bmatrix} = \frac{2}{3} \begin{bmatrix} 1 & -\frac{1}{2} & -\frac{1}{2} \\ 0 & \frac{\sqrt{3}}{2} & -\frac{\sqrt{3}}{2} \end{bmatrix} \times \begin{bmatrix} f_a \\ f_b \\ f_c \end{bmatrix} \quad \begin{bmatrix} f_d \\ f_q \end{bmatrix} = \begin{bmatrix} \cos(\phi) & \sin(\phi) \\ -\sin(\phi) & \cos(\phi) \end{bmatrix} \times \begin{bmatrix} f_\alpha \\ f_\beta \end{bmatrix}$$

$$\begin{bmatrix} f_d \\ f_q \end{bmatrix} = \frac{2}{3} \begin{bmatrix} \cos(\phi) & \cos(\phi - \gamma) & \cos(\phi + \gamma) \\ -\sin(\phi) & -\sin(\phi - \gamma) & -\sin(\phi + \gamma) \end{bmatrix} \times \begin{bmatrix} f_a \\ f_b \\ f_c \end{bmatrix}$$



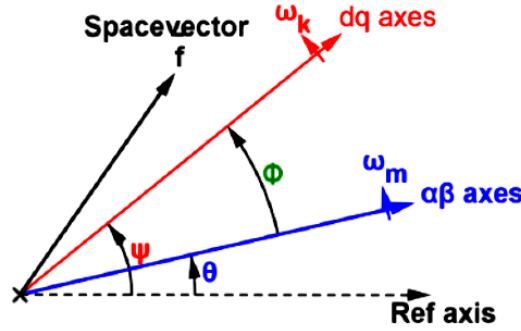
$$\begin{bmatrix} f_\alpha \\ f_\beta \end{bmatrix} = \begin{bmatrix} \cos(\phi) & -\sin(\phi) \\ \sin(\phi) & \cos(\phi) \end{bmatrix} \times \begin{bmatrix} f_d \\ f_q \end{bmatrix} \quad \begin{bmatrix} f_a \\ f_b \\ f_c \end{bmatrix} = \begin{bmatrix} 1 & 0 \\ -\frac{1}{2} & \frac{\sqrt{3}}{2} \\ -\frac{1}{2} & -\frac{\sqrt{3}}{2} \end{bmatrix} \times \begin{bmatrix} f_\alpha \\ f_\beta \end{bmatrix}$$

$$\begin{bmatrix} f_a \\ f_b \\ f_c \end{bmatrix} = \begin{bmatrix} \cos(\phi) & -\sin(\phi) \\ \cos(\phi - \gamma) & -\sin(\phi - \gamma) \\ \cos(\phi + \gamma) & -\sin(\phi + \gamma) \end{bmatrix} \times \begin{bmatrix} f_d \\ f_q \end{bmatrix}$$

$$\gamma = \frac{2\pi}{3}$$

ϕ = angle between dq and $\alpha\beta$ reference frames

A space vector \vec{f}_o and its time rate of change \vec{g}_o are attached to an $\alpha\beta$ coordinate system rotating at the speed $\omega_m = \frac{d\theta}{dt}$. The transformation to a dq coordinate system rotating at the speed $\omega_k = \frac{d\psi}{dt}$ is performed using the rotating matrix $M(\phi)$ where $\phi = \psi - \theta$.



Specifically, in terms of Space vectors and Rotating matrix,

$$\vec{f}_o = \begin{bmatrix} f_\alpha \\ f_\beta \end{bmatrix} \quad \vec{f}_k = \begin{bmatrix} f_d \\ f_q \end{bmatrix} \quad M(\phi) = \begin{bmatrix} \cos(\phi) & -\sin(\phi) \\ \sin(\phi) & \cos(\phi) \end{bmatrix}$$

the transformation of variables takes the form

$$\vec{f}_o = M(\phi)\vec{f}_k \quad \text{or the reverse} \quad \vec{f}_k = M^t(\phi)\vec{f}_o$$

The time rate of change of the initial space vector \vec{f}_o is

$$\vec{g}_o = \frac{d}{dt}\vec{f}_o = \frac{d}{dt}[M(\phi)\vec{f}_k] = M(\phi)\frac{d}{dt}\vec{f}_k + \frac{d}{dt}M(\phi) * \vec{f}_k$$

$$\vec{g}_o = M(\phi)\vec{g}_k = M(\phi)\frac{d}{dt}\vec{f}_k + (\omega_k - \omega_m)M(\phi)M\left(\frac{\pi}{2}\right)\vec{f}_k$$

so that, after cancelling $M(\phi)$, the time derivative in the k frame becomes

$$\vec{g}_k = \frac{d}{dt}\vec{f}_k + (\omega_k - \omega_m)M\left(\frac{\pi}{2}\right)\vec{f}_k$$

Note that $\frac{d}{dt}M(\phi) = \frac{d\phi}{dt}\frac{d}{d\phi}M(\phi) = (\omega_k - \omega_m)\frac{d}{d\phi}M(\phi)$ and

$$\begin{aligned} \frac{d}{d\phi}M(\phi) &= \begin{bmatrix} -\sin(\phi) & -\cos(\phi) \\ \cos(\phi) & -\sin(\phi) \end{bmatrix} = \begin{bmatrix} \cos(\phi) & -\sin(\phi) \\ \sin(\phi) & \cos(\phi) \end{bmatrix} \times \begin{bmatrix} 0 & -1 \\ 1 & 0 \end{bmatrix} \\ &= M(\phi)M\left(\frac{\pi}{2}\right) \end{aligned}$$

A matter of scale in 3 \Rightarrow 2 and 2 \Rightarrow 3 phase transformations:

$$\begin{bmatrix} f_d \\ f_q \end{bmatrix} = \kappa \begin{bmatrix} \cos(\phi) & \cos(\phi - \gamma) & \cos(\phi + \gamma) \\ -\sin(\phi) & -\sin(\phi - \gamma) & -\sin(\phi + \gamma) \end{bmatrix} \times \begin{bmatrix} f_a \\ f_b \\ f_c \end{bmatrix} \text{ or}$$

$$f_{dq} = \kappa T f_{abc}$$

Pseudo-inverse conversion:

$$f_{abc} = k_i T^t f_{dq} \quad \text{where } k_i = \frac{2}{3} \frac{1}{\kappa} \quad \text{and} \quad \frac{2}{3} T T^t = U_2$$

Quadratic form conversion:

$$f_a^2 + f_b^2 + f_c^2 = k_p (f_d^2 + f_q^2) \quad \text{where } k_p = \frac{2}{3} \frac{1}{\kappa^2}$$

Magnitude conversion:

$$f_\alpha = k_m f_a \quad \text{where } k_m = \frac{3}{2} \kappa$$

Common conventions:

	a	b	c	d
κ	$2/3$	$\sqrt{2/3}$	1	$\sqrt{2}/3$
k_i	1	$\sqrt{2/3}$	$2/3$	$\sqrt{2}$
k_p	$3/2$	1	$2/3$	3
k_m	1	$\sqrt{3/2}$	$3/2$	$1/\sqrt{2}$

a : Equal magnitude of 2- and 3-phase balanced sinusoidal signals

b : Equal 2- and 3-phase power (power invariant)

c : 2-phase amplitude equals 3/2 3-phase amplitude

d : 2-phase amplitude equals rms of 3-phase signal